

The Rabbit Ears Pulse-Envelope Phenomenon in Off-Fundamental Detection of Pulsed Signals

Frank H. Sanders



report series

The Rabbit Ears Pulse-Envelope Phenomenon in Off-Fundamental Detection of Pulsed Signals

Frank H. Sanders



U.S. DEPARTMENT OF COMMERCE

July 2012

DISCLAIMER

Certain commercial equipment and materials are identified in this report to specify adequately the technical aspects of the reported results. In no case does such identification imply recommendation or endorsement by the National Telecommunications and Information Administration, nor does it imply that the material or equipment identified is the best available for this purpose.

CONTENTS

Figures.....	vi
Tables.....	xi
Abbreviations/Acronyms	xii
1 Mathematical Demonstration of the Rabbit Ears Effect	1
1.1 Time-Domain Envelopes of Spectrum Power Measured Across the Central Spectrum Lobe.....	1
1.2 Time-Domain Envelopes of Spectrum Power <i>Not</i> Measured Across the Central Spectrum Lobe.....	3
2 Measured Rabbit Ears Pulses in Radar Emission Spectra	6
2.1 Real-World Pulse Envelope Characteristics	6
2.2 Expectations for Real-World Rabbit Ears Characteristics.....	6
2.3 Rabbit Ears Pulse Envelopes Across a Real-World 5 GHz Radar Spectrum	6
2.4 Rabbit Ears Pulse Envelopes Across the Spectrum of Another 5 GHz Radar.....	20
3 Observations of Rabbit Ears Morphologies and Implications for Off-Fundamental Detection of Pulsed Signals	42
3.1 Observed Rabbit Ears Morphologies.....	42
3.2 Implications for Off-Fundamental Detection of Pulsed Signals.....	42
3.3 Multipath Effects	42
4 Practical Application: Using the Rabbit Ears Effect to Measure Parameters Of Chirped- Frequency Pulses	43
4.1 Frequency-Modulated (Chirped) Pulses	43
4.2 Measurement of Chirped Pulse Parameters through Use of the Rabbit Ears Effect.....	43
4.3 Example Chirp-Parameter Measurement Using the Rabbit Ears Effect.....	44
5 Summary	48
6 Acknowledgements.....	49
7 References.....	50

FIGURES

Figure 1. Time-domain view of a sequence of simulated RF pulses. In this simulation the parameters are $f_0 = 10$ MHz, $\tau_{pulse} = 100$ μ s, $PRI = 3$ ms.....	2
Figure 2. Fourier transform of the pulse sequence of Figure 1. A classic sinc ² power spectrum is generated. Power is plotted linearly.	2
Figure 3. Inverse Fourier transform of the spectrum of Figure 2, from 0 MHz to 20 MHz. The original pulse sequence of Figure 1 is reconstructed in the time domain.....	3
Figure 4. Inverse Fourier transform of spectrum 5 MHz off-tuned from f_0 showing two pulses in the time domain. Convolution bandwidth = 20 MHz. The rabbit ears effect is barely visible.	4
Figure 5. Inverse Fourier transform of spectrum 10 MHz off-tuned from f_0 showing two pulses in the time domain. Convolution bandwidth = 20 MHz. The rabbit ears effect is easily visible.	4
Figure 6. Inverse Fourier transform of spectrum 15 MHz off-tuned from f_0 showing two pulses in the time domain. Convolution bandwidth = 20 MHz. The rabbit ears troughs deepen as the off-tuned distance from f_0 increases.	5
Figure 7. Inverse Fourier transform of spectrum 20 MHz off-tuned from f_0 showing two pulses in the time domain. Convolution bandwidth = 20 MHz.	5
Figure 8. Radiated emission spectrum of a WR-100 (WSR-74C) weather radar, measured in an 8-MHz bandwidth. The transmitter used a magnetron oscillator as its final-stage output device. Pulse envelopes were measured at each of the frequencies labeled A-Z.....	7
Figure 9. Pulse envelope in an 8-MHz bandwidth, Point A ($\Delta f = -1500$ MHz) in the WR-100 spectrum. The red line shows the radar's pulse envelope at its fundamental frequency.....	7
Figure 10. Pulse envelope, Point B ($\Delta f = -1490$ MHz) in the WR-100 spectrum.	8
Figure 11. Pulse envelope, Point C ($\Delta f = -1430$ MHz) in the WR-100 spectrum.	8
Figure 12. Pulse envelope, Point D ($\Delta f = -1360$ MHz) in the WR-100 spectrum.....	9
Figure 13. Pulse envelope, Point E ($\Delta f = -1330$ MHz) in the WR-100 spectrum.	9
Figure 14. Pulse envelope, Point F ($\Delta f = -1250$ MHz) in the WR-100 spectrum.....	10
Figure 15. Pulse envelope, Point G ($\Delta f = -1150$ MHz) in the WR-100 spectrum.....	10

Figure 16. Pulse envelope, Point H ($\Delta f = -1000$ MHz) in the WR-100 spectrum.	11
Figure 17. Classical rabbit ears, Point I ($\Delta f = -850$ MHz) in the WR-100 spectrum.	11
Figure 18. Pulse envelope, Point J ($\Delta f = -670$ MHz) in the WR-100 spectrum.	12
Figure 19. Pulse envelope, Point K ($\Delta f = -550$ MHz) in the WR-100 spectrum.	12
Figure 20. Pulse envelope, Point L ($\Delta f = -490$ MHz) in the WR-100 spectrum.	13
Figure 21. Pulse envelope, Point M ($\Delta f = -300$ MHz) in the WR-100 spectrum.	13
Figure 22. Pulse envelope, Point N ($\Delta f = -160$ MHz) in the WR-100 spectrum.	14
Figure 23. Pulse envelope, Point P ($\Delta f = -100$ MHz) in the WR-100 spectrum.	14
Figure 24. Pulse envelope, Point Q (f_0) in the WR-100 spectrum.	15
Figure 25. Pulse envelope, Point R ($\Delta f = +150$ MHz) in the WR-100 spectrum.	15
Figure 26. Pulse envelope, Point S ($\Delta f = +490$ MHz) in the WR-100 spectrum.	16
Figure 27. Pulse envelope, Point T ($\Delta f = +650$ MHz) in the WR-100 spectrum.	16
Figure 28. Pulse envelope, Point U ($\Delta f = +730$ MHz) in the WR-100 spectrum.	17
Figure 29. Pulse envelope, Point V ($\Delta f = +900$ MHz) in the WR-100 spectrum.	17
Figure 30. Pulse envelope, Point W ($\Delta f = +1040$ MHz) in the WR-100 spectrum.	18
Figure 31. Pulse envelope, Point X ($\Delta f = +1250$ MHz) in the WR-100 spectrum.	18
Figure 32. Pulse envelope, Point Y ($\Delta f = +1350$ MHz) in the WR-100 spectrum.	19
Figure 33. Pulse envelope, Point Z ($\Delta f = +1430$ MHz) in the WR-100 spectrum.	19
Figure 34. TDWR spectrum formed with Channel A (analog) pulse modulator. Off-fundamental pulse envelopes were measured every 10 MHz as indicated.	20
Figure 35. TDWR spectrum formed with Channel B (digital) pulse modulator. Off-fundamental pulse envelopes were measured every 10 MHz as indicated.	20
Figure 36. Pulse envelope, Point A ($\Delta f = -100$ MHz) in the TDWR Channel A spectrum. The red curve is a graphical aid showing the pulse envelope at f_0	21
Figure 37. Pulse envelope, Point B ($\Delta f = -90$ MHz) in the TDWR Channel A spectrum.	21

Figure 38. Pulse envelope, Point C ($\Delta f = -80$ MHz) in the TDWR Channel A spectrum.....	22
Figure 39. Pulse envelope, Point D ($\Delta f = -70$ MHz) in the TDWR Channel A spectrum.....	22
Figure 40. Pulse envelope, Point E ($\Delta f = -60$ MHz) in the TDWR Channel A spectrum.....	23
Figure 41. Pulse envelope, Point F ($\Delta f = -50$ MHz) in the TDWR Channel A spectrum.....	23
Figure 42. Pulse envelope, Point G ($\Delta f = -40$ MHz) in the TDWR Channel A spectrum.....	24
Figure 43. Pulse envelope, Point H ($\Delta f = -30$ MHz) in the TDWR Channel A spectrum.....	24
Figure 44. Pulse envelope, Point I ($\Delta f = -20$ MHz) in the TDWR Channel A spectrum.....	25
Figure 45. Pulse envelope, Point J ($\Delta f = -10$ MHz) in the TDWR Channel A spectrum.....	25
Figure 46. Pulse envelope, Point K (f_0) in the TDWR Channel A spectrum.....	26
Figure 47. Pulse envelope, Point L ($\Delta f = +10$ MHz) in the TDWR Channel A spectrum.....	26
Figure 48. Pulse envelope, Point M ($\Delta f = +20$ MHz) in the TDWR Channel A spectrum.....	27
Figure 49. Pulse envelope, Point N ($\Delta f = +30$ MHz) in the TDWR Channel A spectrum.....	27
Figure 50. Pulse envelope, Point P ($\Delta f = +40$ MHz) in the TDWR Channel A spectrum.....	28
Figure 51. Pulse envelope, Point Q ($\Delta f = +50$ MHz) in the TDWR Channel A spectrum.....	28
Figure 52. Pulse envelope, Point R ($\Delta f = +60$ MHz) in the TDWR Channel A spectrum.....	29
Figure 53. Pulse envelope, Point S ($\Delta f = +70$ MHz) in the TDWR Channel A spectrum.....	29

Figure 54. Pulse envelope, Point T ($\Delta f = +80$ MHz) in the TDWR Channel A spectrum.....	30
Figure 55. Pulse envelope, Point U ($\Delta f = +90$ MHz) in the TDWR Channel A spectrum.....	30
Figure 56. Pulse envelope, Point V ($\Delta f = +100$ MHz) in the TDWR Channel A spectrum.....	31
Figure 57. Pulse envelope, Point A ($\Delta f = -100$ MHz) in the TDWR Channel B spectrum.....	31
Figure 58. Pulse envelope, Point B ($\Delta f = -90$ MHz) in the TDWR Channel B spectrum.....	32
Figure 59. Pulse envelope, Point C ($\Delta f = -80$ MHz) in the TDWR Channel B spectrum.....	32
Figure 60. Pulse envelope, Point D ($\Delta f = -70$ MHz) in the TDWR Channel B spectrum.....	33
Figure 61. Pulse envelope, Point E ($\Delta f = -60$ MHz) in the TDWR Channel B spectrum.....	33
Figure 62. Pulse envelope, Point F ($\Delta f = -50$ MHz) in the TDWR Channel B spectrum.....	34
Figure 63. Pulse envelope, Point G ($\Delta f = -40$ MHz) in the TDWR Channel B spectrum.....	34
Figure 64. Pulse envelope, Point H ($\Delta f = -30$ MHz) in the TDWR Channel B spectrum.....	35
Figure 65. Pulse envelope, Point I ($\Delta f = -20$ MHz) in the TDWR Channel B spectrum.....	35
Figure 66. Classic rabbit ears pulse envelope, Point J ($\Delta f = -10$ MHz) in the TDWR Channel B spectrum.....	36
Figure 67. Pulse envelope, Point K (f_0) in the TDWR Channel B spectrum.....	36
Figure 68. Classic rabbit ears pulse envelope, Point L ($\Delta f = +10$ MHz) in the TDWR Channel B spectrum.....	37
Figure 69. Pulse envelope, Point M ($\Delta f = +20$ MHz) in the TDWR Channel B spectrum.....	37

Figure 70. Pulse envelope, Point N ($\Delta f = +30$ MHz) in the TDWR Channel B spectrum.....	38
Figure 71. Pulse envelope, Point P ($\Delta f = +40$ MHz) in the TDWR Channel B spectrum.....	38
Figure 72. Pulse envelope, Point Q ($\Delta f = +50$ MHz) in the TDWR Channel B spectrum.....	39
Figure 73. Pulse envelope, Point R ($\Delta f = +60$ MHz) in the TDWR Channel B spectrum.....	39
Figure 74. Pulse envelope, Point S ($\Delta f = +70$ MHz) in the TDWR Channel B spectrum.....	40
Figure 75. Pulse envelope, Point T ($\Delta f = +80$ MHz) in the TDWR Channel B spectrum.....	40
Figure 76. Pulse envelope, Point U ($\Delta f = +90$ MHz) in the TDWR Channel B spectrum.....	41
Figure 77. Pulse envelope, Point V ($\Delta f = +100$ MHz) in the TDWR Channel B spectrum.....	41
Figure 78. SA display of rabbit ears when SA tuned frequency was 10 MHz below the center of 20 MHz wide chirped-pulse carrier. SA settings were as shown in Table 1, with RBW = 8 MHz.	46
Figure 79. SA display of rabbit ears when SA tuned frequency was 10 MHz above the center of the 20 MHz wide chirped-pulse carrier. Pulse duration of 60 μ s is observed between the rabbit ears in both Figures 78 and 79.	46
Figure 80. SA display when tuned to the center of the chirped-pulse FM range. Calculation of pulse duration and FM range is shown in notes in red.....	47

TABLES

Table 1. SA settings for chirped-pulse parameter measurements.....	45
--	----

ABBREVIATIONS/ACRONYMS

DFS	dynamic frequency selection
FAA	Federal Aviation Administration
FM	frequency modulation
IF	intermediate frequency
ITS	Institute for Telecommunication Sciences (NTIA)
LFM	linear frequency modulation
NEXRAD	Next Generation Weather Radar (WSR-88D)
NLFM	non-linear frequency modulation
NTIA	National Telecommunications and Information Administration
NWS	National Weather Service
OOB	out of band (radio emissions)
PRI	pulse repetition interval
RBW	resolution bandwidth
RF	radio frequency
SA	spectrum analyzer
TDWR	Terminal Doppler Weather Radar (FAA equivalent of the NEXRAD)
VBW	video bandwidth
VSA	vector signal analyzer
VSG	vector signal generator
WR-100	civilian weather radar equivalent to the WSR-74C
WSR-74C	NWS weather radar now supplanted by the WSR-88D (NEXRAD)
WSR-88D	NEXRAD weather surveillance radar, accepted 1988, Doppler-capable

THE RABBIT EARS PULSE-ENVELOPE PHENOMENON IN OFF-FUNDAMENTAL DETECTION OF PULSED SIGNALS

Frank H. Sanders¹

When radiofrequency pulse envelopes are observed away from their fundamental frequency their shapes differ from those at their fundamental frequency. Off-fundamental pulse envelopes tend to exhibit spikes at their rising and falling edges with lower-amplitude energy between the spikes. This phenomenon, called the rabbit ears effect, is described in this NTIA Report. Examples of rabbit ears pulse envelopes are provided in a mathematical simulation and from measurements of off-fundamental pulse envelopes of two models of 5 GHz weather radars. Morphologies of rabbit ears pulses are examined. A method is provided for using this effect to determine the durations and bandwidths of chirped pulses in bandwidth-limited measurement systems. Implications for off-fundamental detection of pulsed signals for dynamic frequency selection (DFS) algorithms are considered.

Key words: chirped pulses; dynamic frequency selection (DFS); off-fundamental signal detection; pulsed radiofrequency (RF) signals; rabbit ears; radar spectrum

1 MATHEMATICAL DEMONSTRATION OF THE RABBIT EARS EFFECT

1.1 Time-Domain Envelopes of Spectrum Power Measured Across the Central Spectrum Lobe

When an energy source is pulsed on and off in the time domain, its emitted energy is spread across a non-zero portion of the radio frequency (RF) domain. When the pulses are generated at a fundamental oscillation frequency, f_0 , the resulting spectrum is distributed across the spectrum at frequencies above and below f_0 . The Fourier transform and inverse Fourier transform connect the time-domain and frequency-domain behaviors of the pulsed energy. An example of a set of theoretically generated time-domain oscillatory-energy pulses and their corresponding theoretical power spectrum is shown in Figures 1 and 2.

As shown in Figure 2, the pulsed-energy power spectrum consists of a set of emission lines spaced at intervals of $(1/PRI)$, where PRI = time-domain pulse repetition interval. The power levels of those individual frequency-domain lines formed as a series of lobes that follow a classical $(\sin(x)/x)^2$ envelope, where x is the separation between any given frequency and f_0 . The null-to-null width of the central lobe is $(2/\tau_{pulse})$ and all other spectrum lobes have a width of $(1/\tau_{pulse})$, where τ_{pulse} is the time-domain pulse width (Figure 2).

¹ The author is with the Institute for Telecommunication Sciences, National Telecommunications and Information Administration, U.S. Department of Commerce, Boulder, Colorado 80305.

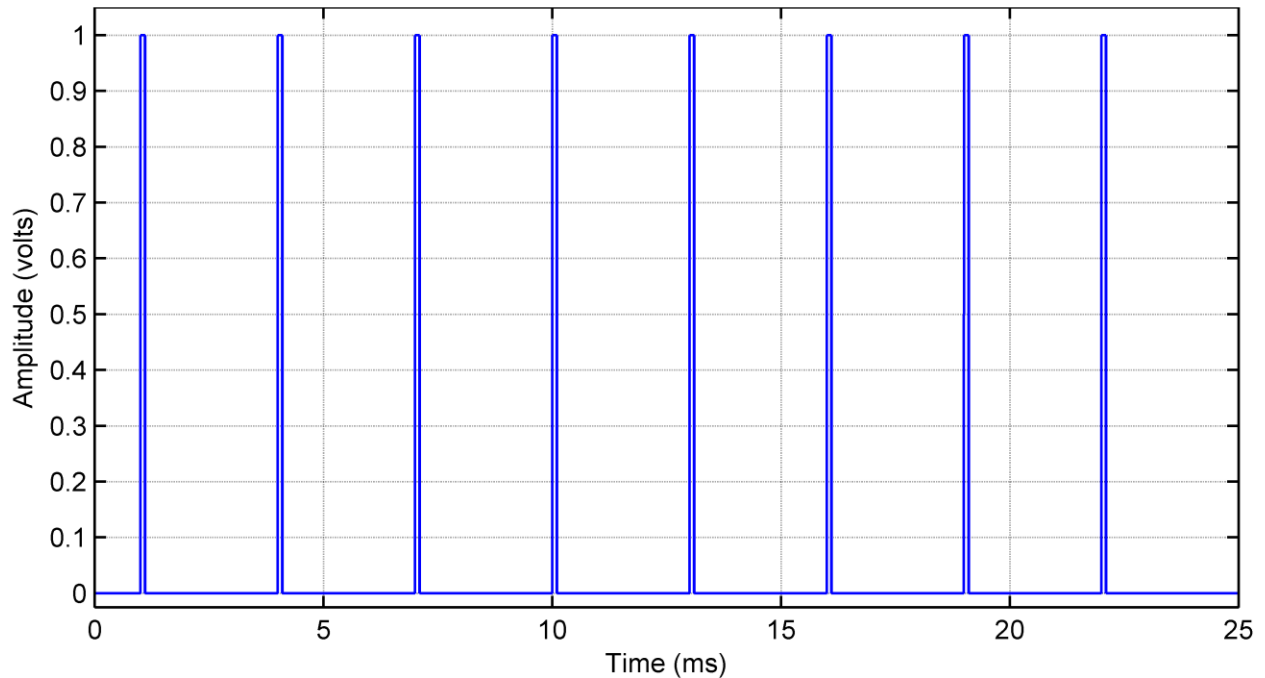


Figure 1. Time-domain view of a sequence of simulated RF pulses. In this simulation the parameters are $f_0 = 10$ MHz, $\tau_{pulse} = 100$ μ s, $PRI = 3$ ms.

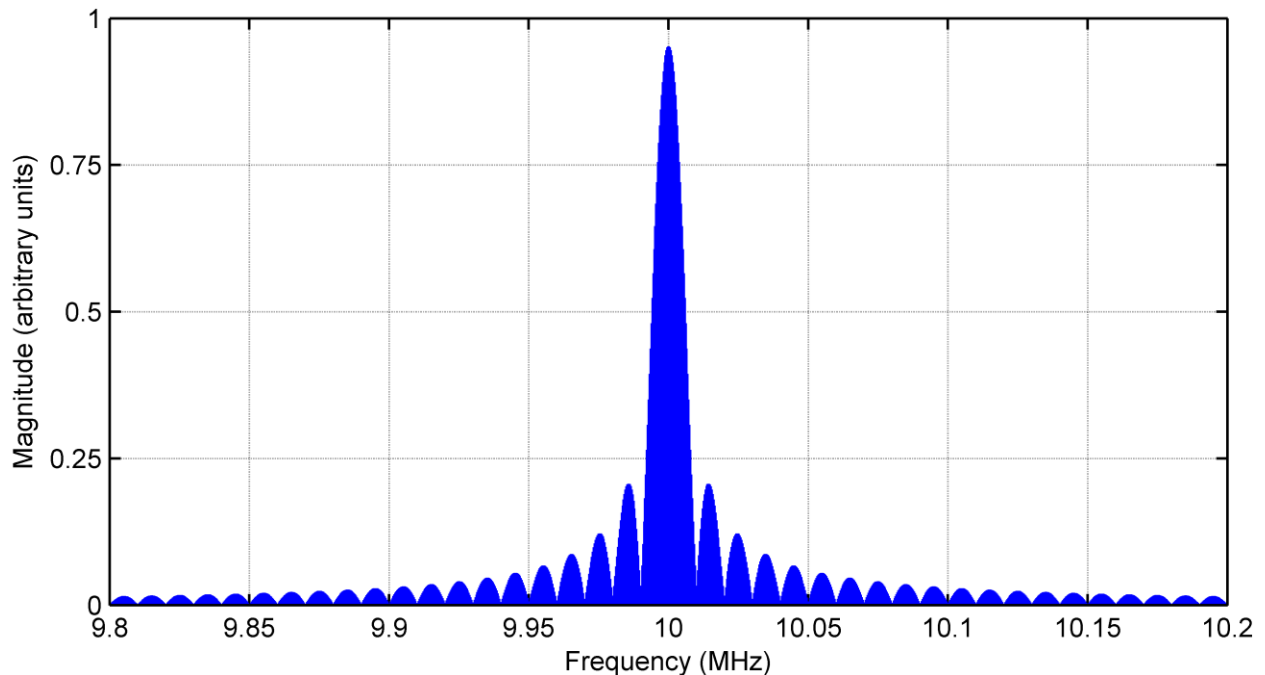


Figure 2. Fourier transform of the pulse sequence of Figure 1. A classic sinc^2 power spectrum is generated. Power is plotted linearly.

Suppose that a transmitter generates pulsed radio frequency energy at frequency f_0 . If a spectrum measurement system collects energy from that transmitter through a bandwidth window that convolves the lines in the central spectrum lobe around f_0 , and if the measurement system output is fed to a time-domain visualization device such as a crystal detector and an oscilloscope, then

the device's display will show pulsed envelopes that are a close approximation of the transmitter's pulse-envelope modulation. This effect is demonstrated in the mathematical simulation of Figure 3, which is an inverse Fourier transform of the spectrum of Figure 2.

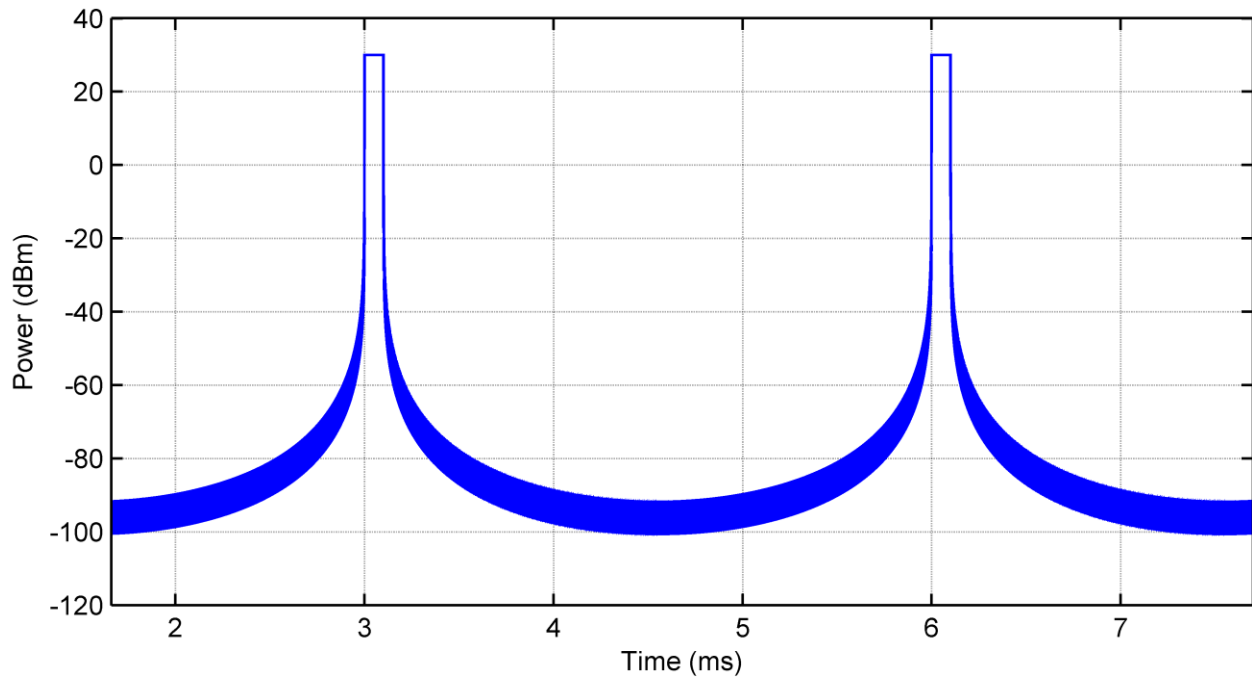


Figure 3. Inverse Fourier transform of the spectrum of Figure 2, from 0 MHz to 20 MHz. The original pulse sequence of Figure 1 is reconstructed in the time domain.

1.2 Time-Domain Envelopes of Spectrum Power *Not* Measured Across the Central Spectrum Lobe

If the convolution bandwidth of a measurement system integrates energy across frequencies that are *exclusive* of the lines in the central spectrum lobe, and the collected energy is again fed to a time-domain display, then the loss of the energy in the central-lobe lines causes a change in the shapes of the detected time-domain pulse envelopes. As shown in the inverse Fourier transforms of Figures 4–7, under this circumstance there is a tendency for the centers of the pulses to be reduced in power; center-pulse energy goes missing. Relatively high levels of energy remain in the rising and falling edges of the pulses. As a result, off-fundamental pulse envelopes tend to be pairs of spikes separated by the transmitted pulse width, τ_{pulse} , with relatively low power levels observed in the center of each pulse. This visual signature is called the rabbit ears effect due to its putative resemblance to a long-eared lagomorph seen face-on. *The pulse-to-pulse PRI is unaffected by this phenomenon* (as demonstrated in Figures 4–7).

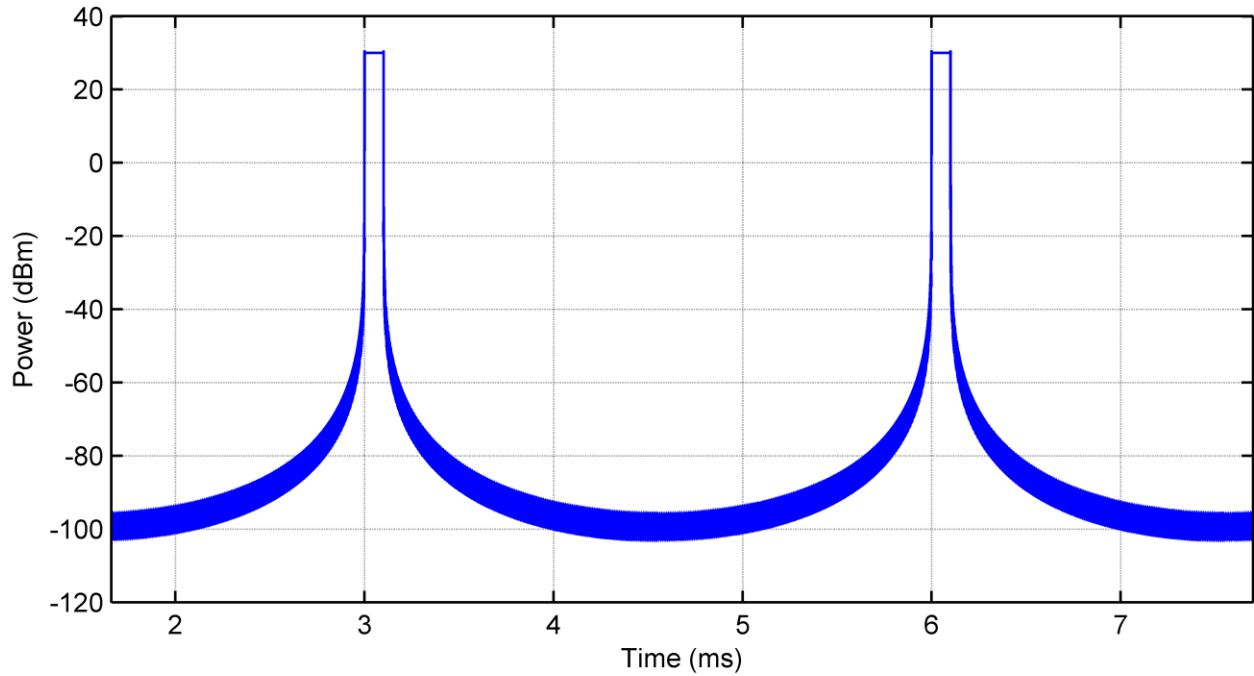


Figure 4. Inverse Fourier transform of spectrum 5 MHz off-tuned from f_0 showing two pulses in the time domain. Convolution bandwidth = 20 MHz. The rabbit ears effect is barely visible.

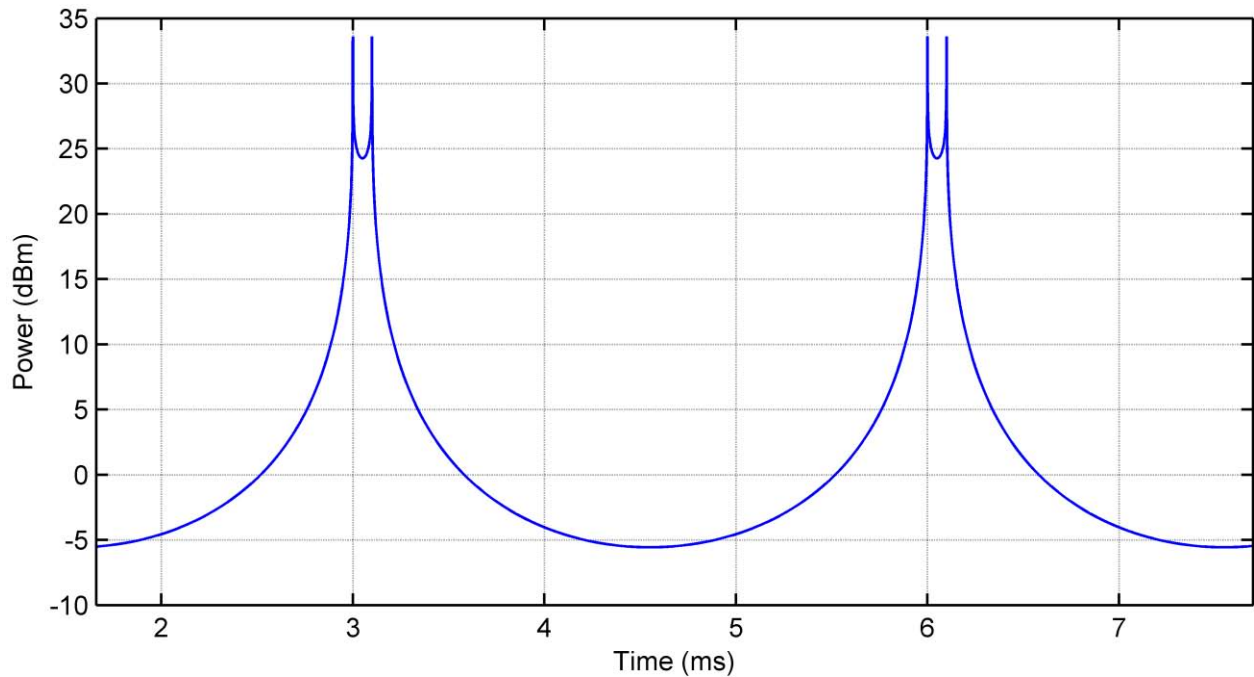


Figure 5. Inverse Fourier transform of spectrum 10 MHz off-tuned from f_0 showing two pulses in the time domain. Convolution bandwidth = 20 MHz. The rabbit ears effect is easily visible.

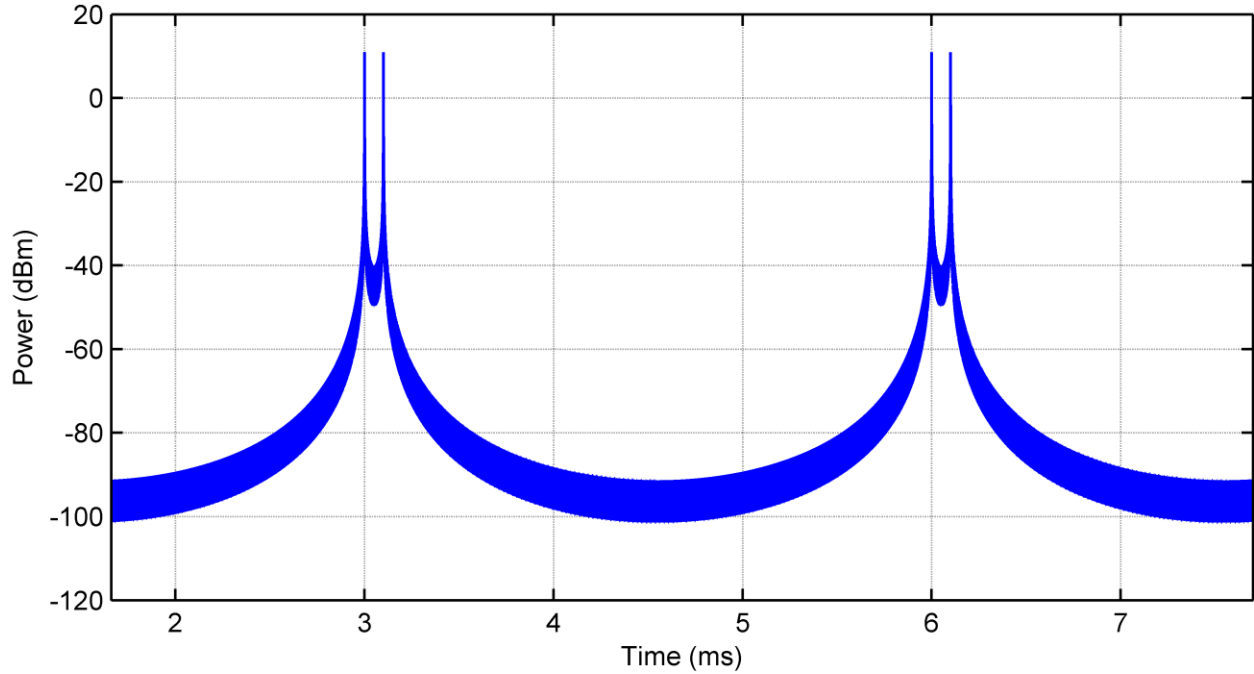


Figure 6. Inverse Fourier transform of spectrum 15 MHz off-tuned from f_0 showing two pulses in the time domain. Convolution bandwidth = 20 MHz. The rabbit ears troughs deepen as the off-tuned distance from f_0 increases.

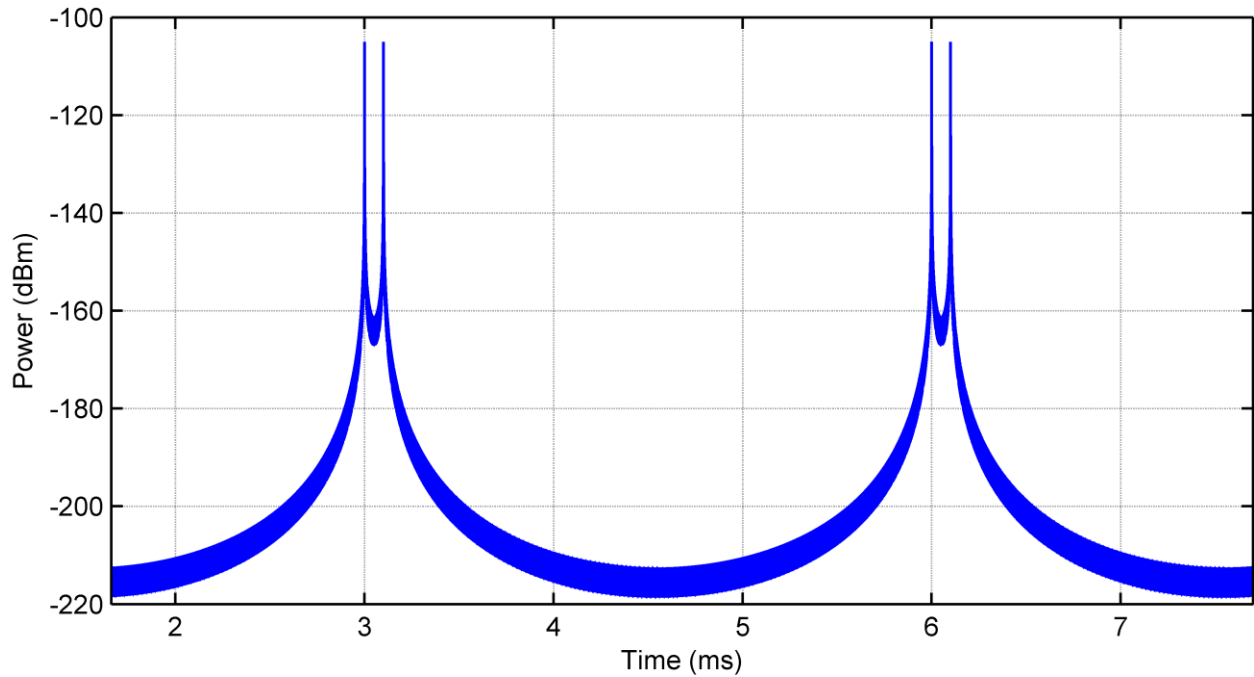


Figure 7. Inverse Fourier transform of spectrum 20 MHz off-tuned from f_0 showing two pulses in the time domain. Convolution bandwidth = 20 MHz.

2 MEASURED RABBIT EARS PULSES IN RADAR EMISSION SPECTRA

2.1 Real-World Pulse Envelope Characteristics

Although the rabbit ears effect can be demonstrated mathematically as in Figures 4–7 the simulation is a highly simplified representation of the emissions of actual radio transmitters. Real-world RF pulse envelopes, as generated for example by radar transmitters, are more complexly shaped. They do not have rectangular envelopes, their rising and falling edges have non-zero lengths and are not entirely smooth, and they usually exhibit some transient features. The transitions between pulse centers and their rising and falling edges are complexly shaped and sometimes exhibit transient features. The pulse centers are neither completely smooth nor flat. The falling edges of real pulses are usually longer than the rising edges and thus the pulse envelopes are unsymmetrical in the time domain. All of these complexities of real pulse envelopes result from inherent and unavoidable behaviors of radio transmitters' baseband pulse-forming networks and final-stage RF amplifiers.

2.2 Expectations for Real-World Rabbit Ears Characteristics

Complexities in the time-domain envelopes of transmitted pulses translate into complexities in the emission spectra of transmitters, causing those spectra to deviate from the ideal sinc^2 shape shown in Figure 2. If the off-fundamental emission lines of real-world spectra are convolved by measurement systems while the center-lobe lines of the spectra are excluded, then rabbit ears envelopes will be observed in the time domain outputs of such measurement systems. Qualitatively these real-world rabbit ears envelopes will resemble the idealized representations of Figures 4–7. But the non-ideal characteristics of real-world pulses and their emission spectra mean that real-world rabbit ears can be expected to deviate from idealized rabbit ears in many of their details.

2.3 Rabbit Ears Pulse Envelopes Across a Real-World 5 GHz Radar Spectrum

The author has measured and recorded rabbit ears pulse envelopes at frequencies between 4 to 7 GHz across the emission spectrum of a 5 GHz weather radar. The measured emission spectrum of this WR-100 radar, a civilian version of the WSR-74C,² is shown in Figure 8. The spectrum was measured in an 8 MHz bandwidth. This bandwidth, wider than recommended in [1], exaggerates the amplitudes of the radar's out-of-band (OOB) and spurious emission levels relative to the power at the fundamental. That bandwidth was used to collect time-domain measurements of pulse envelopes at each of the frequencies indicated by letters A-Z in Figure 8. The spectrum of Figure 8 and the pulse envelopes of Figures 9–33 were all measured via radiated energy from the radar. Aside from the wide bandwidth, the spectrum was measured in accordance with the guidelines in [1], including the stepped-frequency algorithm described in that document. The pulse envelopes were measured with a crystal detector and digital oscilloscope connected to the output of the wideband video output of the measurement system. The center-frequency pulse shape of the radar is superimposed in red on each of the measured rabbit ears envelopes as a visualization aid.

² WSR-74C radars were once used by the United States National Weather Service but have been superseded by WSR-88D NEXRAD radars.

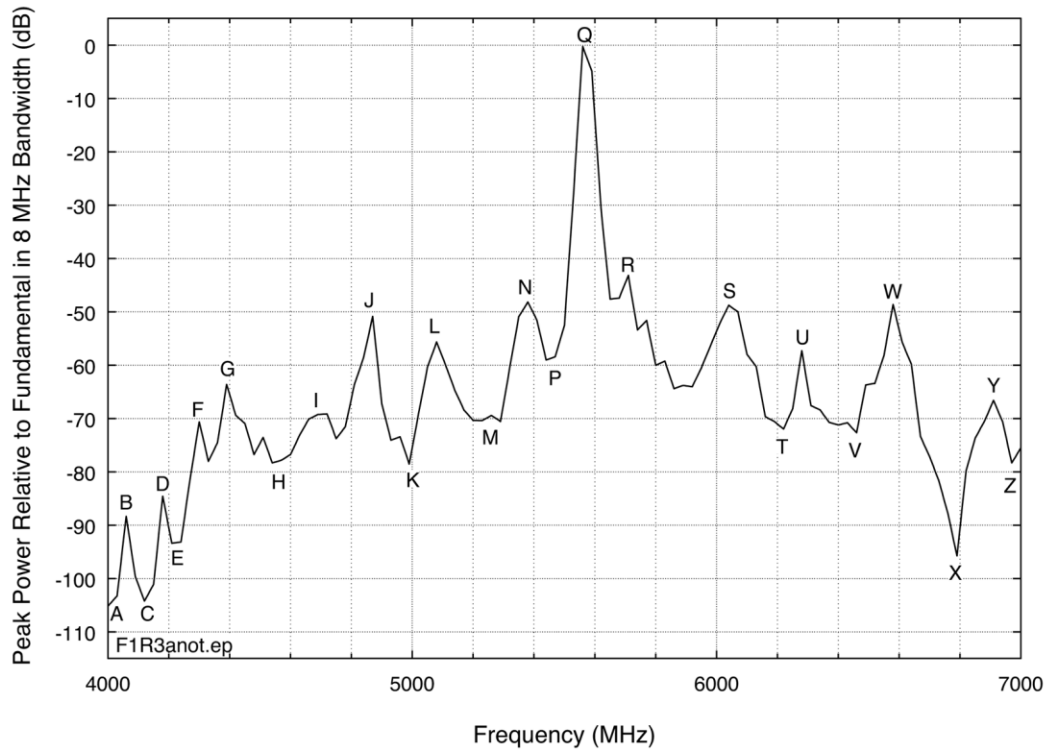


Figure 8. Radiated emission spectrum of a WR-100 (WSR-74C) weather radar, measured in an 8-MHz bandwidth. The transmitter used a magnetron oscillator as its final-stage output device. Pulse envelopes were measured at each of the frequencies labeled A-Z.

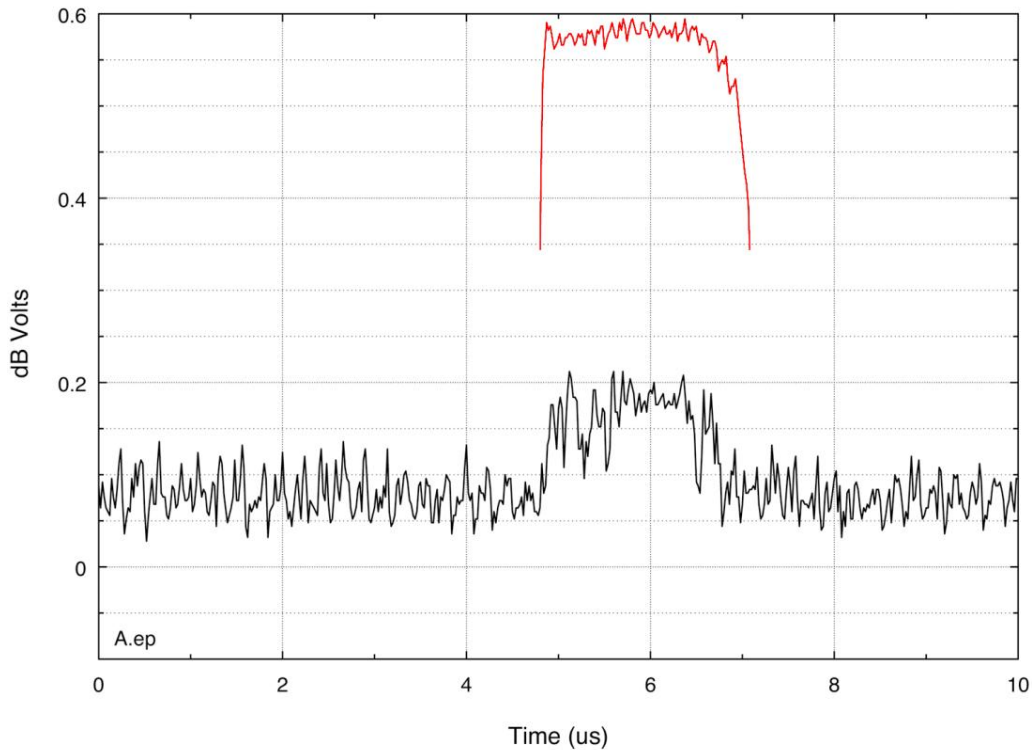


Figure 9. Pulse envelope in an 8-MHz bandwidth, Point A ($\Delta f = -1500$ MHz) in the WR-100 spectrum. The red line shows the radar's pulse envelope at its fundamental frequency.

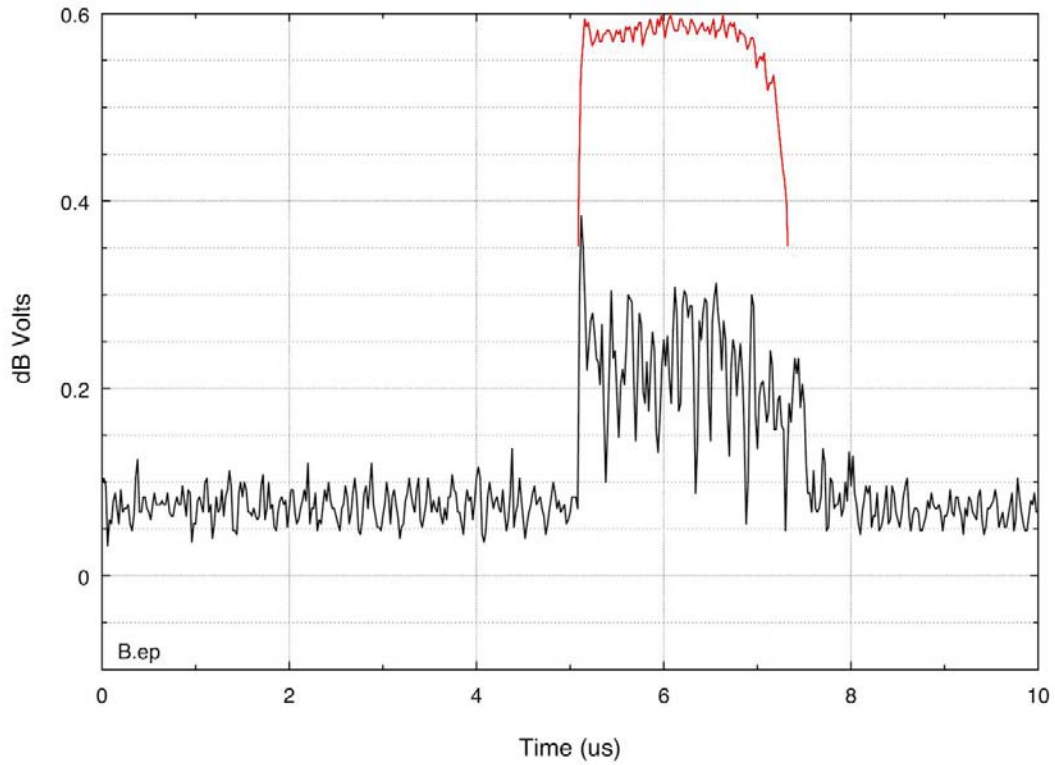


Figure 10. Pulse envelope, Point B ($\Delta f = -1490$ MHz) in the WR-100 spectrum.

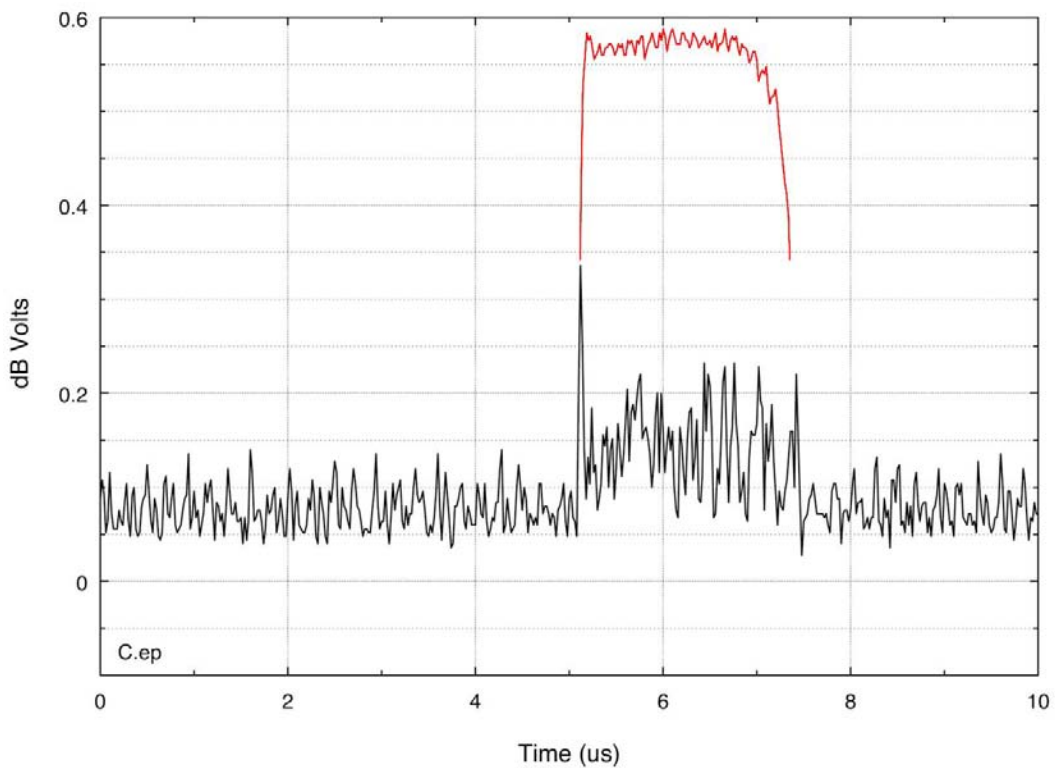


Figure 11. Pulse envelope, Point C ($\Delta f = -1430$ MHz) in the WR-100 spectrum.

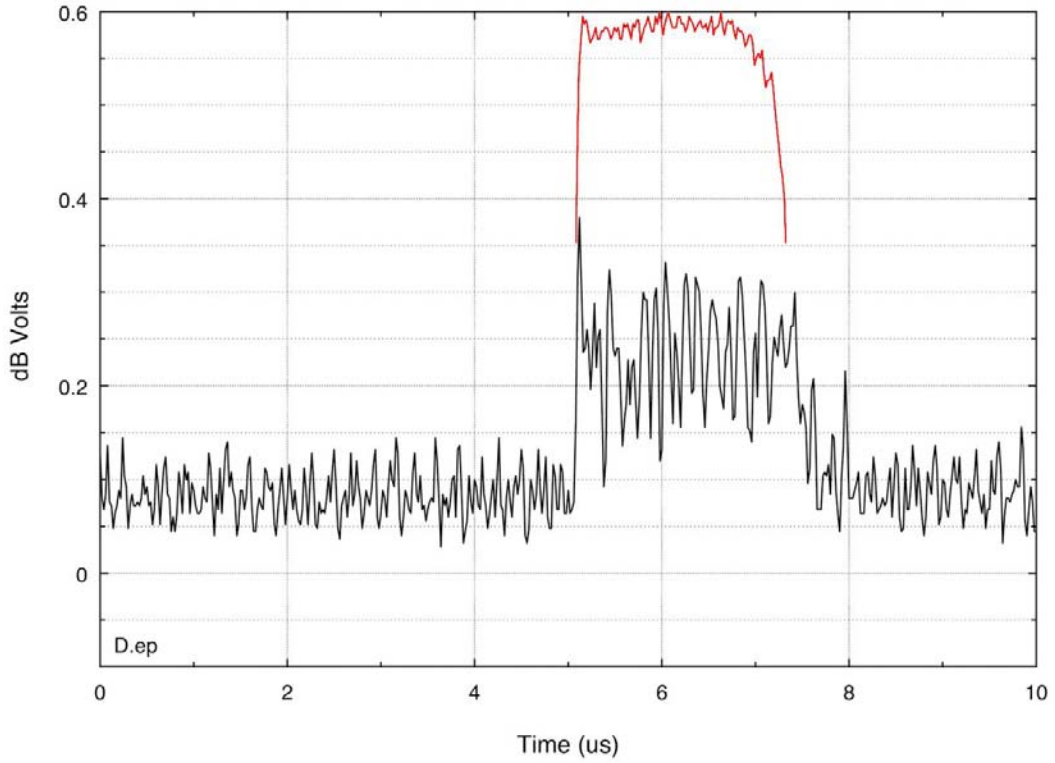


Figure 12. Pulse envelope, Point D ($\Delta f = -1360$ MHz) in the WR-100 spectrum.

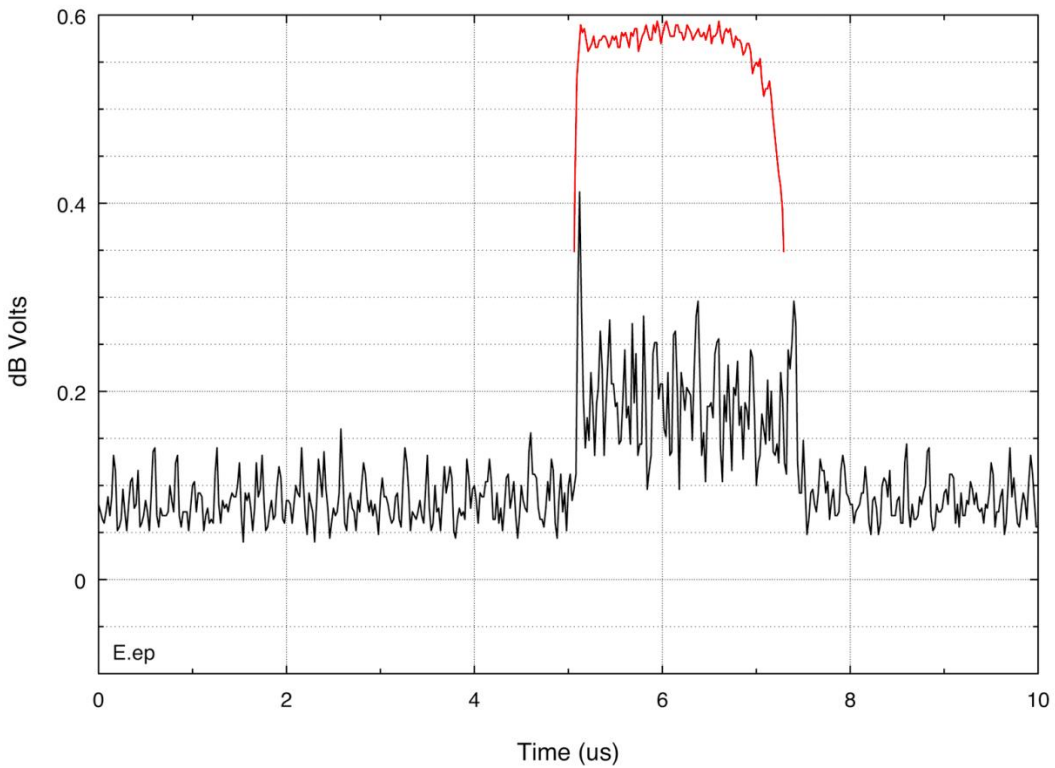


Figure 13. Pulse envelope, Point E ($\Delta f = -1330$ MHz) in the WR-100 spectrum.

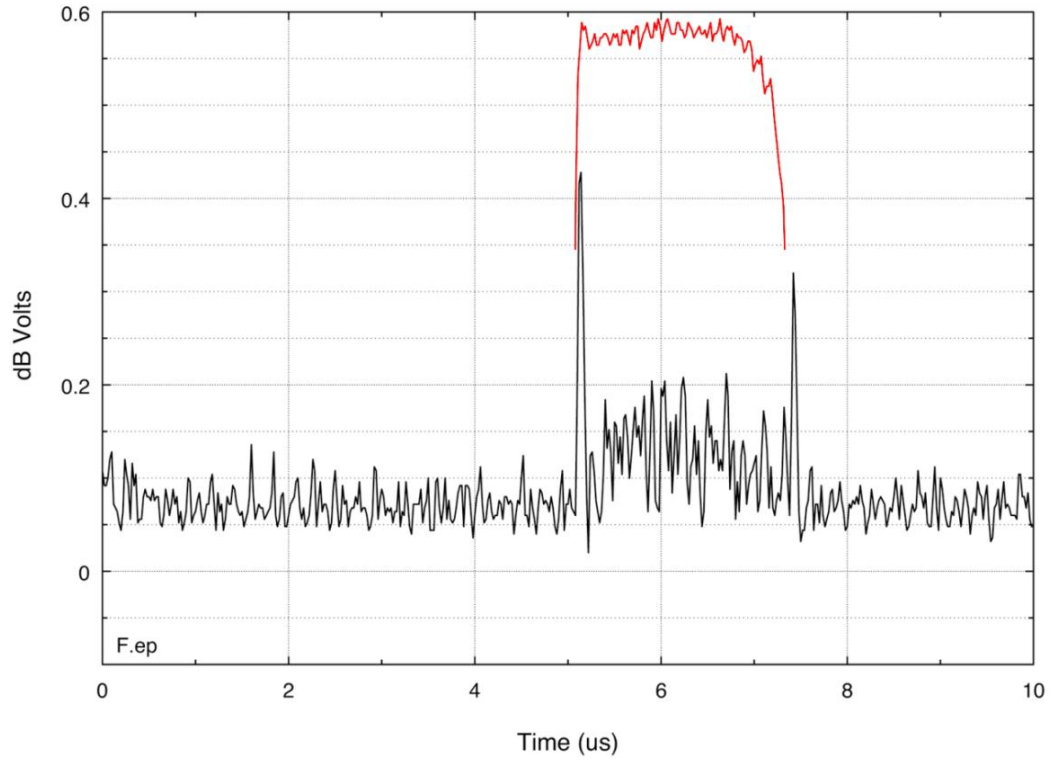


Figure 14. Pulse envelope, Point F ($\Delta f = -1250$ MHz) in the WR-100 spectrum.

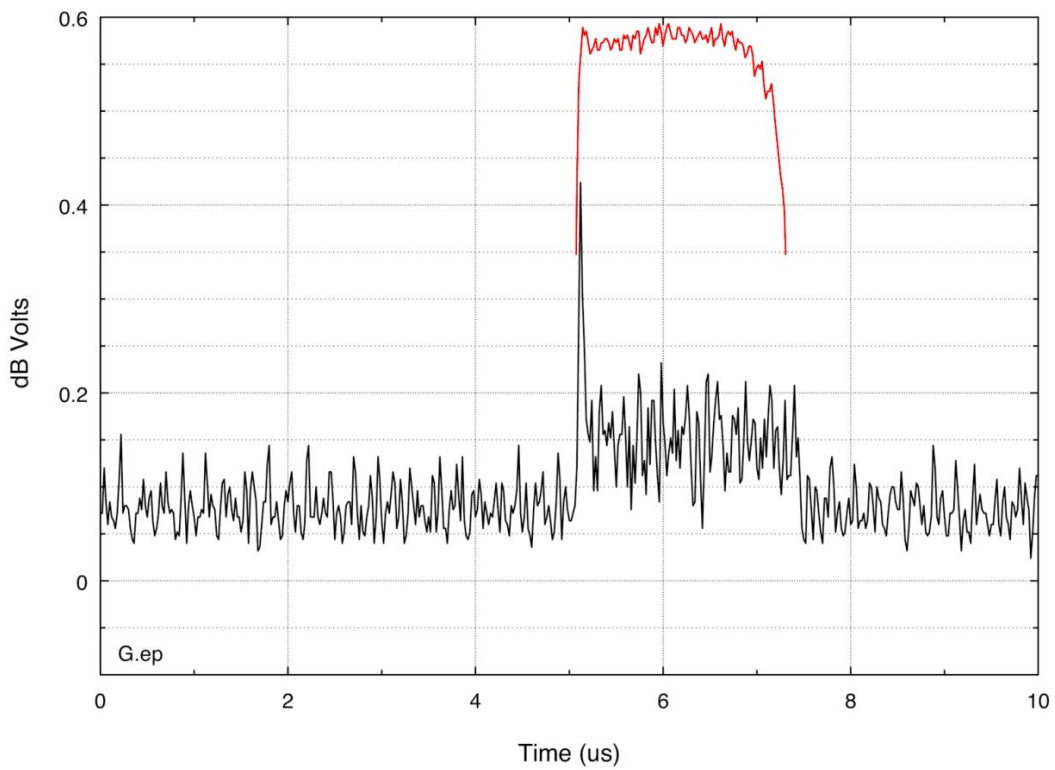


Figure 15. Pulse envelope, Point G ($\Delta f = -1150$ MHz) in the WR-100 spectrum.

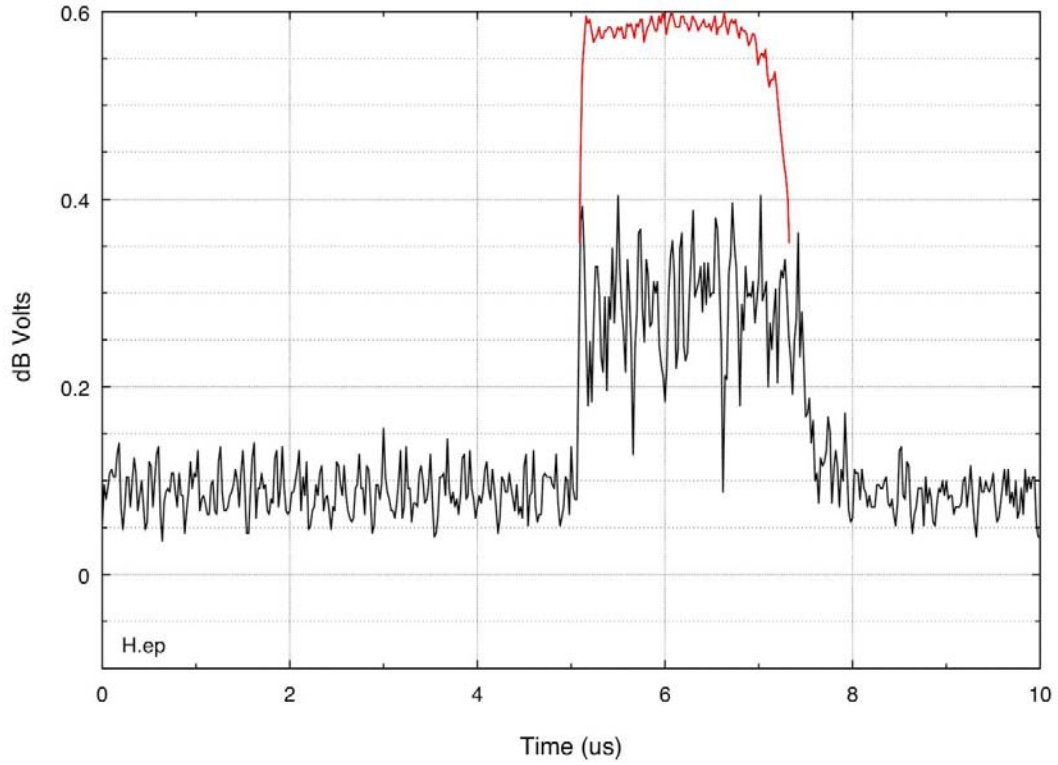


Figure 16. Pulse envelope, Point H ($\Delta f = -1000$ MHz) in the WR-100 spectrum.

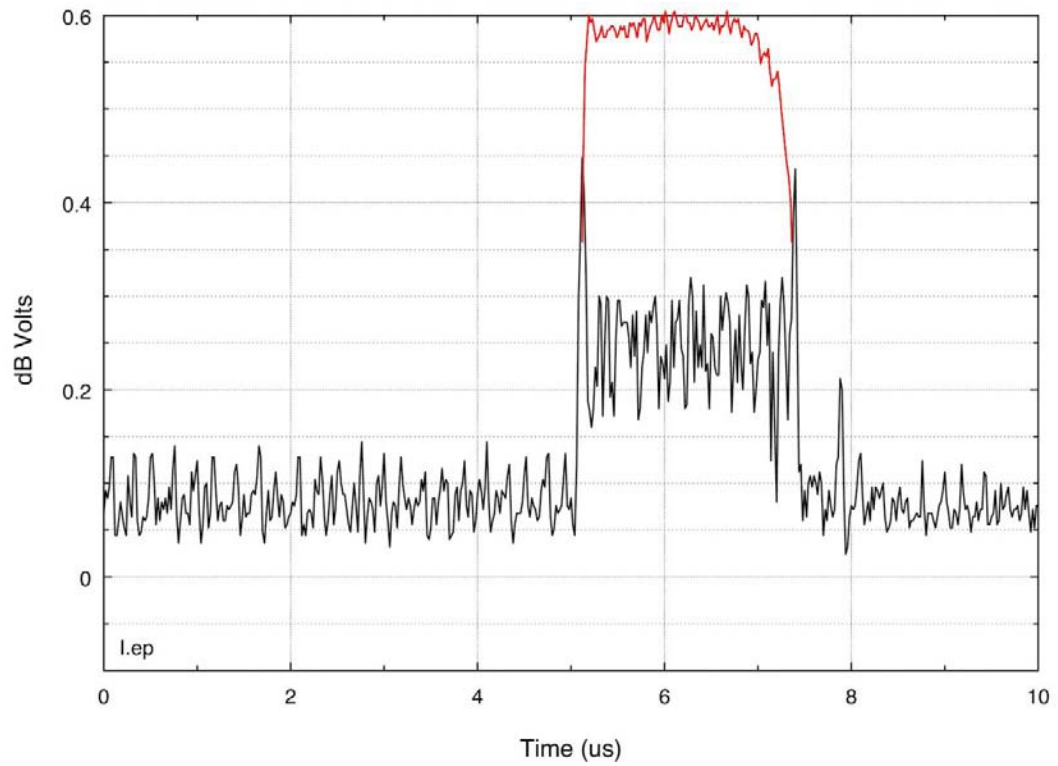


Figure 17. Classical rabbit ears, Point I ($\Delta f = -850$ MHz) in the WR-100 spectrum.

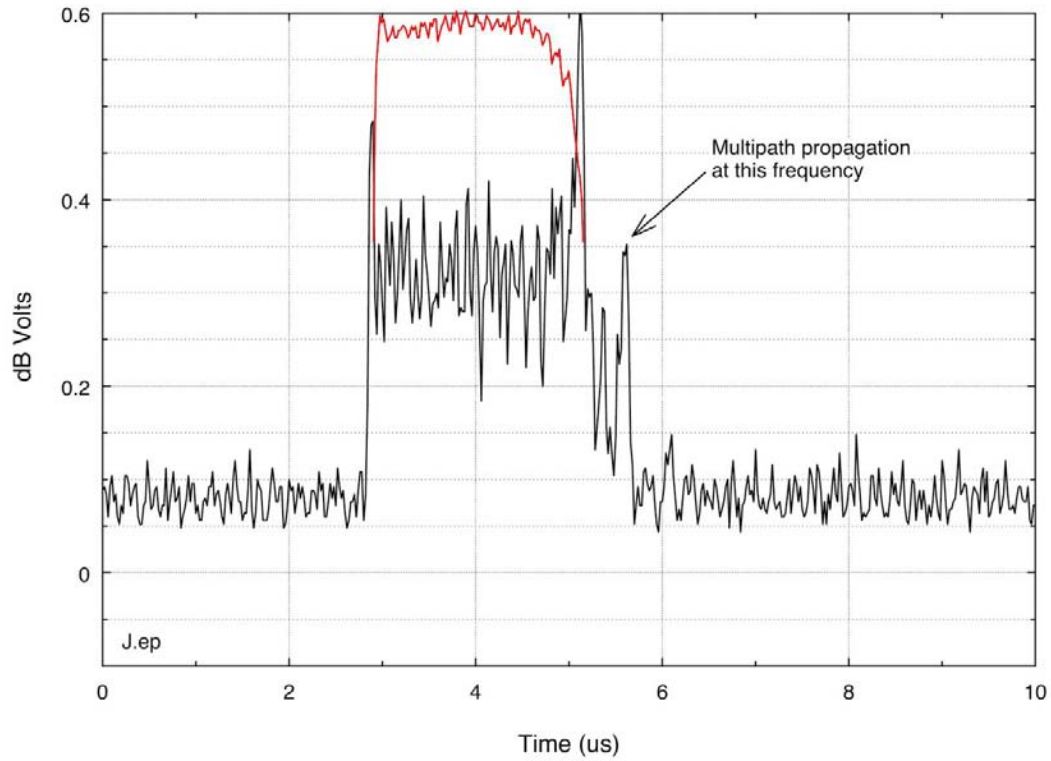


Figure 18. Pulse envelope, Point J ($\Delta f = -670$ MHz) in the WR-100 spectrum.

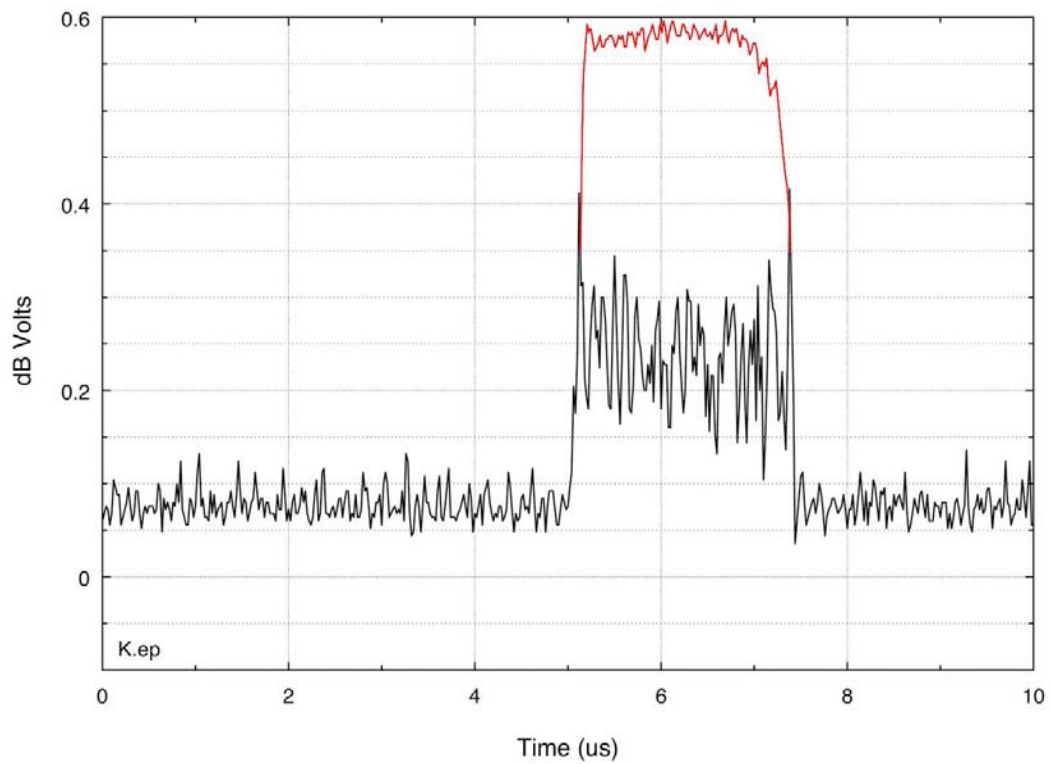


Figure 19. Pulse envelope, Point K ($\Delta f = -550$ MHz) in the WR-100 spectrum.

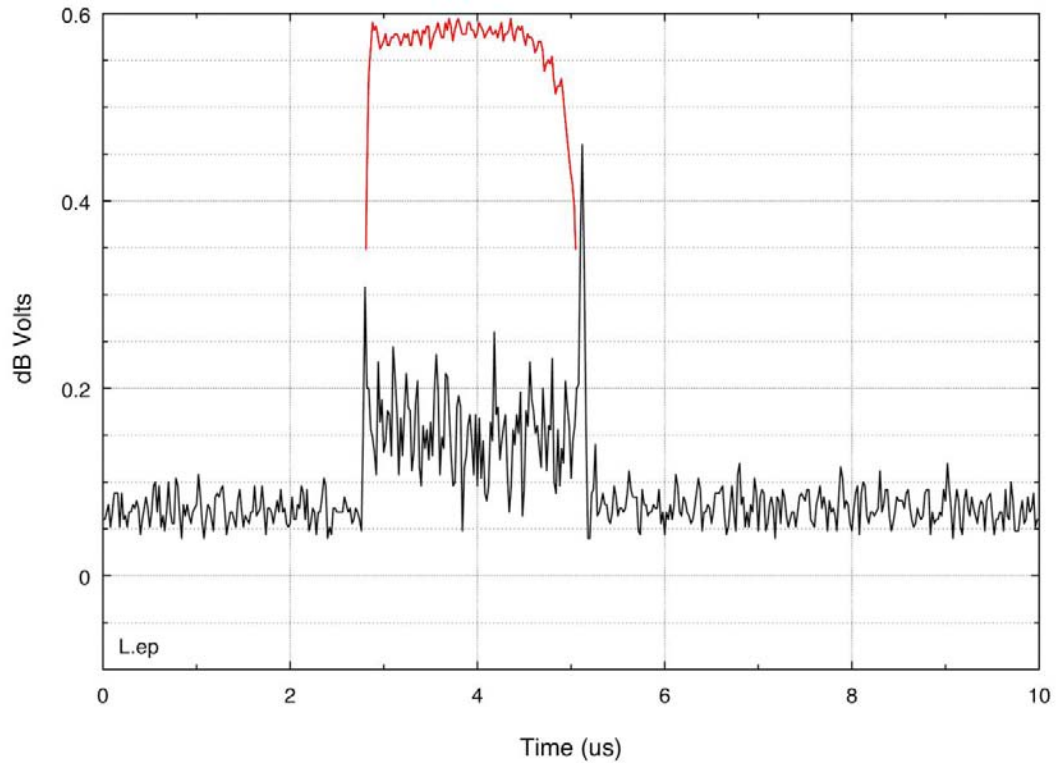


Figure 20. Pulse envelope, Point L ($\Delta f = -490$ MHz) in the WR-100 spectrum.

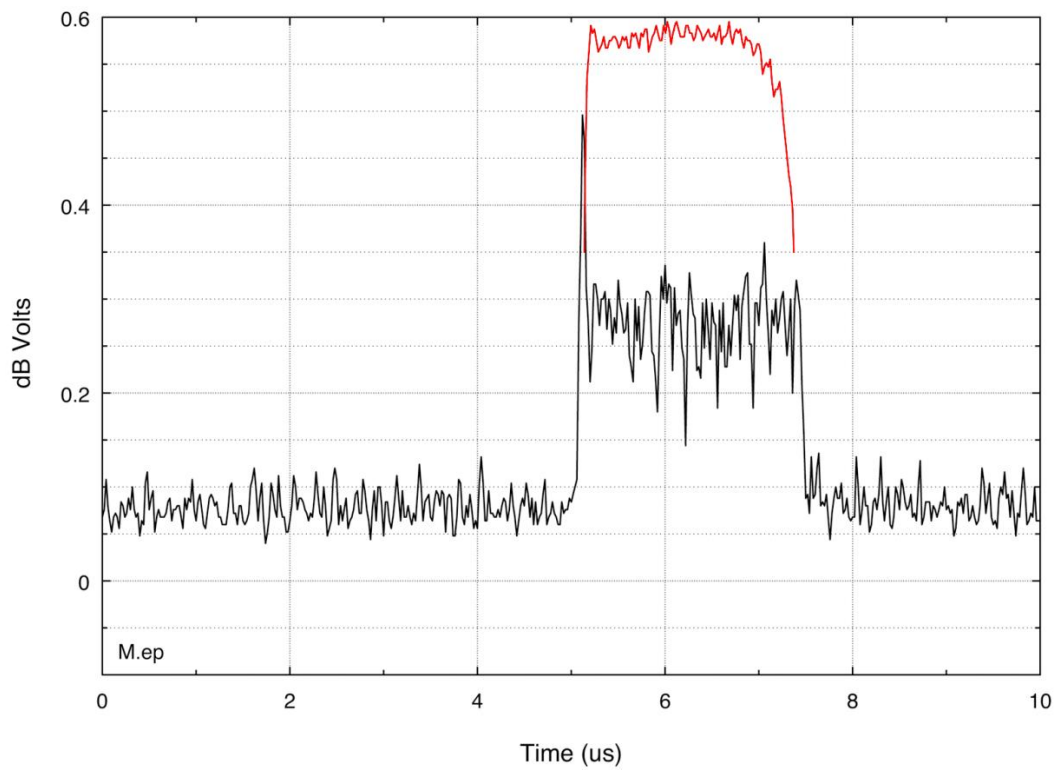


Figure 21. Pulse envelope, Point M ($\Delta f = -300$ MHz) in the WR-100 spectrum.

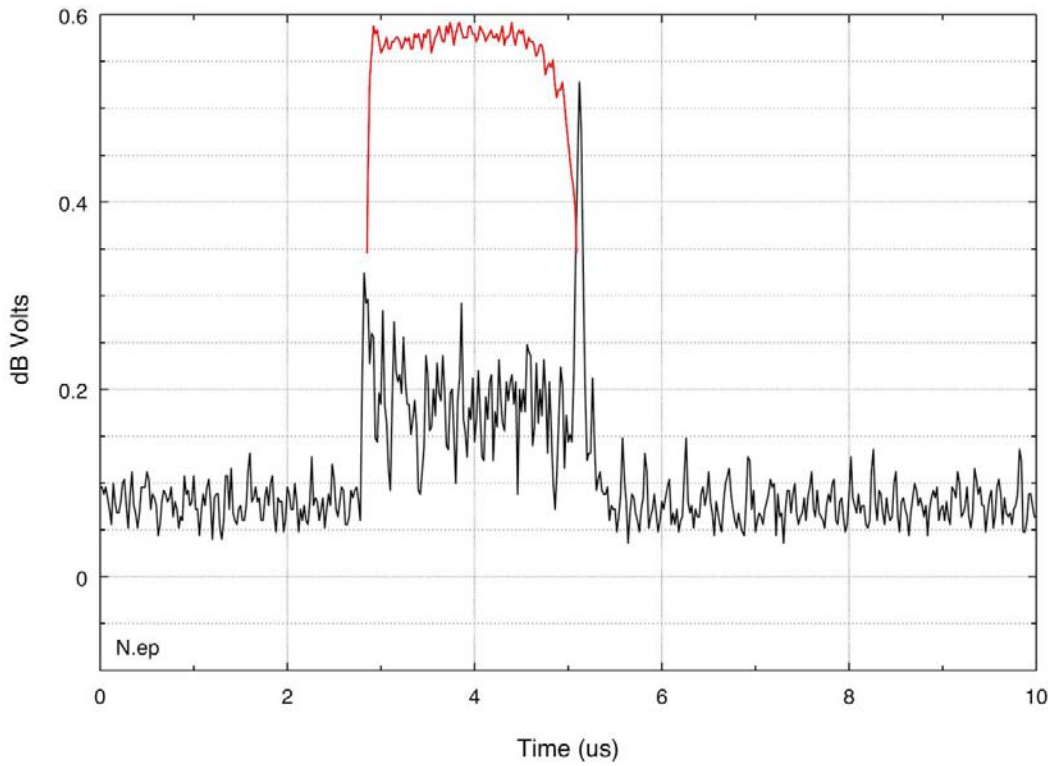


Figure 22. Pulse envelope, Point N ($\Delta f = -160$ MHz) in the WR-100 spectrum.

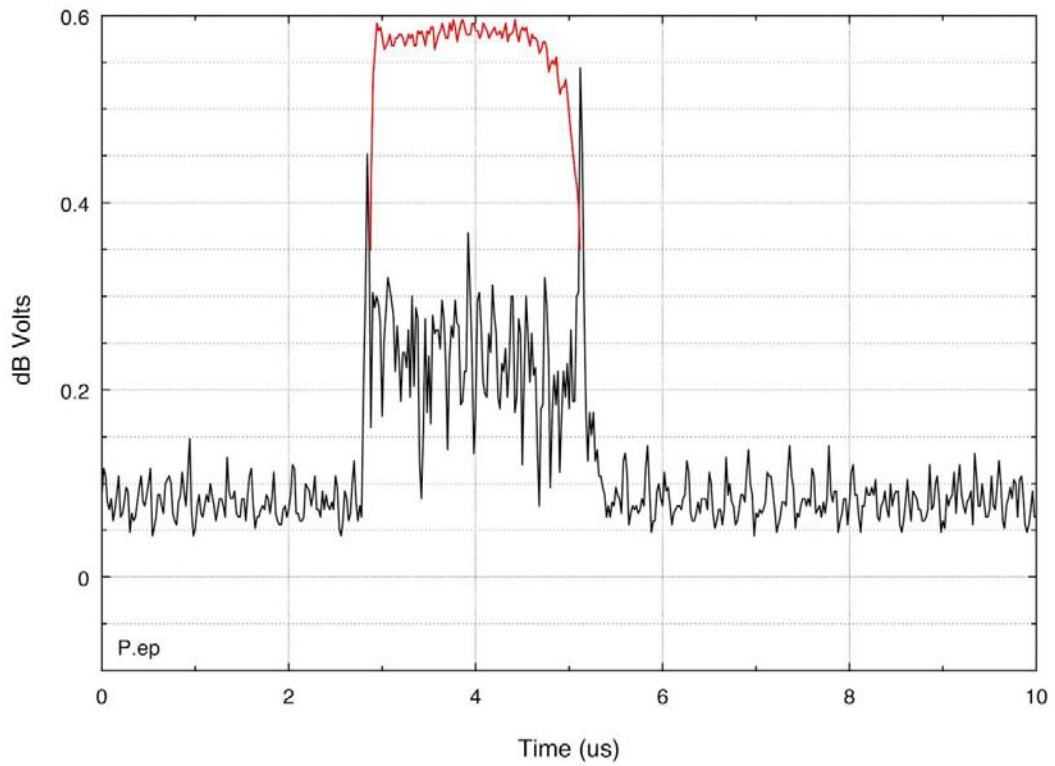


Figure 23. Pulse envelope, Point P ($\Delta f = -100$ MHz) in the WR-100 spectrum.

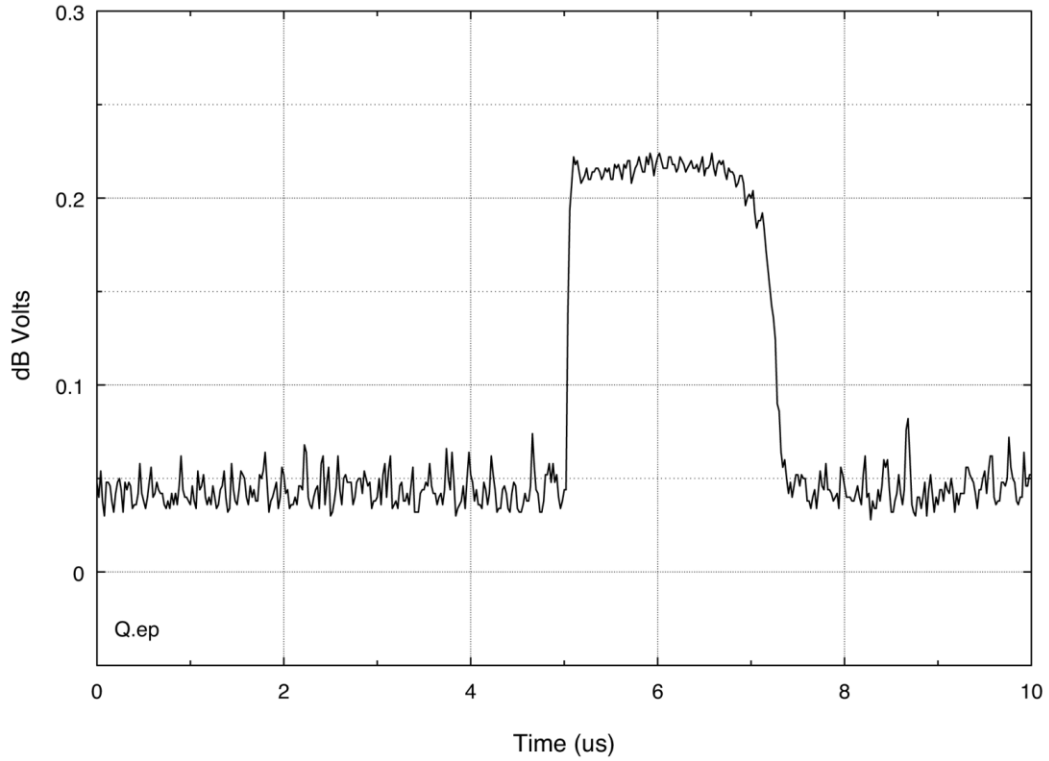


Figure 24. Pulse envelope, Point Q (f_0) in the WR-100 spectrum.

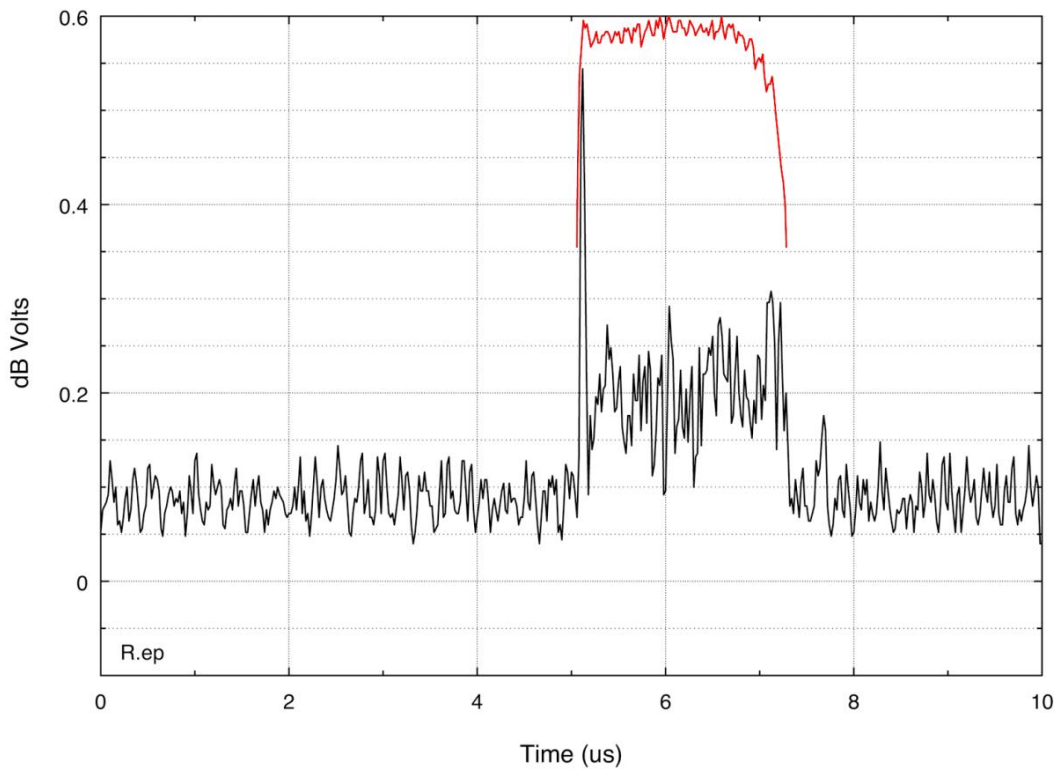


Figure 25. Pulse envelope, Point R ($\Delta f = +150$ MHz) in the WR-100 spectrum.

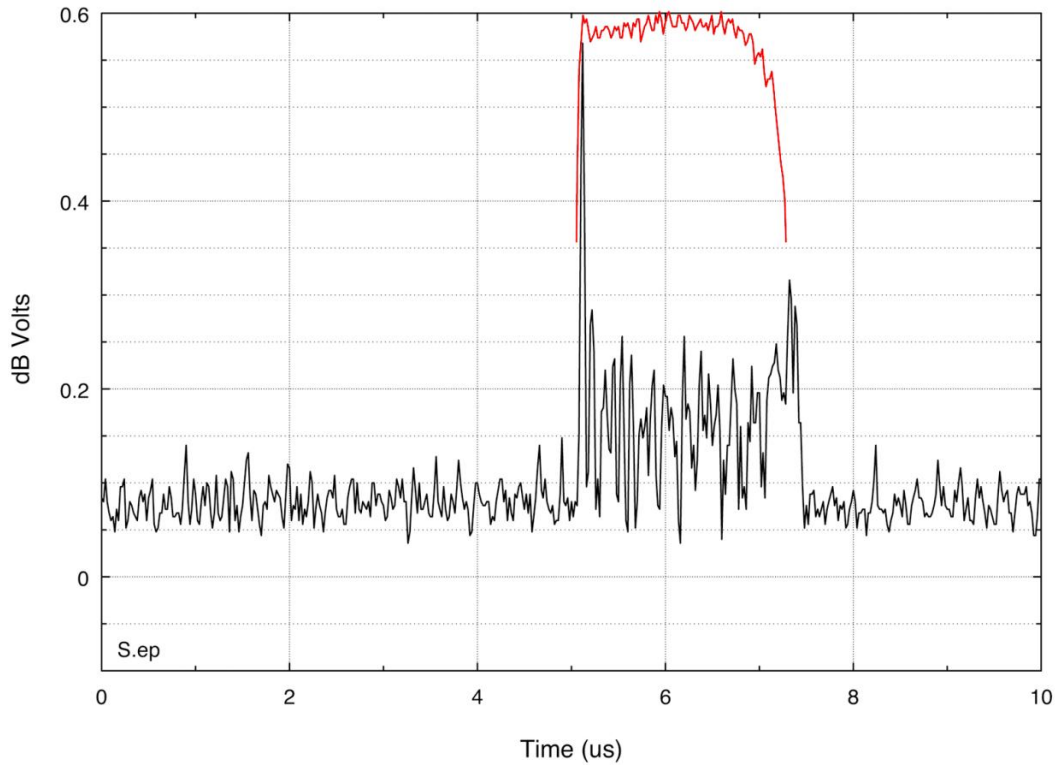


Figure 26. Pulse envelope, Point S ($\Delta f = +490$ MHz) in the WR-100 spectrum.

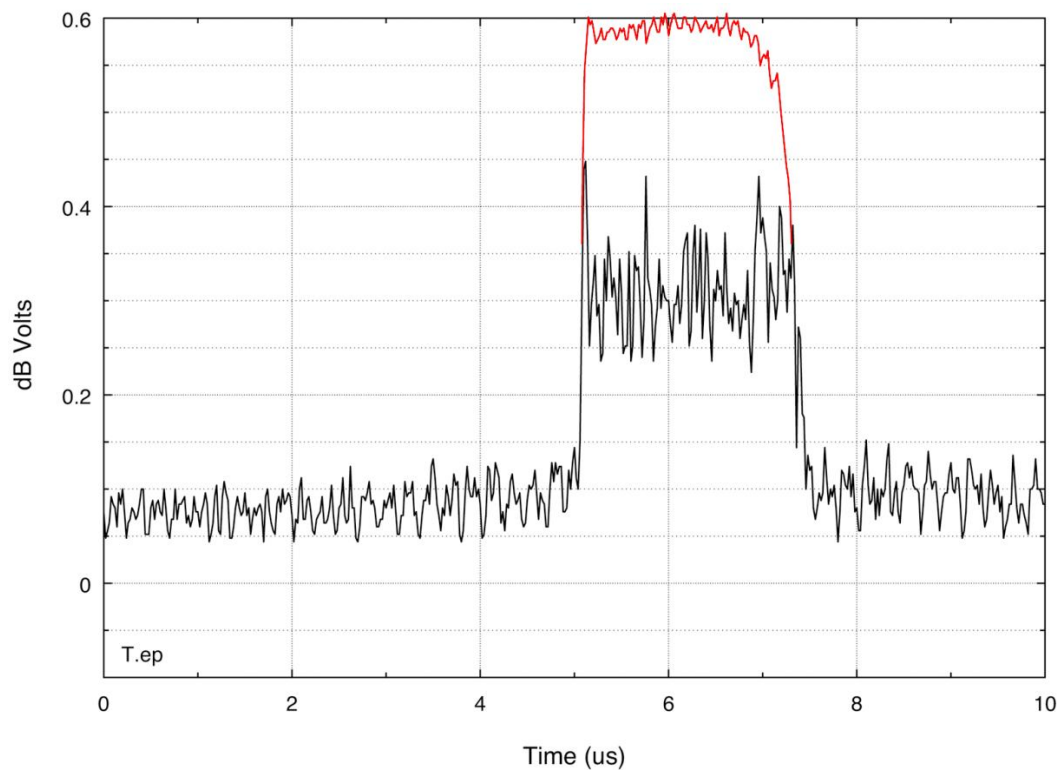


Figure 27. Pulse envelope, Point T ($\Delta f = +650$ MHz) in the WR-100 spectrum.

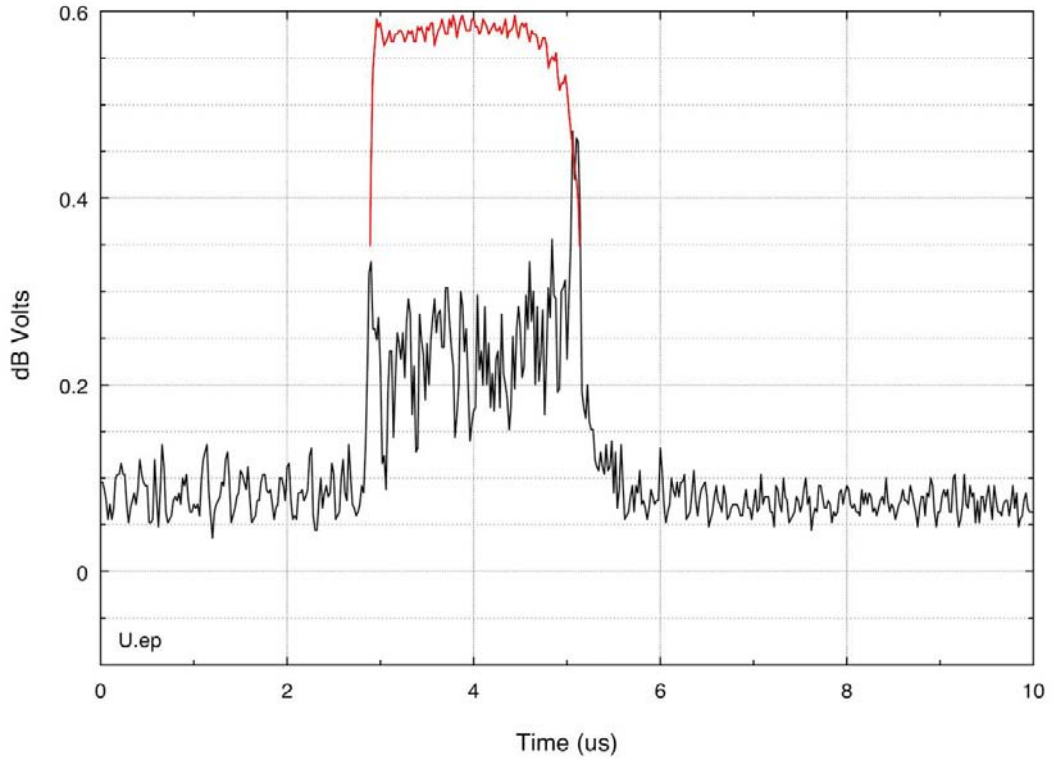


Figure 28. Pulse envelope, Point U ($\Delta f = +730$ MHz) in the WR-100 spectrum.

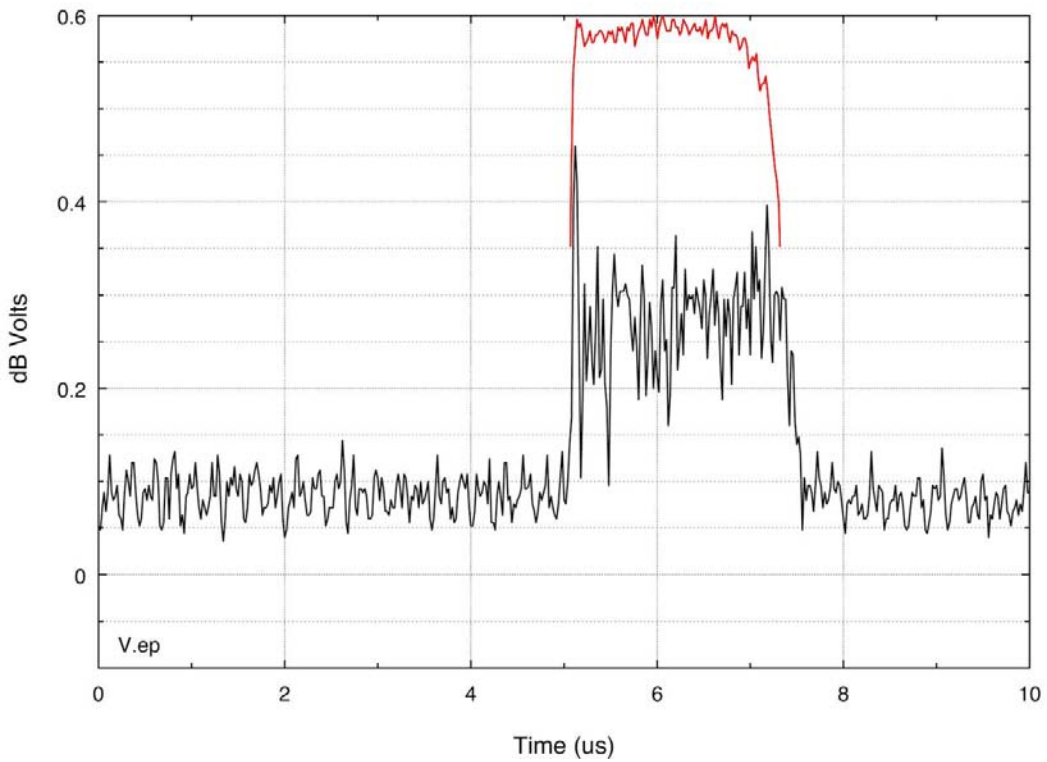


Figure 29. Pulse envelope, Point V ($\Delta f = +900$ MHz) in the WR-100 spectrum.

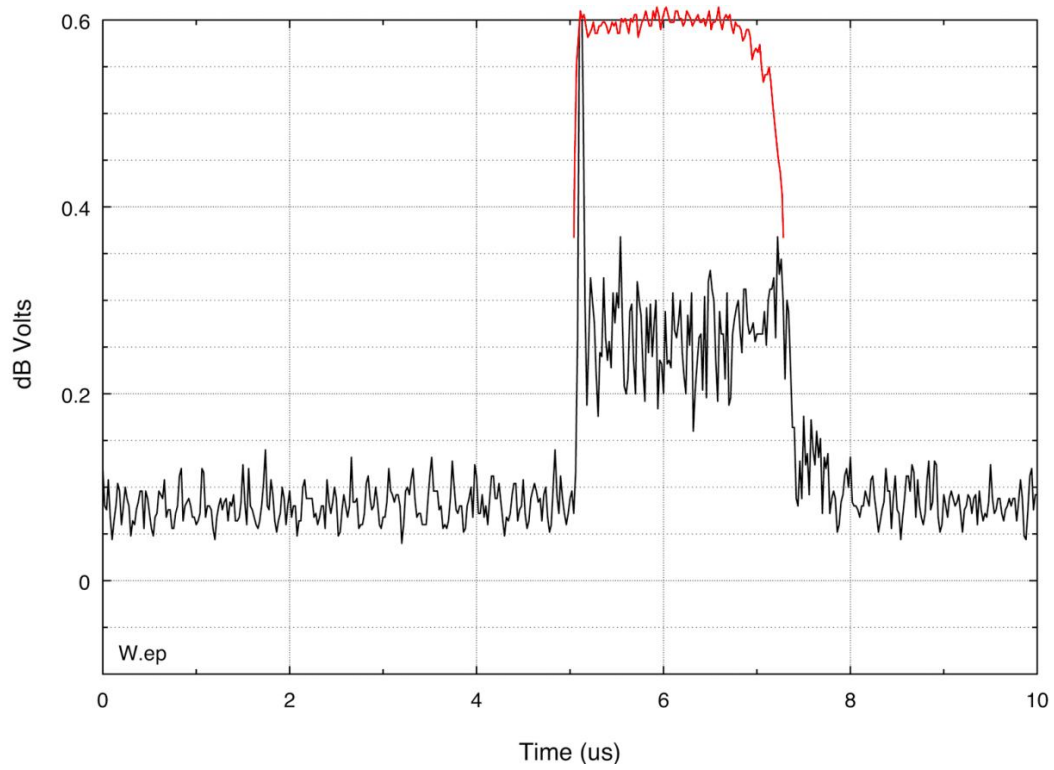


Figure 30. Pulse envelope, Point W ($\Delta f = +1040$ MHz) in the WR-100 spectrum.

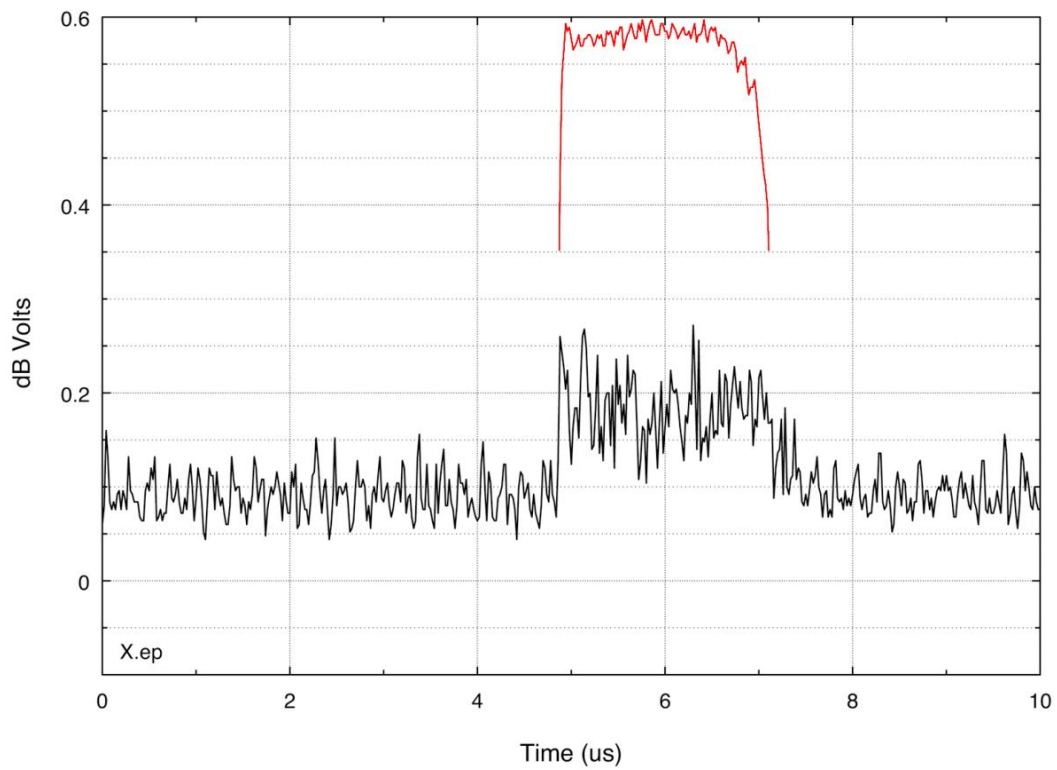


Figure 31. Pulse envelope, Point X ($\Delta f = +1250$ MHz) in the WR-100 spectrum.

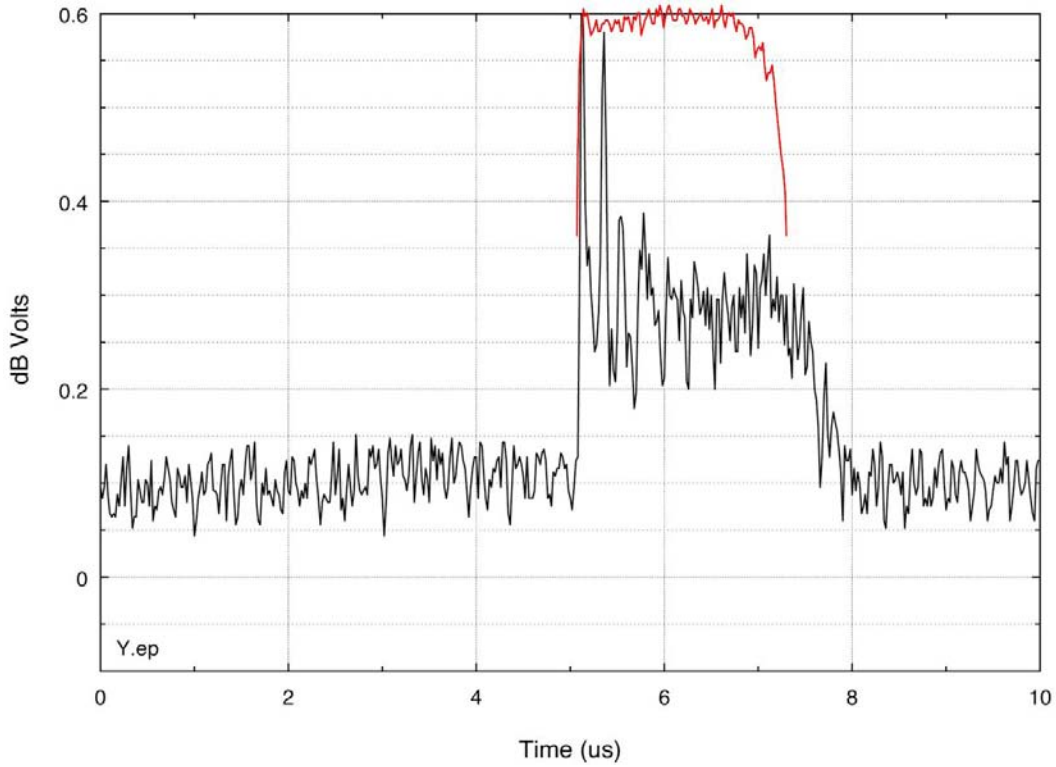


Figure 32. Pulse envelope, Point Y ($\Delta f = +1350$ MHz) in the WR-100 spectrum.

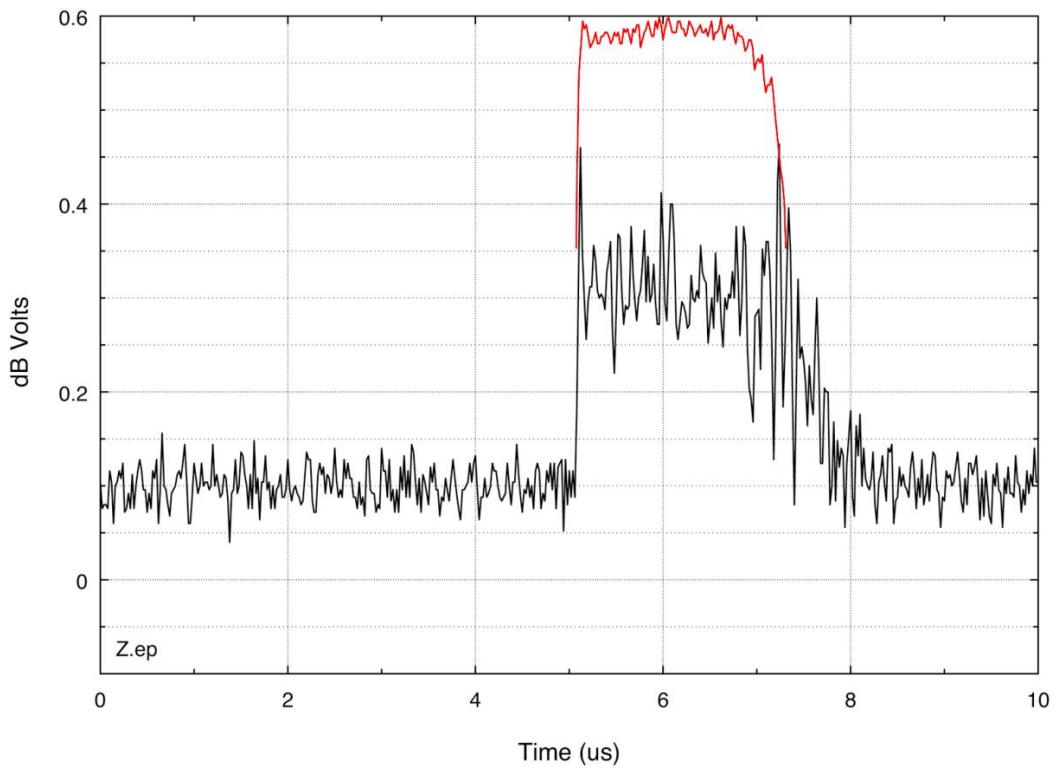


Figure 33. Pulse envelope, Point Z ($\Delta f = +1430$ MHz) in the WR-100 spectrum.

2.4 Rabbit Ears Pulse Envelopes Across the Spectrum of Another 5 GHz Radar

The author has measured and recorded rabbit ears pulse envelopes across the spectrum of a 5 GHz Federal Aviation Administration (FAA) Terminal Doppler Weather Radar (TDWR). This was an engineering test-bed unit that drives a high-power klystron final RF output stage with either a conventional pulse-forming network or else a newly designed digital pulse former. The two options are called Channels A and B respectively. Their spectra are shown in Figures 34–35. Pulse envelopes measured in an 8-MHz bandwidth are shown in Figures 36–77.

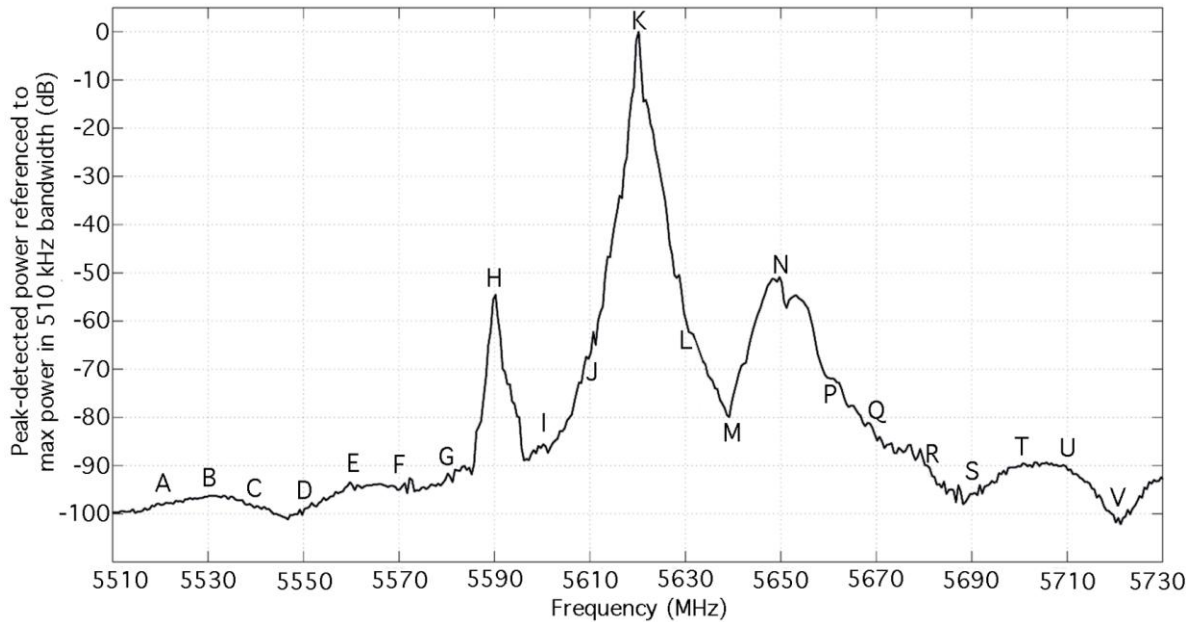


Figure 34. TDWR spectrum formed with Channel A (analog) pulse modulator. Off-fundamental pulse envelopes were measured every 10 MHz as indicated.

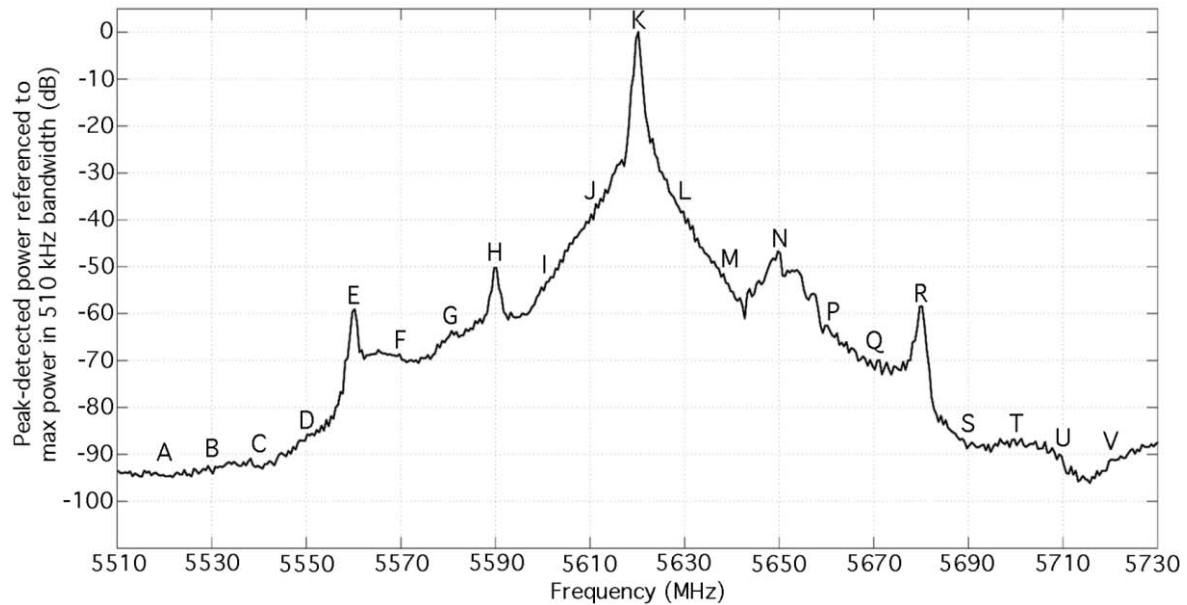


Figure 35. TDWR spectrum formed with Channel B (digital) pulse modulator. Off-fundamental pulse envelopes were measured every 10 MHz as indicated.

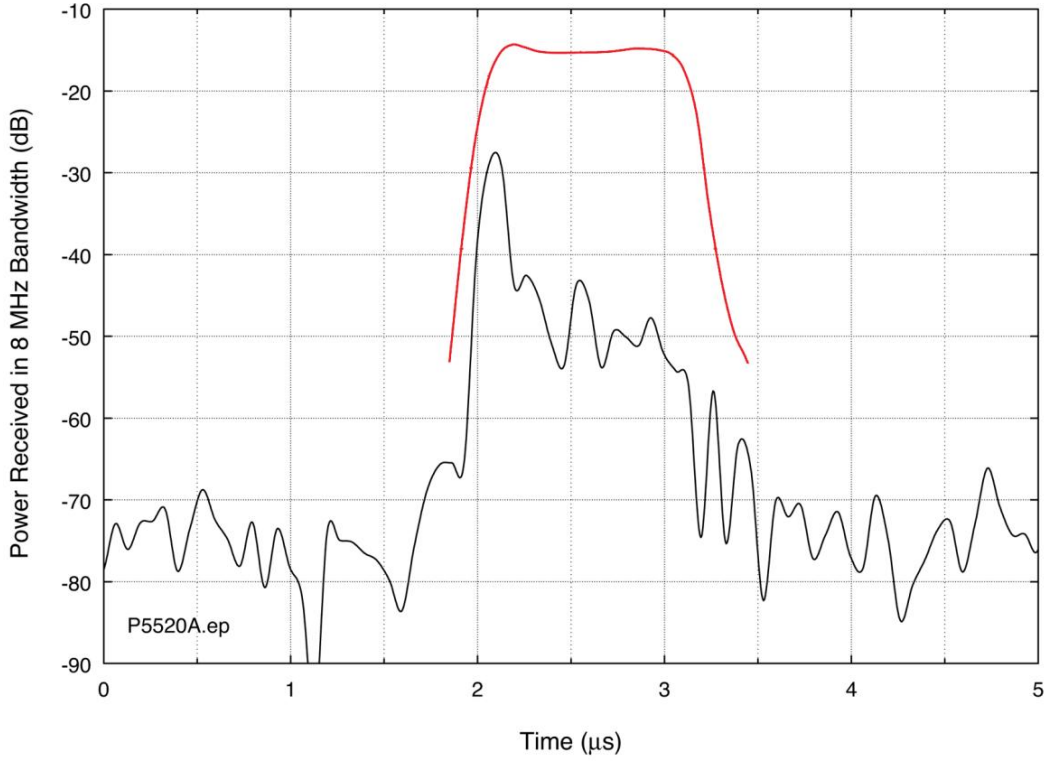


Figure 36. Pulse envelope, Point A ($\Delta f = -100$ MHz) in the TDWR Channel A spectrum. The red curve is a graphical aid showing the pulse envelope at f_0 .

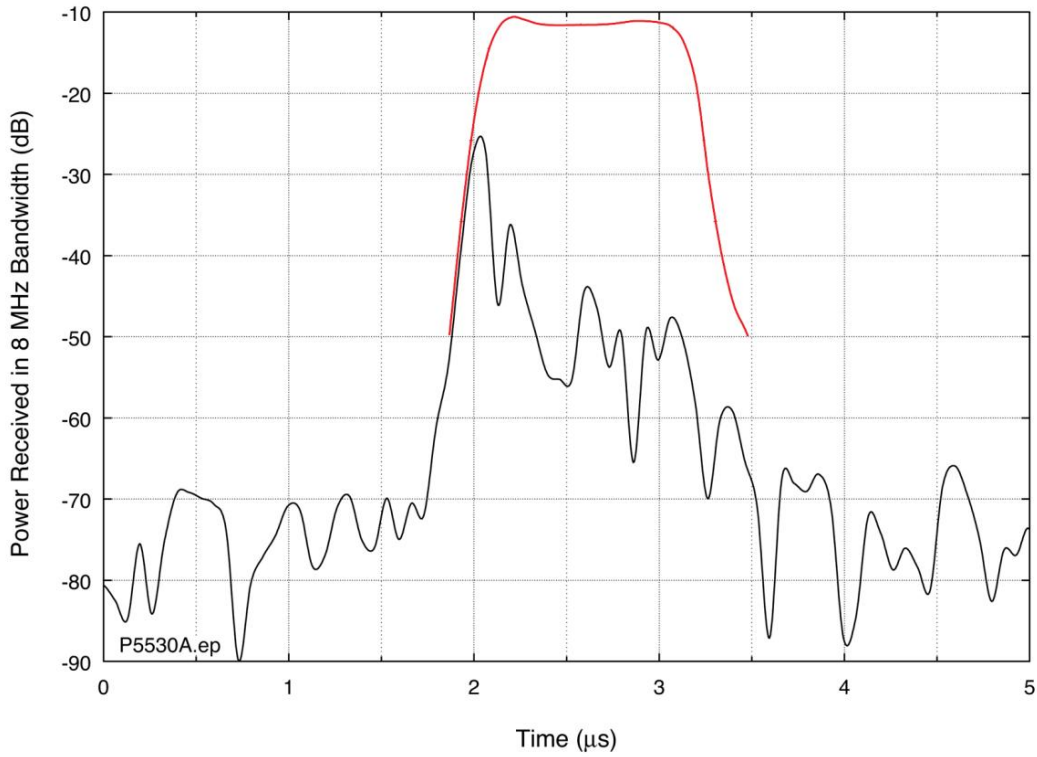


Figure 37. Pulse envelope, Point B ($\Delta f = -90$ MHz) in the TDWR Channel A spectrum.

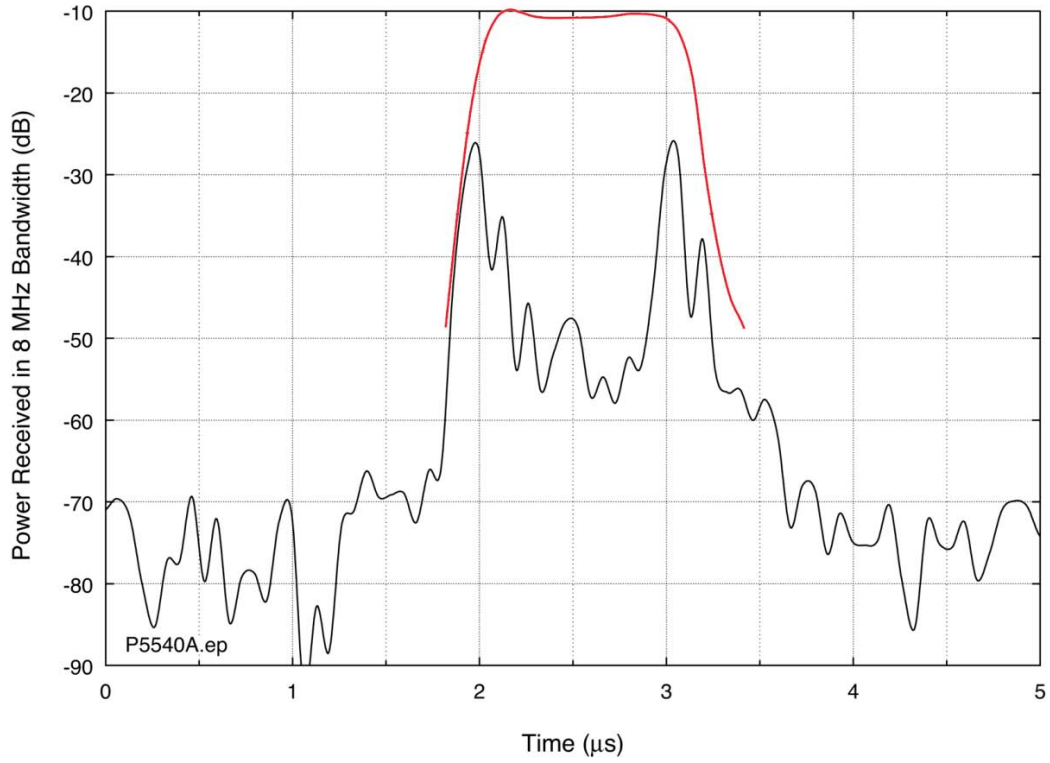


Figure 38. Pulse envelope, Point C ($\Delta f = -80$ MHz) in the TDWR Channel A spectrum.

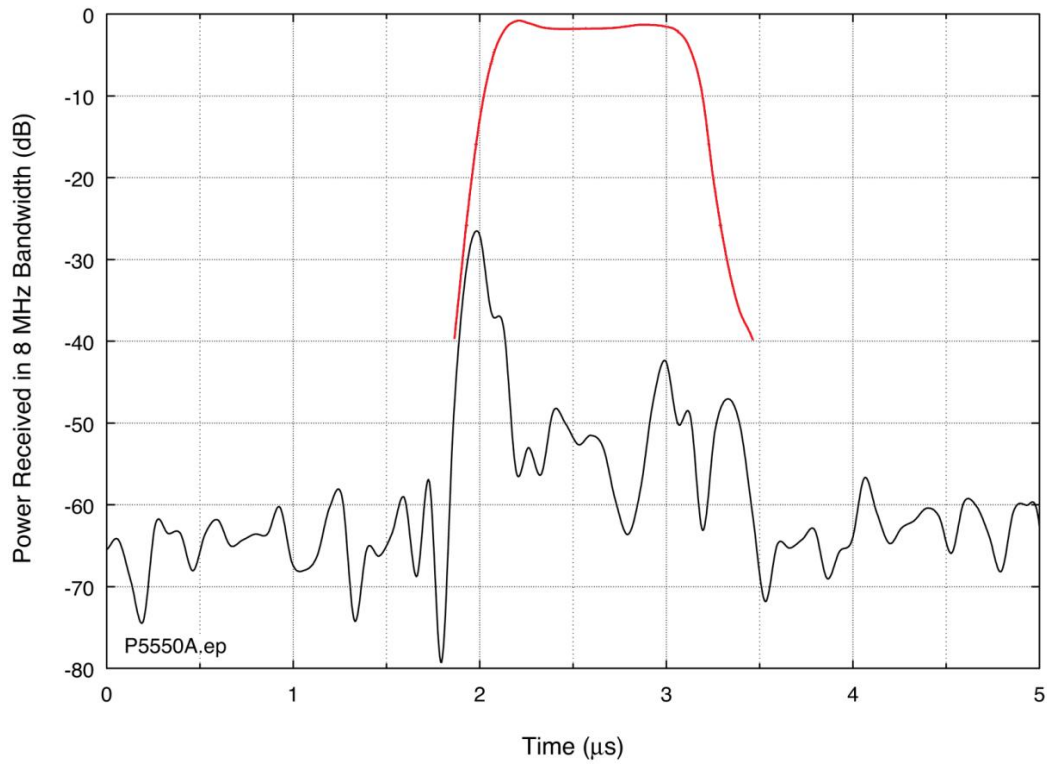


Figure 39. Pulse envelope, Point D ($\Delta f = -70$ MHz) in the TDWR Channel A spectrum.

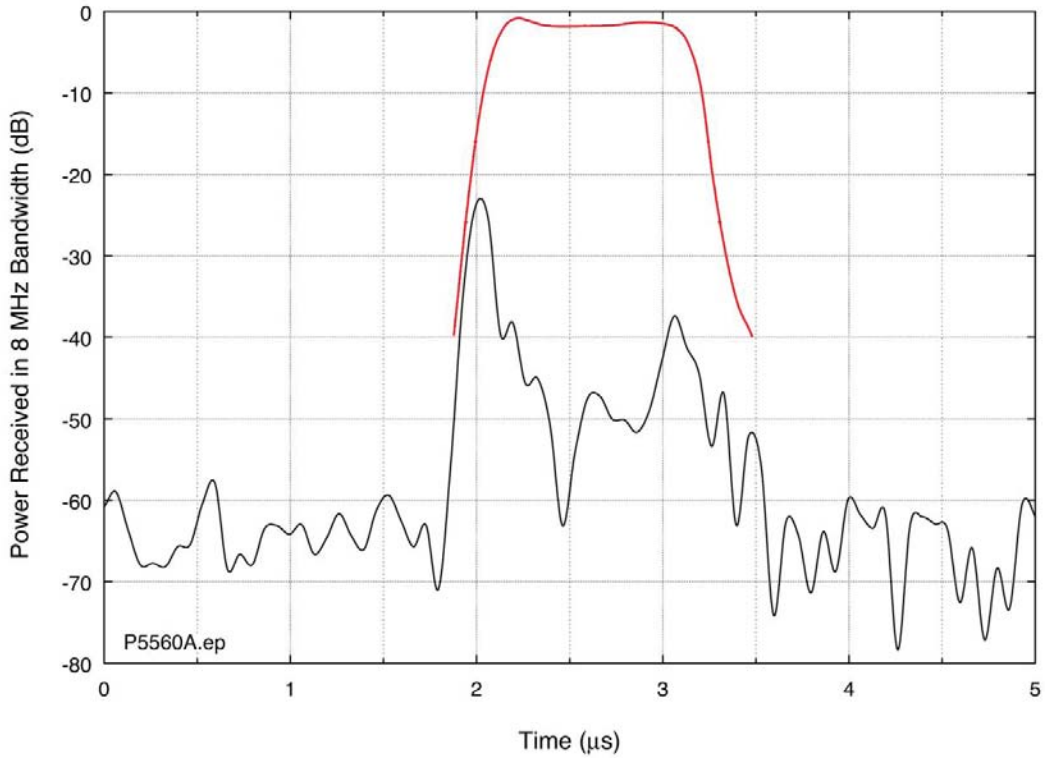


Figure 40. Pulse envelope, Point E ($\Delta f = -60$ MHz) in the TDWR Channel A spectrum.

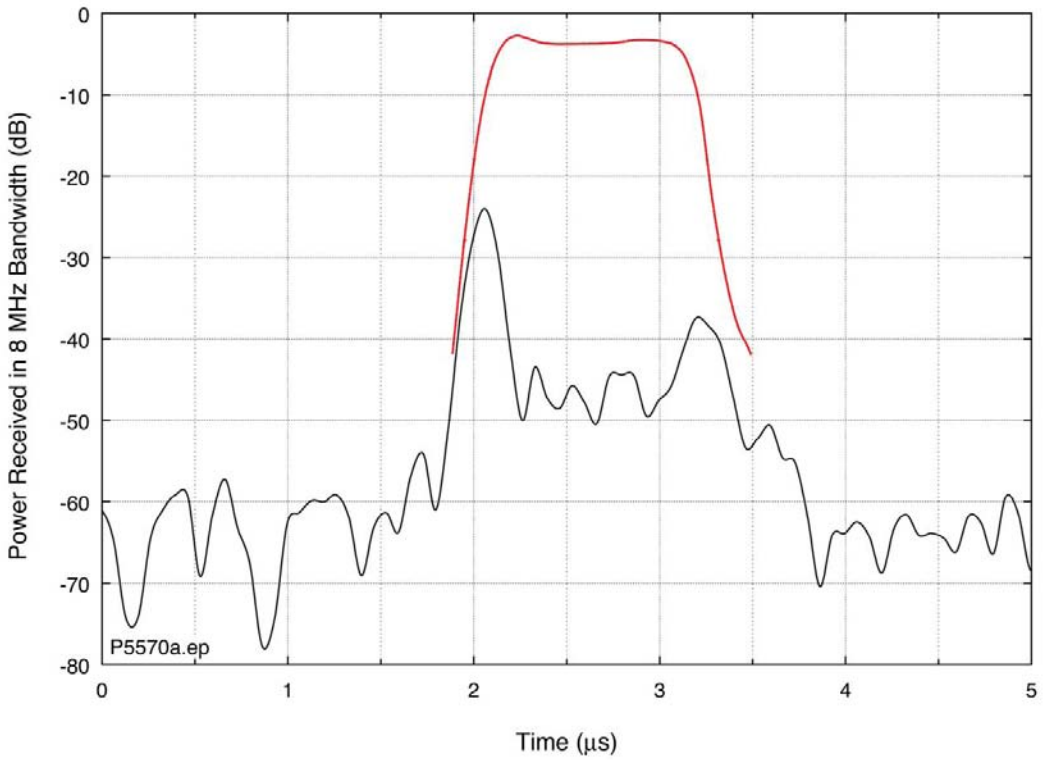


Figure 41. Pulse envelope, Point F ($\Delta f = -50$ MHz) in the TDWR Channel A spectrum.

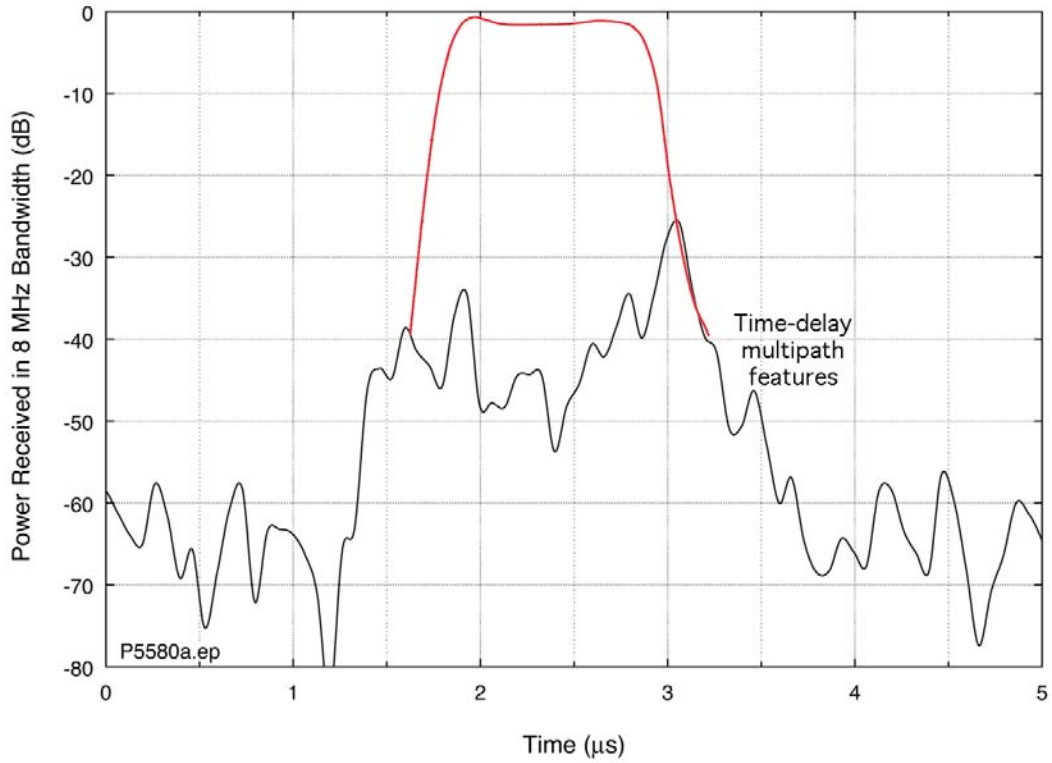


Figure 42. Pulse envelope, Point G ($\Delta f = -40$ MHz) in the TDWR Channel A spectrum.

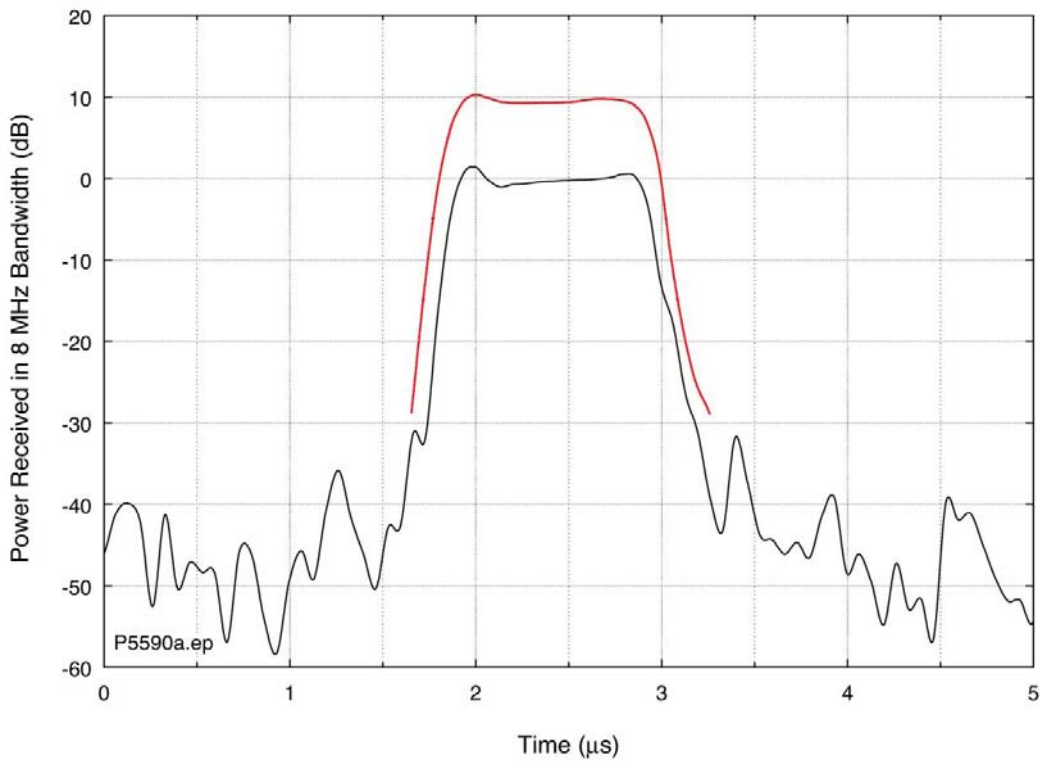


Figure 43. Pulse envelope, Point H ($\Delta f = -30$ MHz) in the TDWR Channel A spectrum.

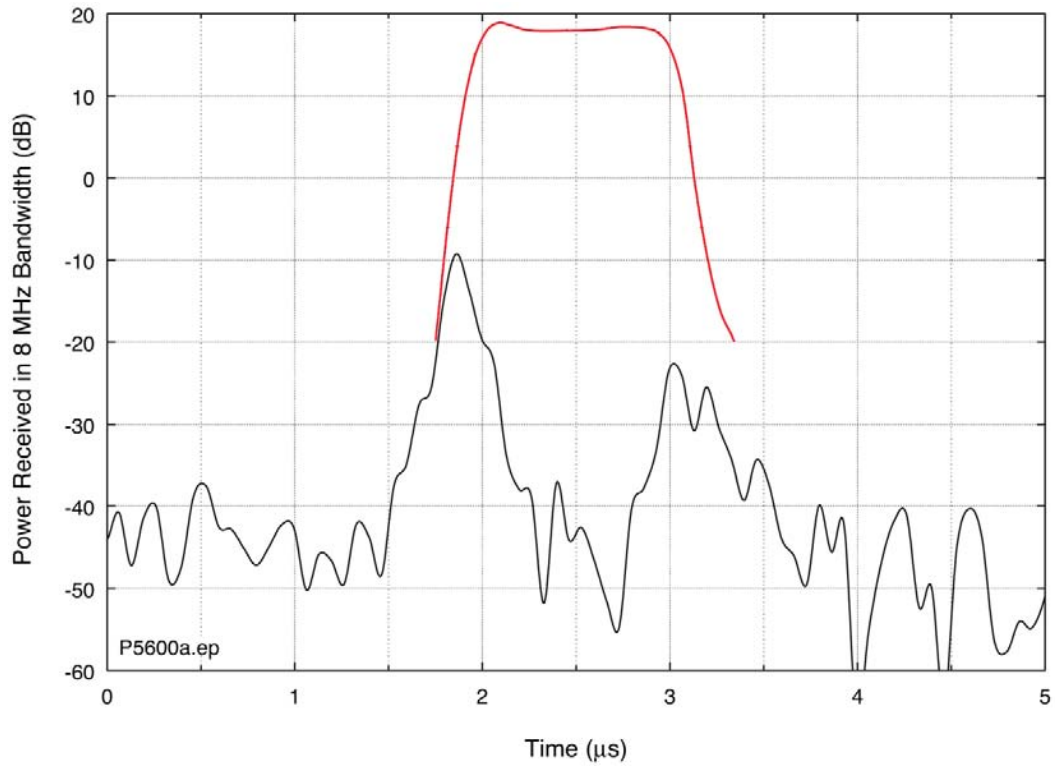


Figure 44. Pulse envelope, Point I ($\Delta f = -20$ MHz) in the TDWR Channel A spectrum.

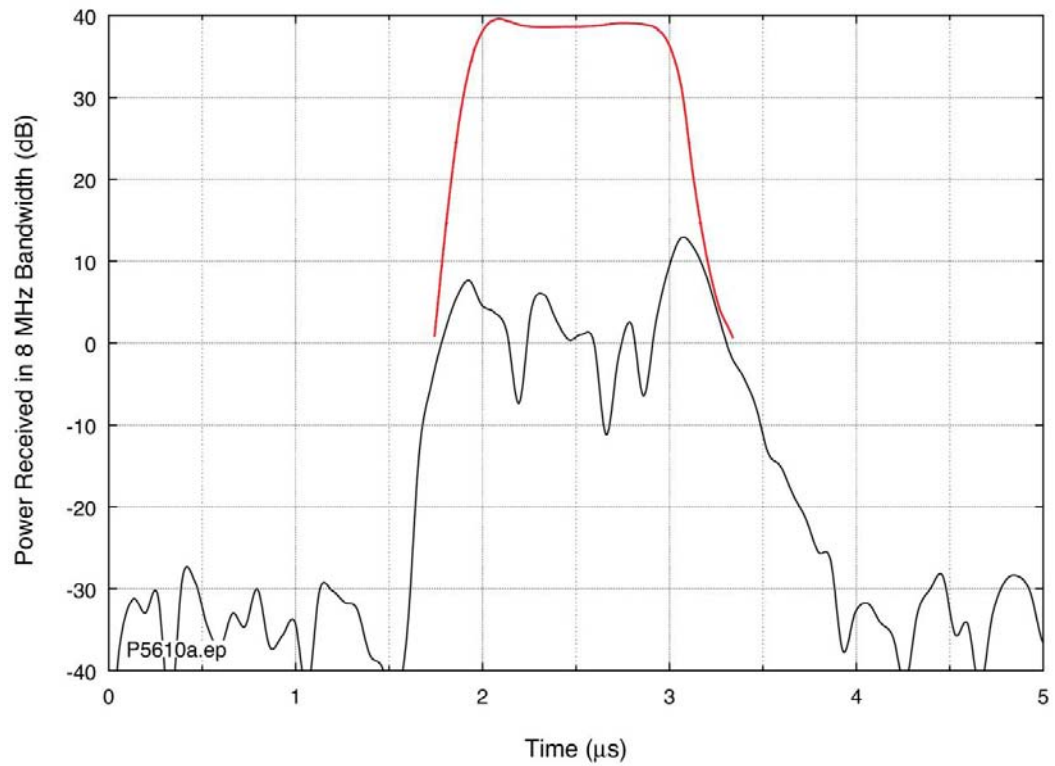


Figure 45. Pulse envelope, Point J ($\Delta f = -10$ MHz) in the TDWR Channel A spectrum.

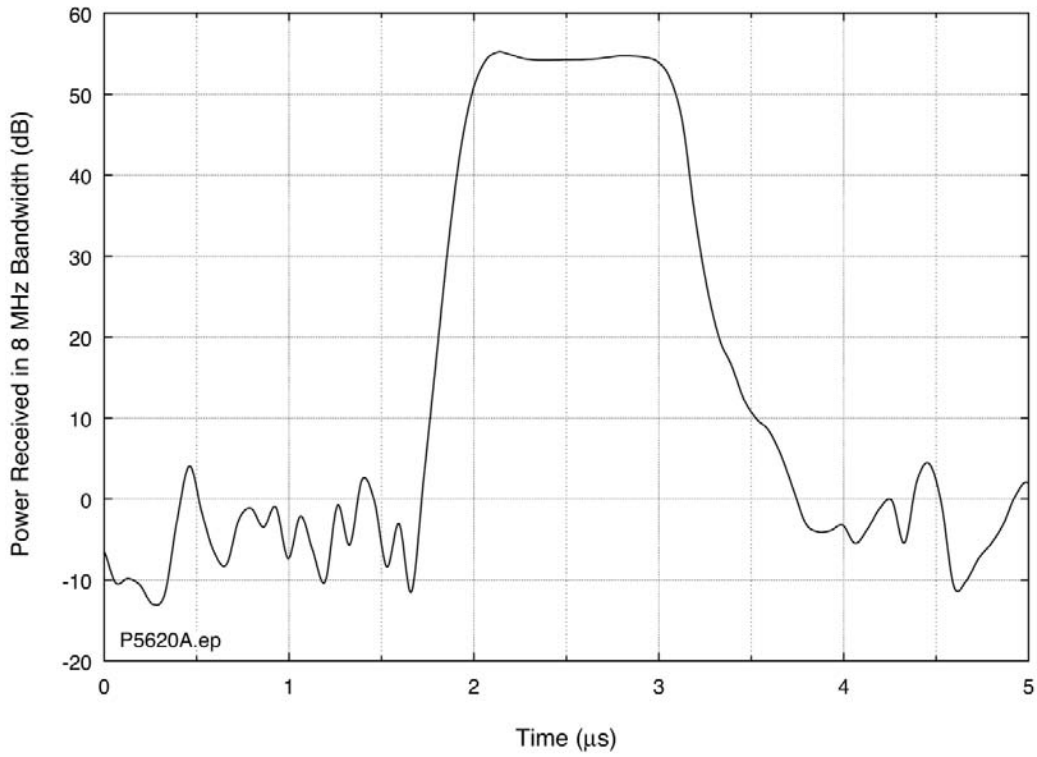


Figure 46. Pulse envelope, Point K (f_0) in the TDWR Channel A spectrum.

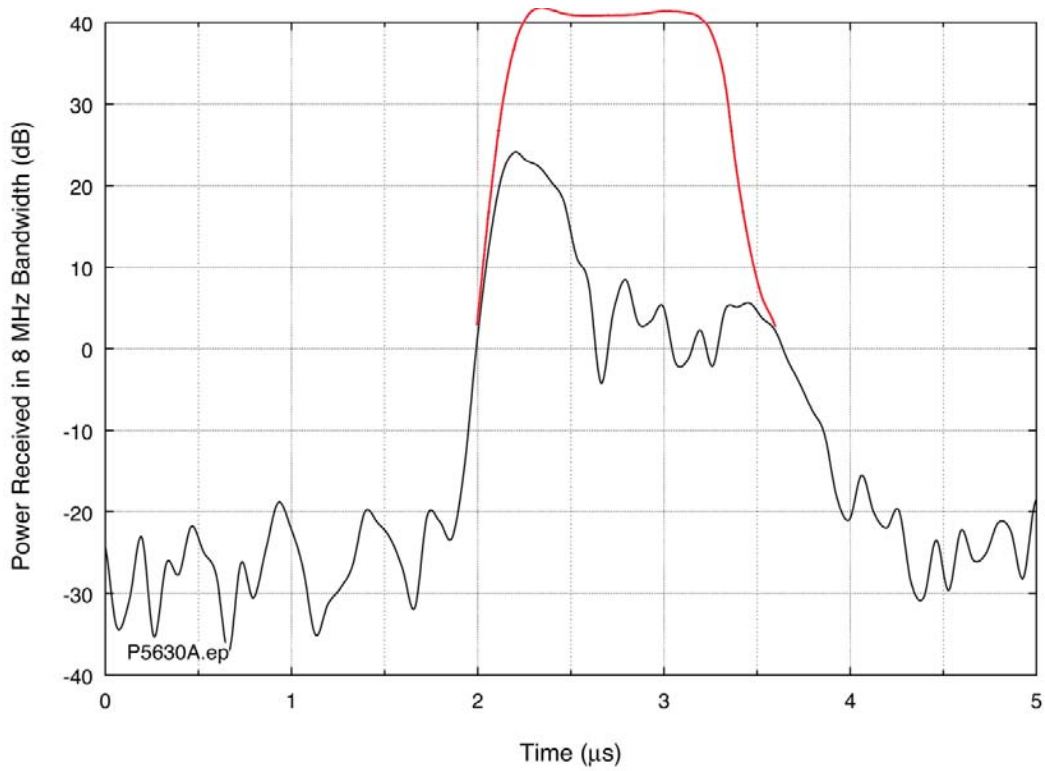


Figure 47. Pulse envelope, Point L ($\Delta f = +10$ MHz) in the TDWR Channel A spectrum.

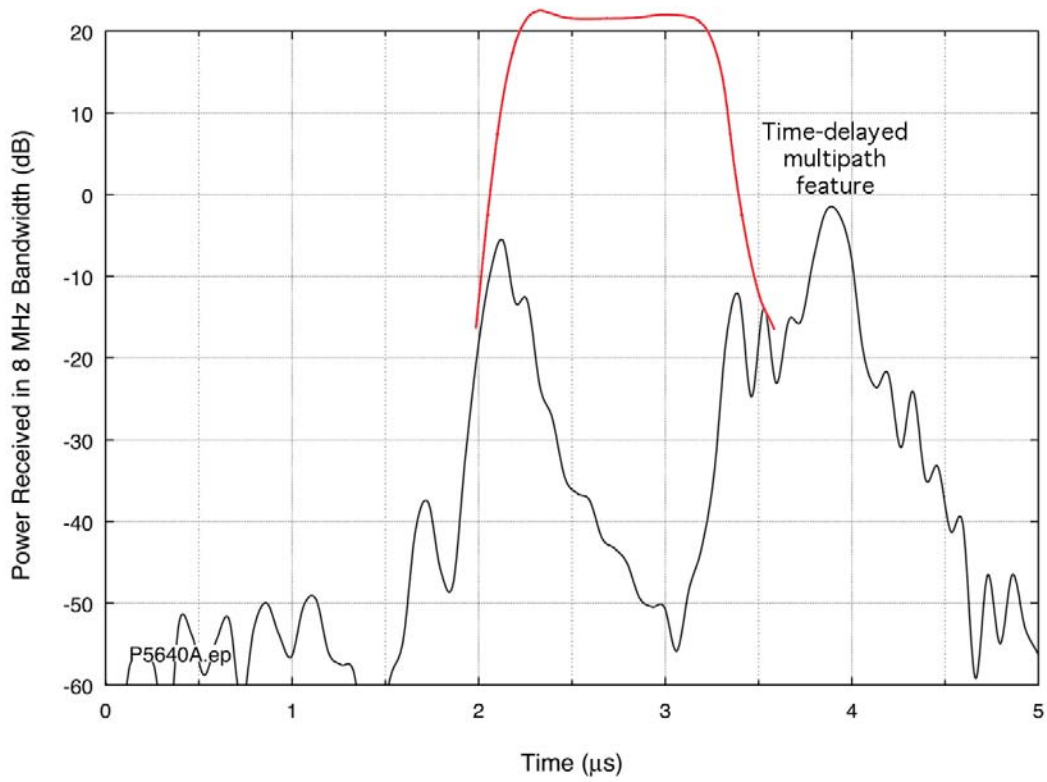


Figure 48. Pulse envelope, Point M ($\Delta f = +20$ MHz) in the TDWR Channel A spectrum.

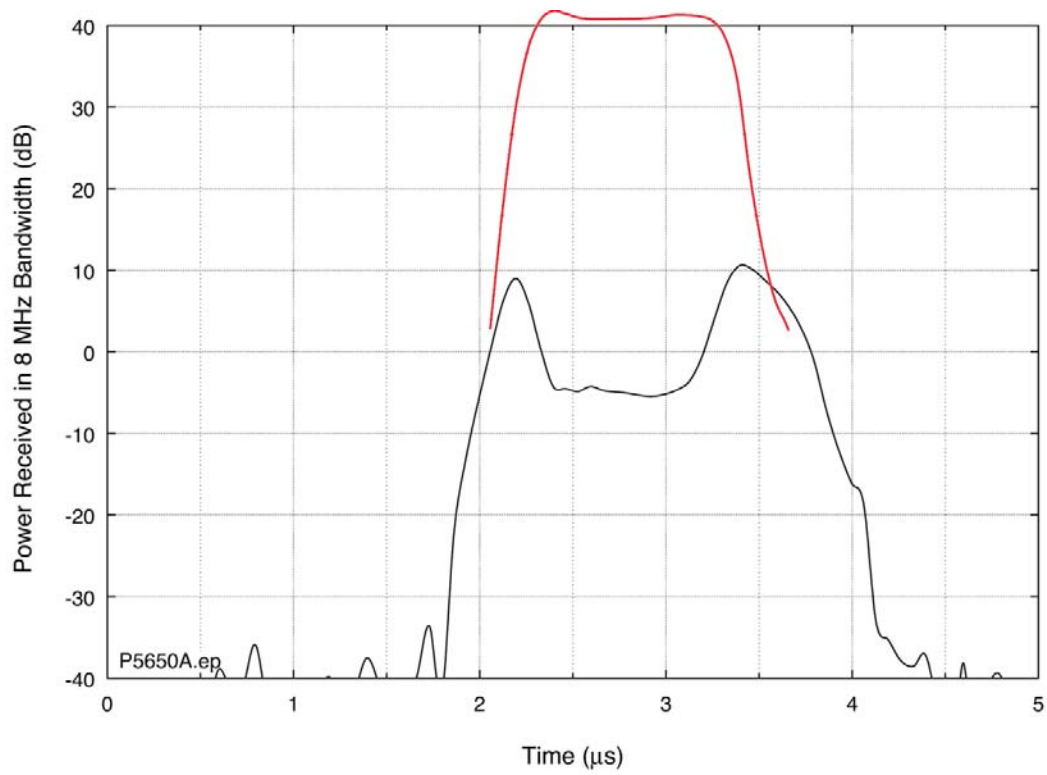


Figure 49. Pulse envelope, Point N ($\Delta f = +30$ MHz) in the TDWR Channel A spectrum.

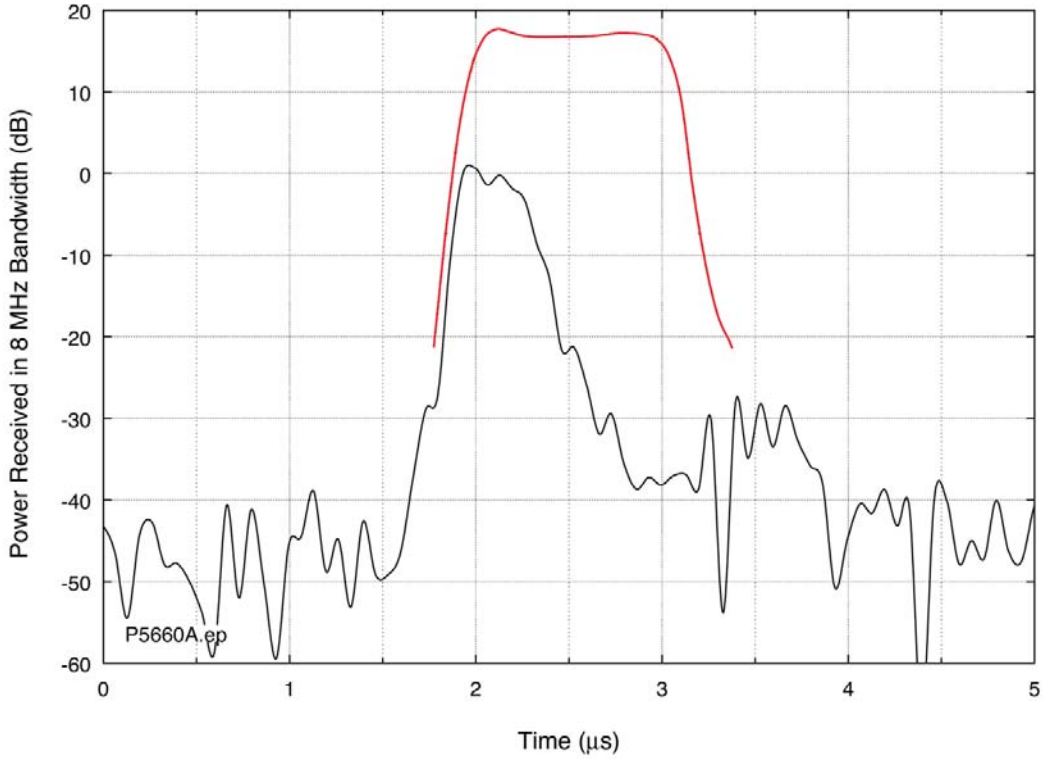


Figure 50. Pulse envelope, Point P ($\Delta f = +40$ MHz) in the TDWR Channel A spectrum.

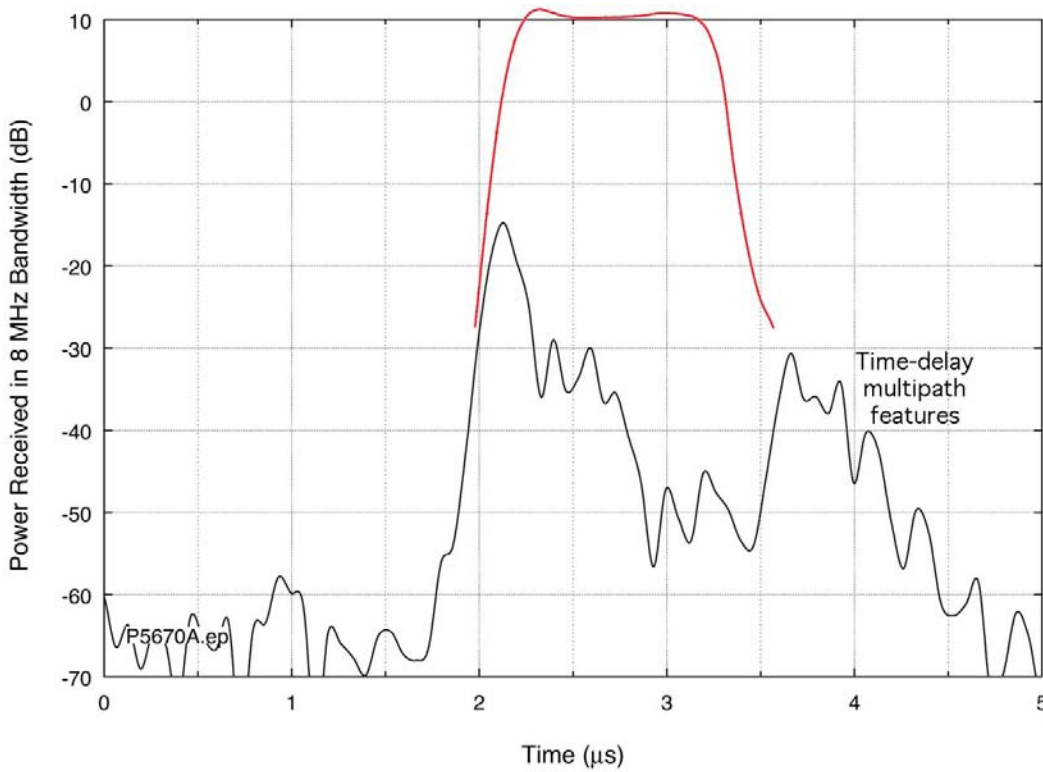


Figure 51. Pulse envelope, Point Q ($\Delta f = +50$ MHz) in the TDWR Channel A spectrum.

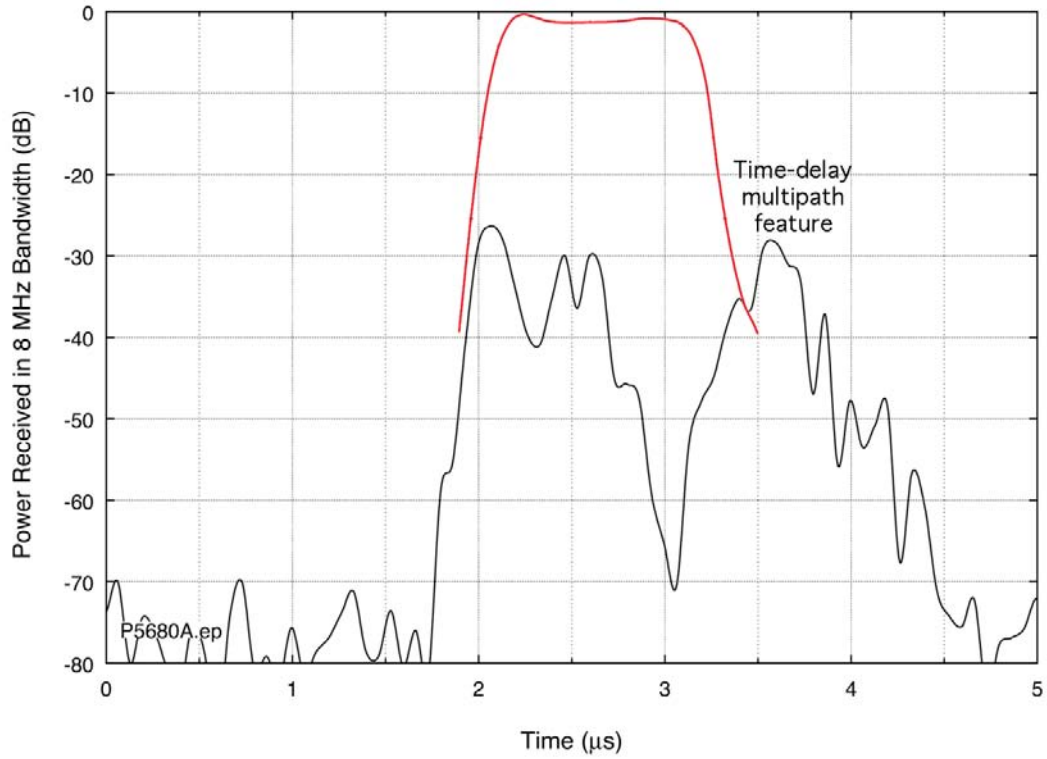


Figure 52. Pulse envelope, Point R ($\Delta f = +60$ MHz) in the TDWR Channel A spectrum.

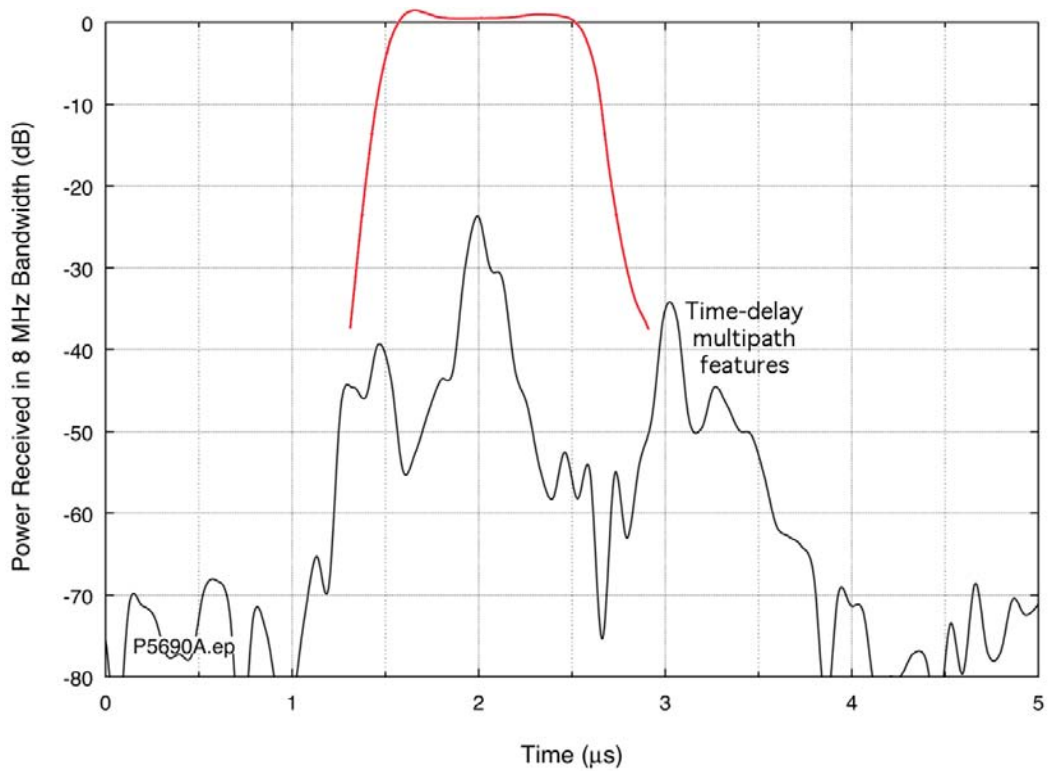


Figure 53. Pulse envelope, Point S ($\Delta f = +70$ MHz) in the TDWR Channel A spectrum.

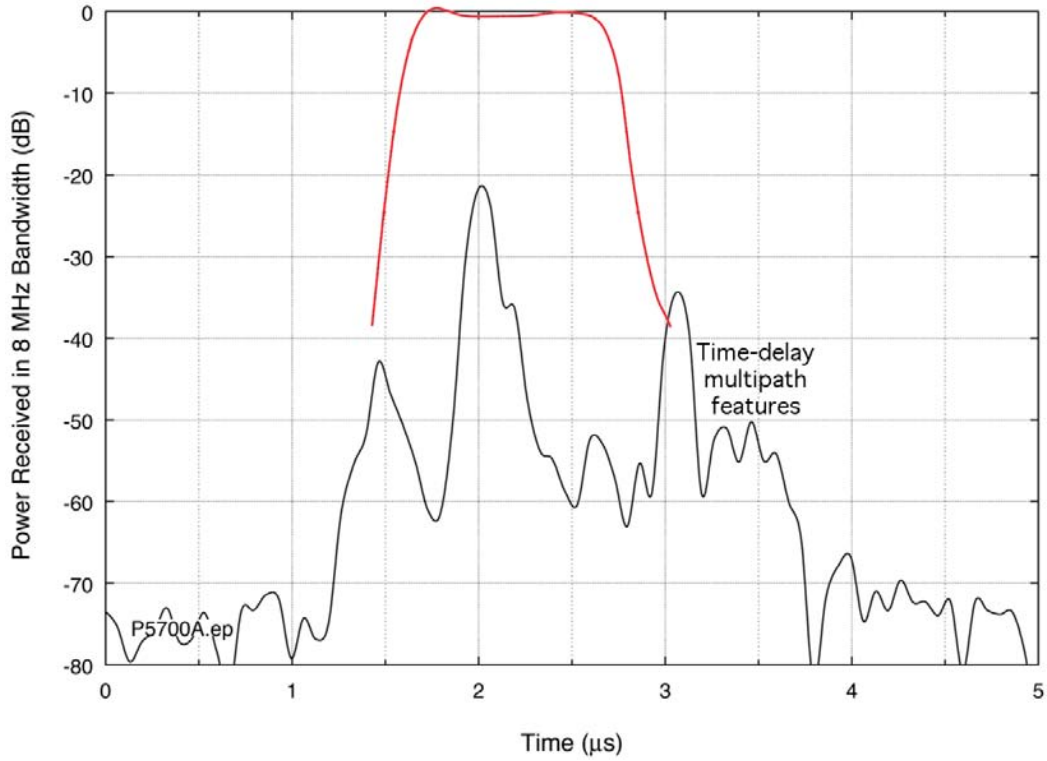


Figure 54. Pulse envelope, Point T ($\Delta f = +80$ MHz) in the TDWR Channel A spectrum.

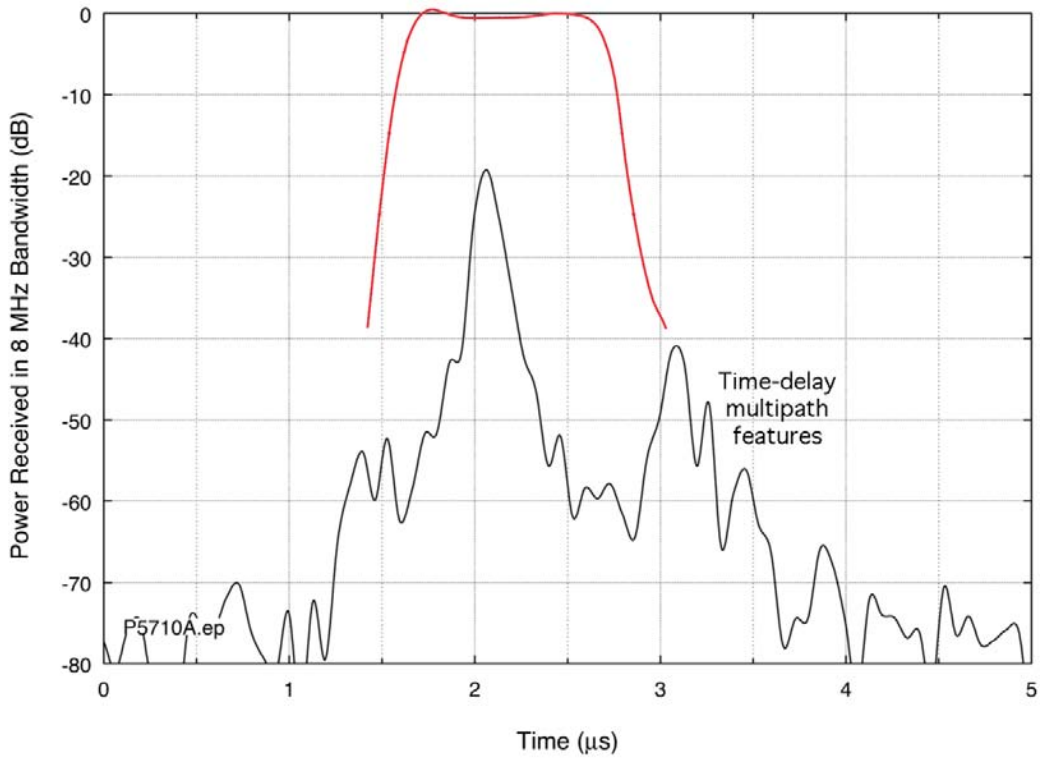


Figure 55. Pulse envelope, Point U ($\Delta f = +90$ MHz) in the TDWR Channel A spectrum.

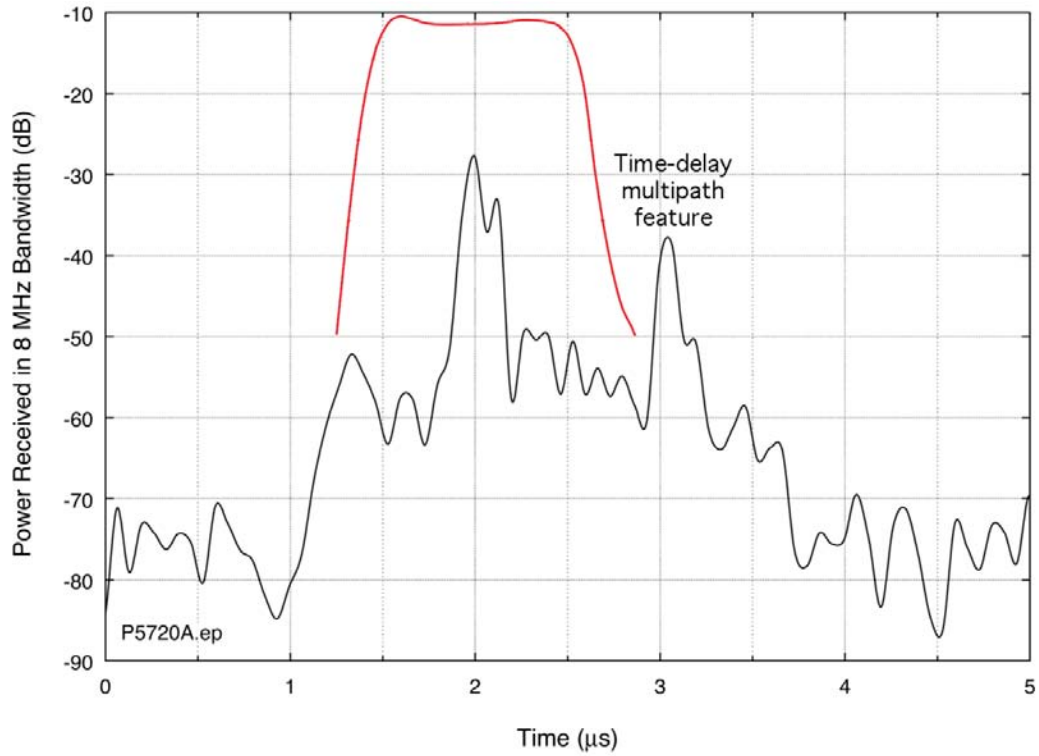


Figure 56. Pulse envelope, Point V ($\Delta f = +100$ MHz) in the TDWR Channel A spectrum.

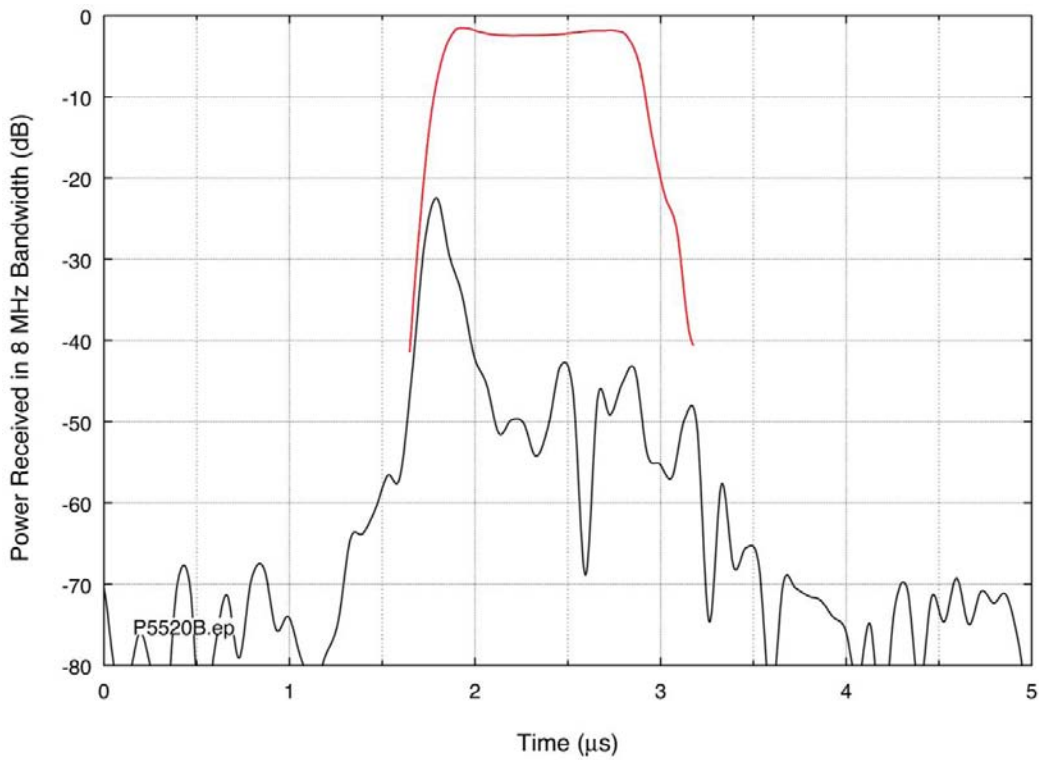


Figure 57. Pulse envelope, Point A ($\Delta f = -100$ MHz) in the TDWR Channel B spectrum.

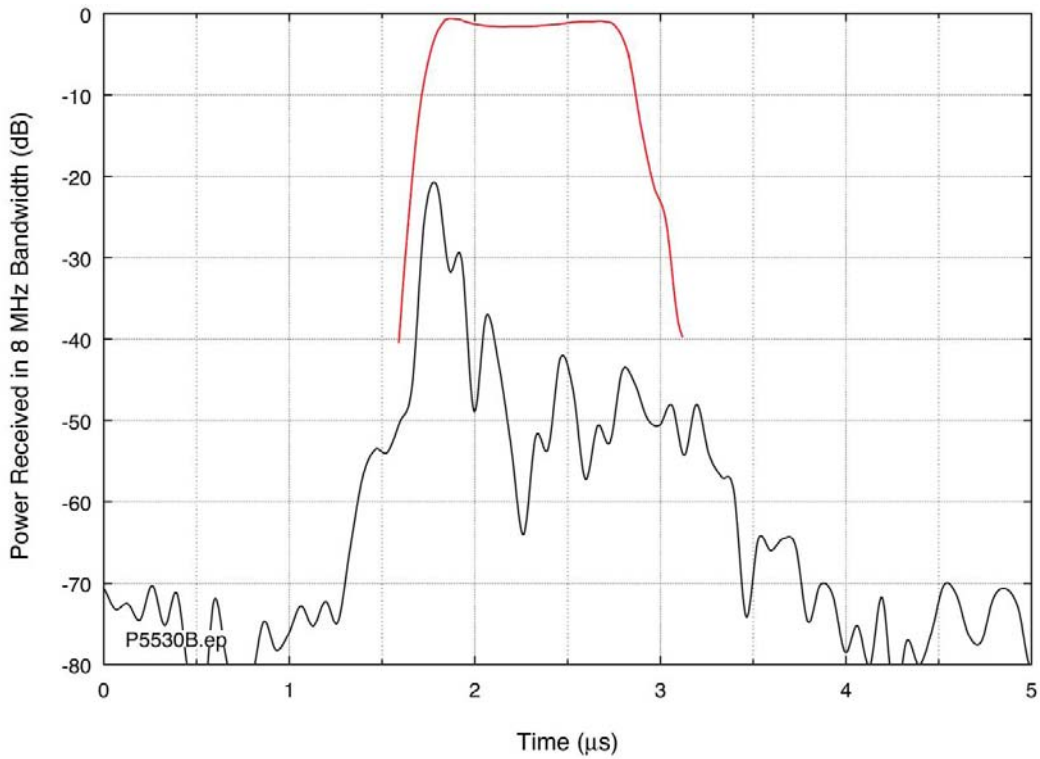


Figure 58. Pulse envelope, Point B ($\Delta f = -90$ MHz) in the TDWR Channel B spectrum.

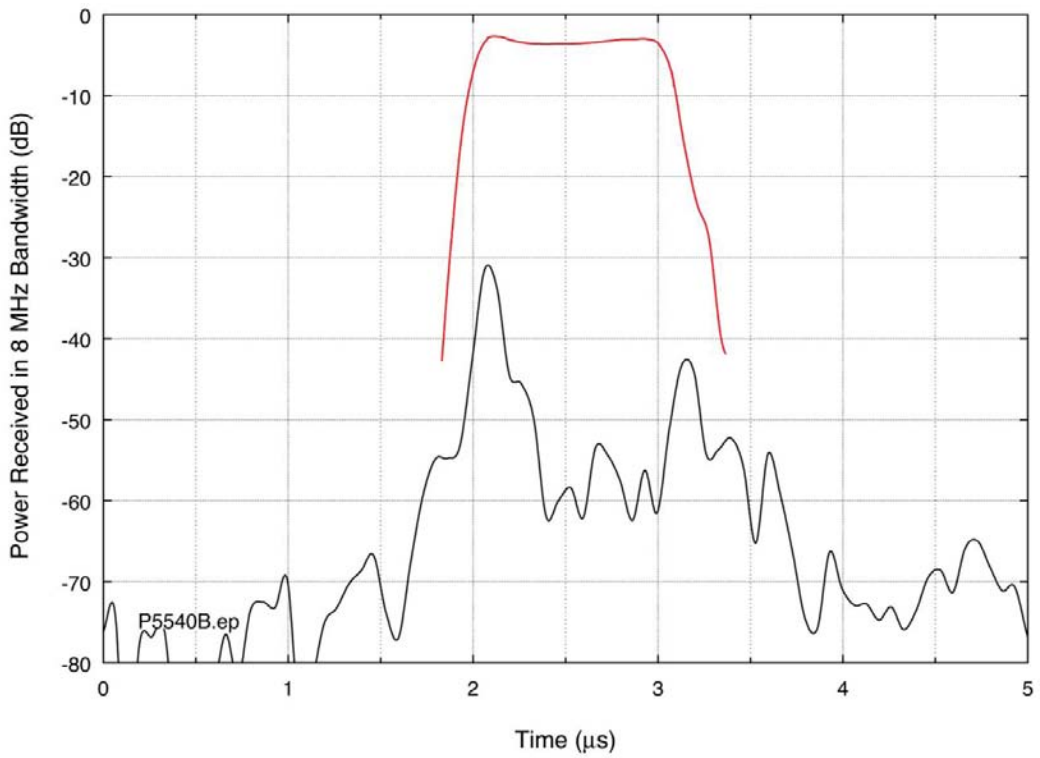


Figure 59. Pulse envelope, Point C ($\Delta f = -80$ MHz) in the TDWR Channel B spectrum.

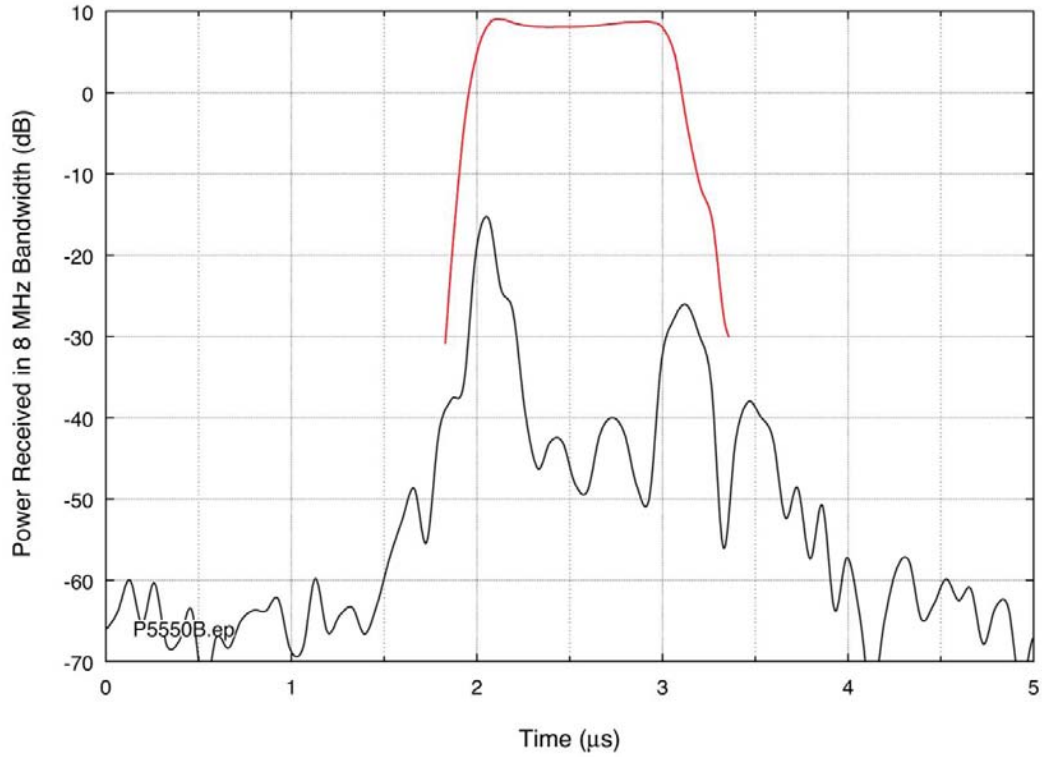


Figure 60. Pulse envelope, Point D ($\Delta f = -70$ MHz) in the TDWR Channel B spectrum.

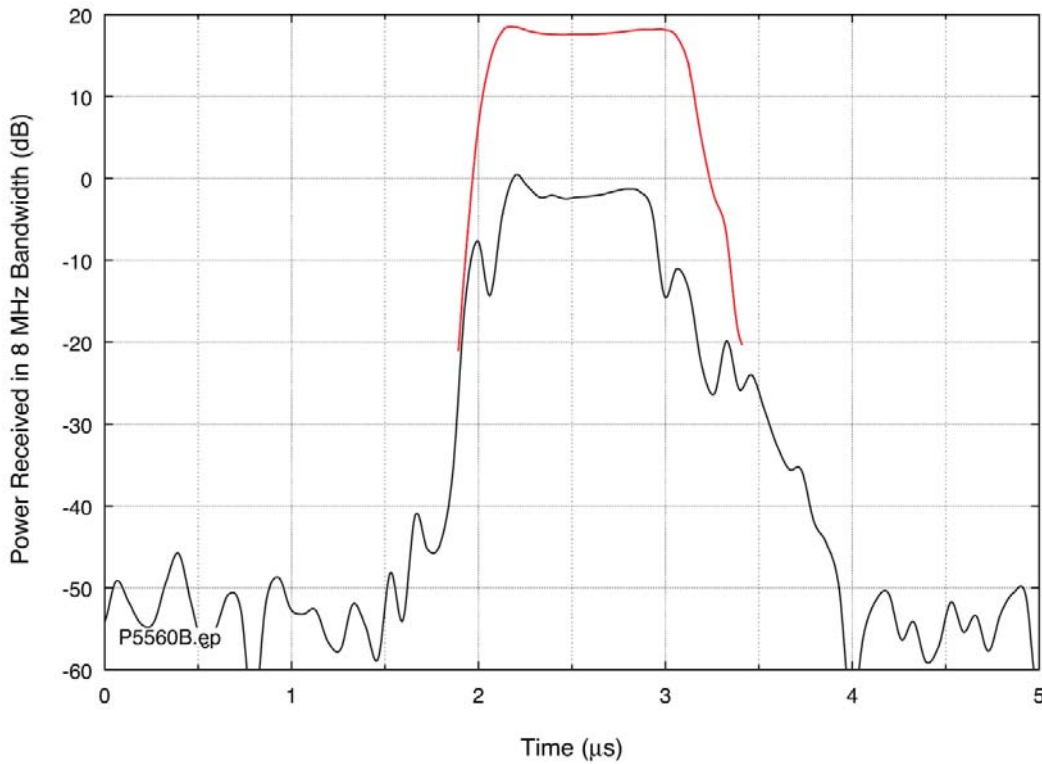


Figure 61. Pulse envelope, Point E ($\Delta f = -60$ MHz) in the TDWR Channel B spectrum.

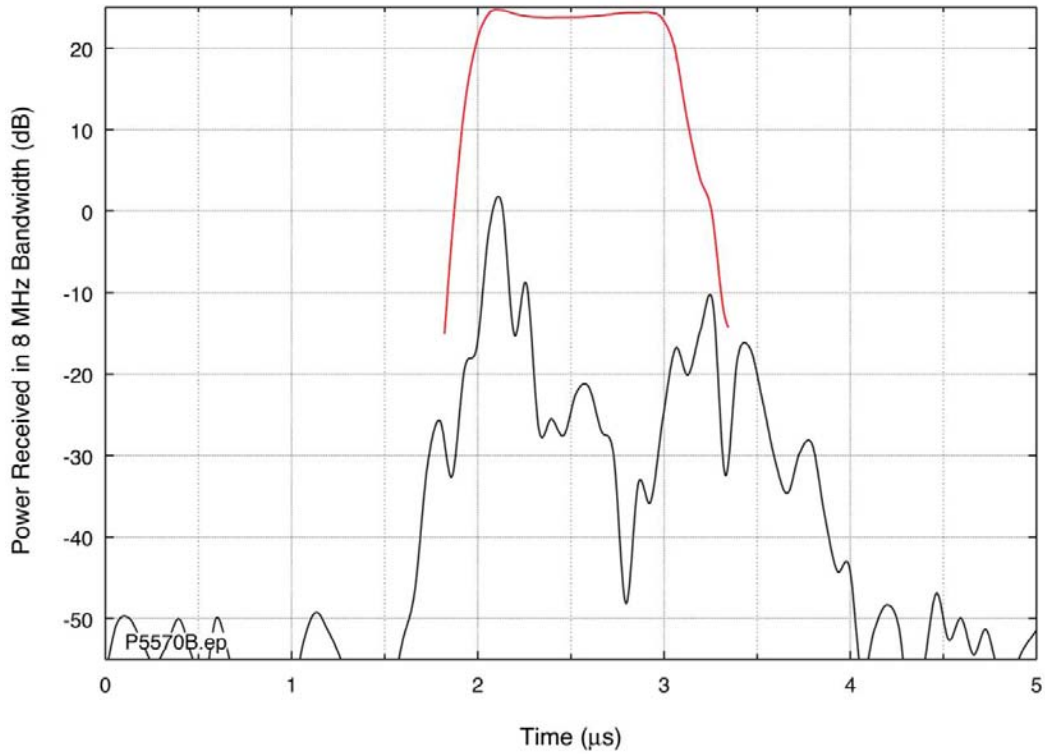


Figure 62. Pulse envelope, Point F ($\Delta f = -50$ MHz) in the TDWR Channel B spectrum.

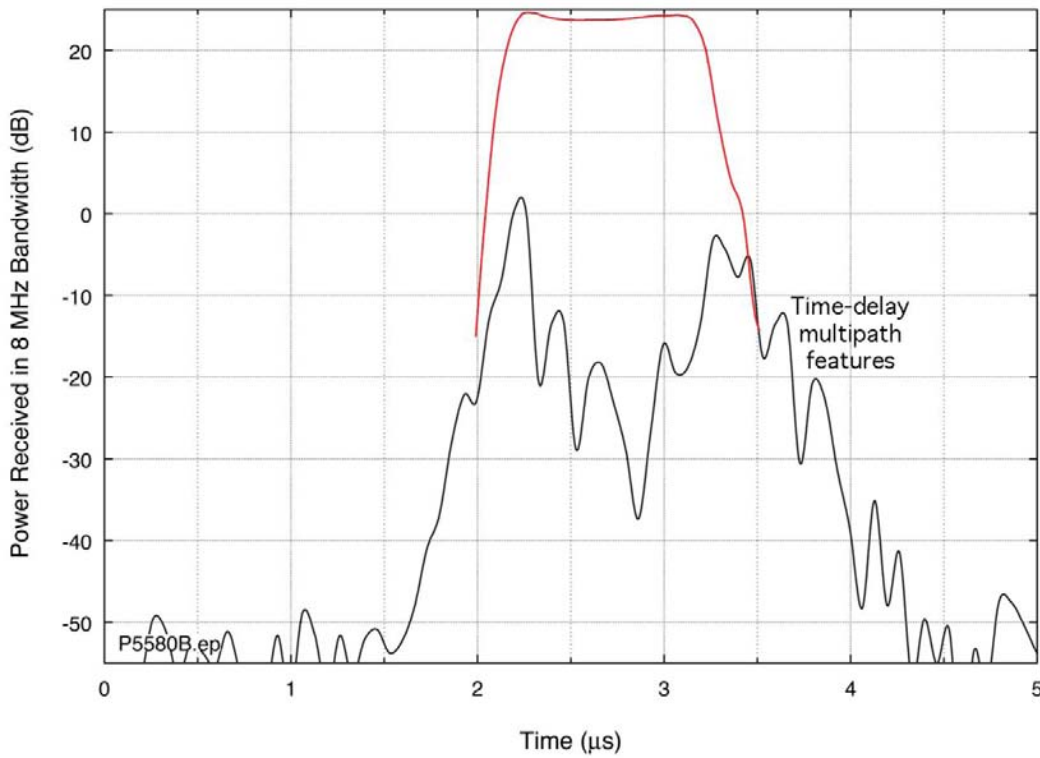


Figure 63. Pulse envelope, Point G ($\Delta f = -40$ MHz) in the TDWR Channel B spectrum.

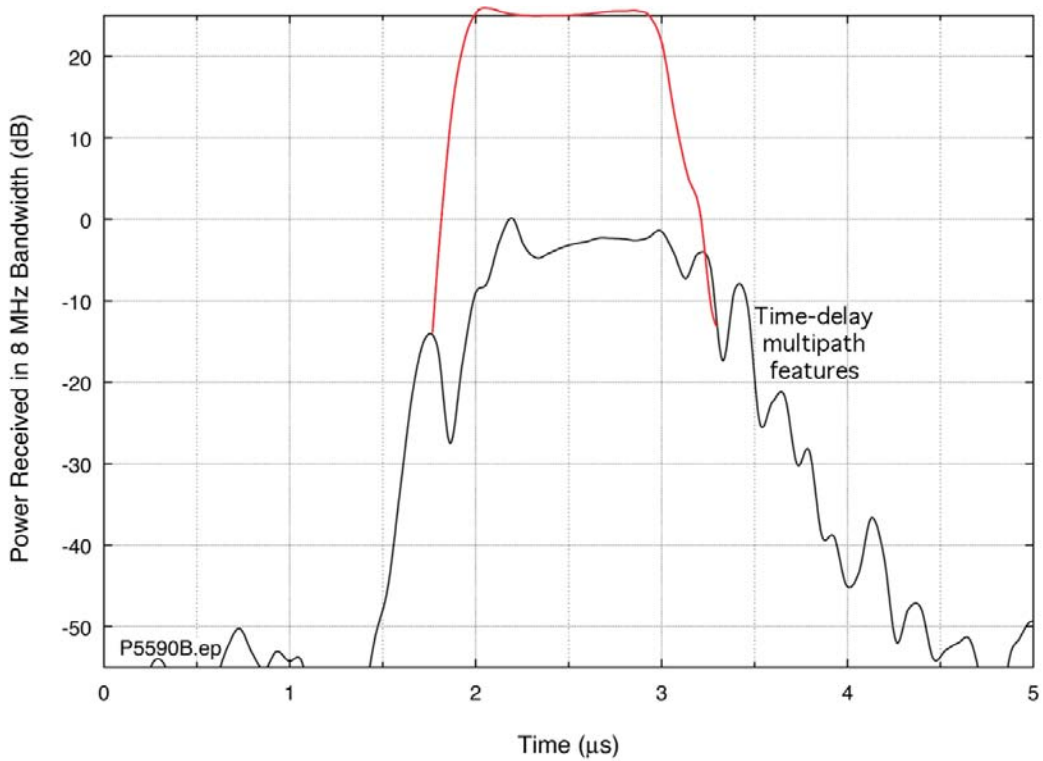


Figure 64. Pulse envelope, Point H ($\Delta f = -30$ MHz) in the TDWR Channel B spectrum.

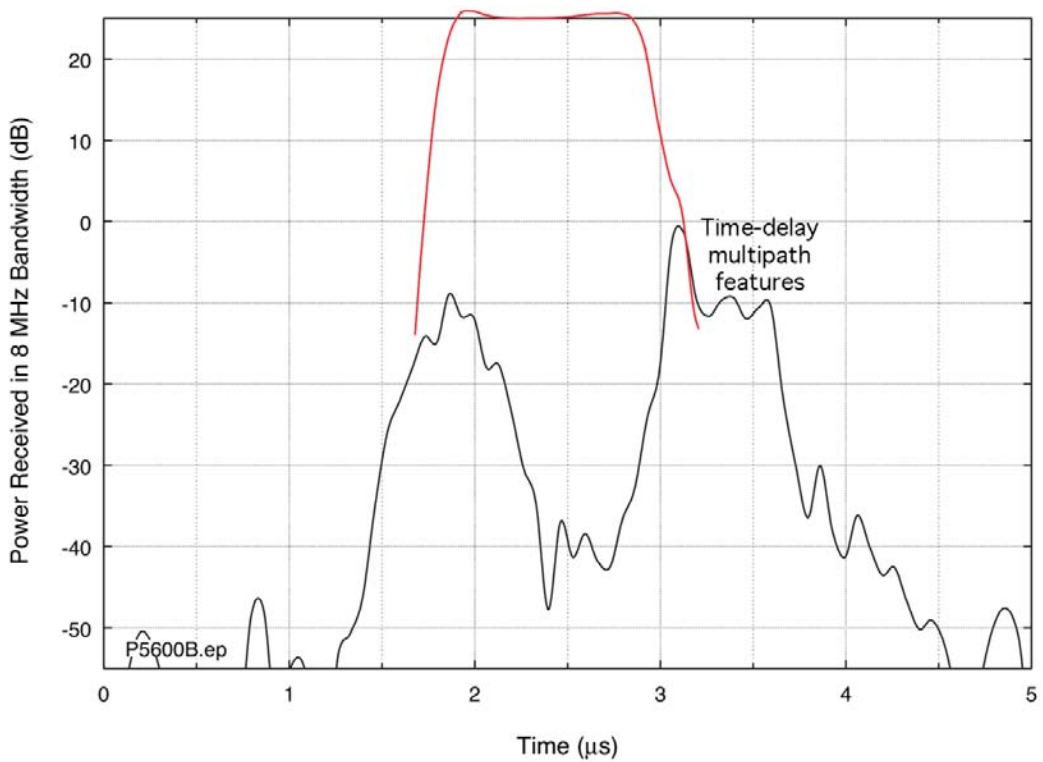


Figure 65. Pulse envelope, Point I ($\Delta f = -20$ MHz) in the TDWR Channel B spectrum.

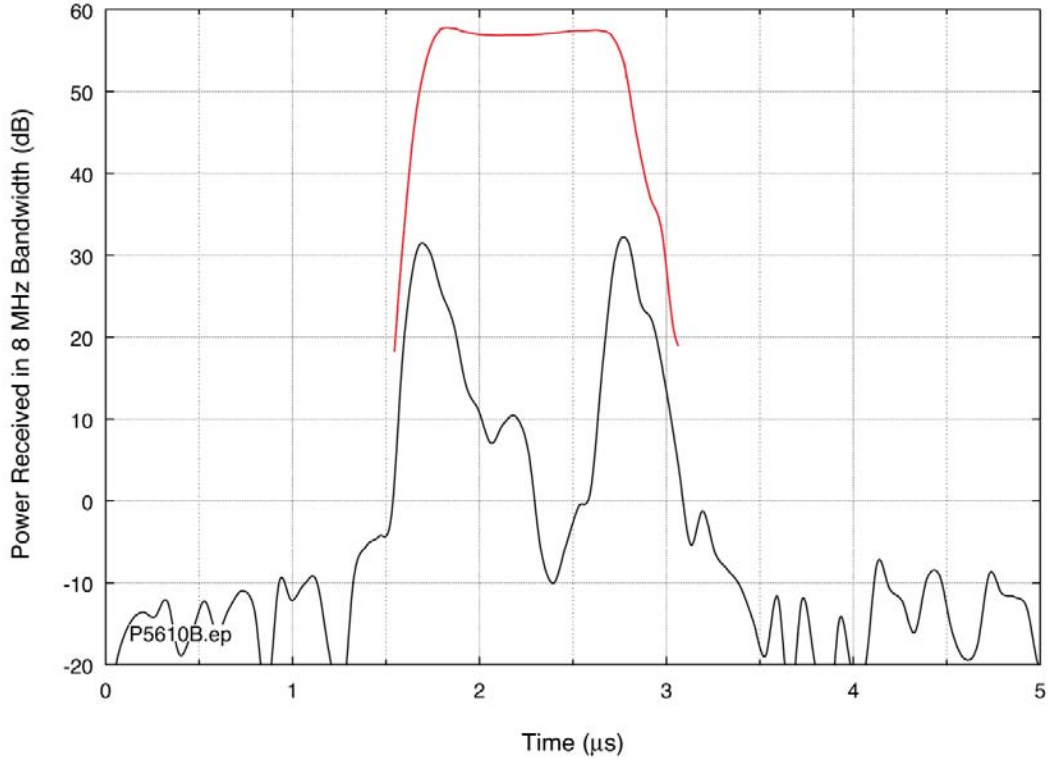


Figure 66. Classic rabbit ears pulse envelope, Point J ($\Delta f = -10$ MHz) in the TDWR Channel B spectrum.

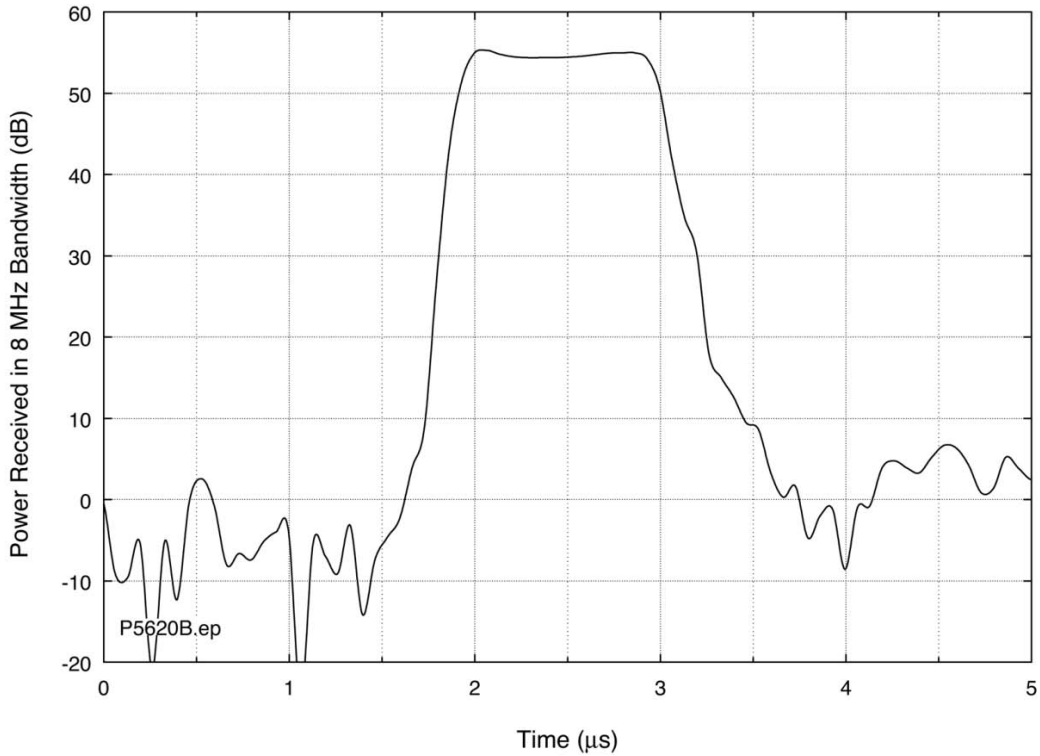


Figure 67. Pulse envelope, Point K (f_0) in the TDWR Channel B spectrum.

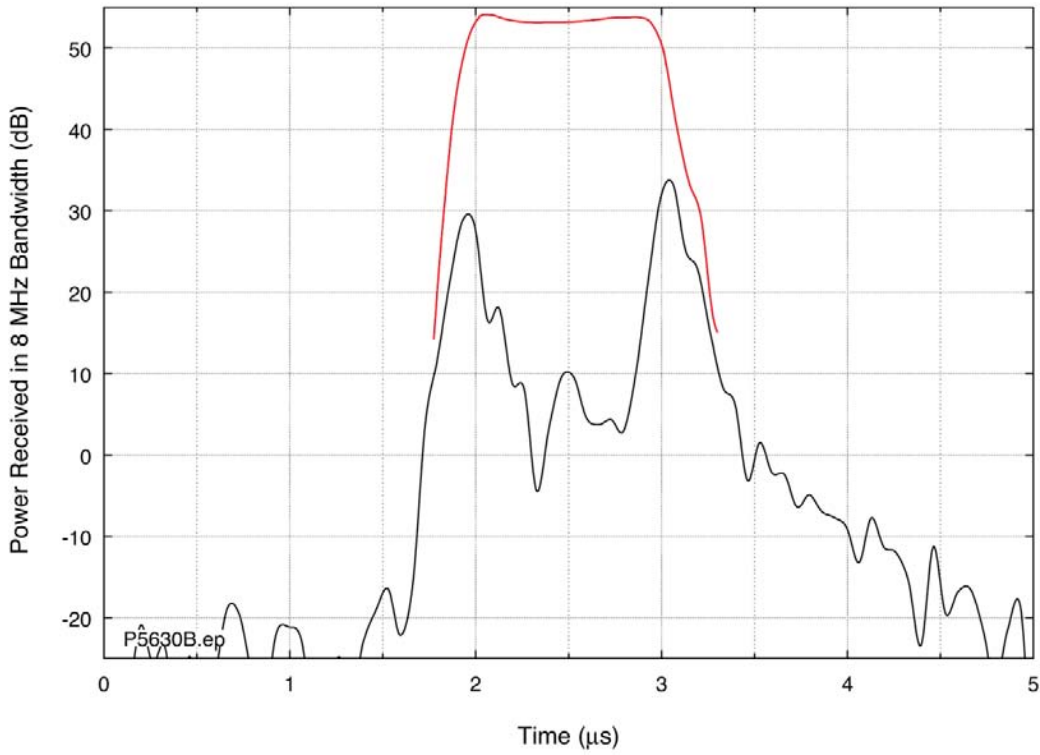


Figure 68. Classic rabbit ears pulse envelope, Point L ($\Delta f = +10$ MHz) in the TDWR Channel B spectrum.

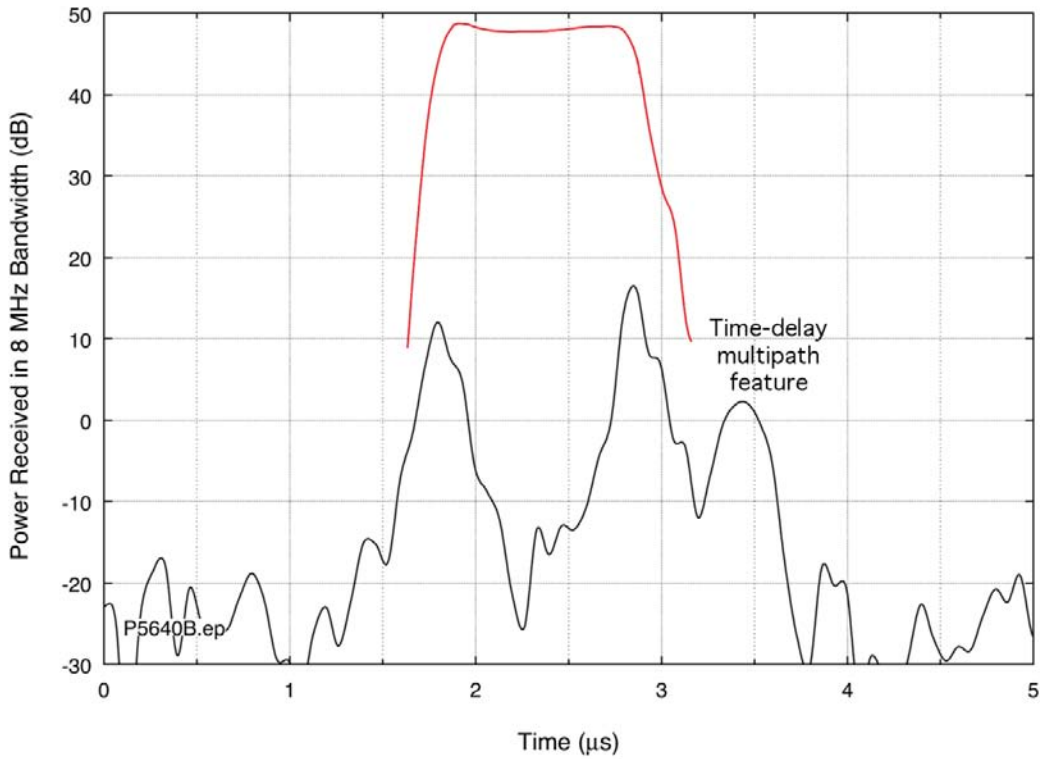


Figure 69. Pulse envelope, Point M ($\Delta f = +20$ MHz) in the TDWR Channel B spectrum.

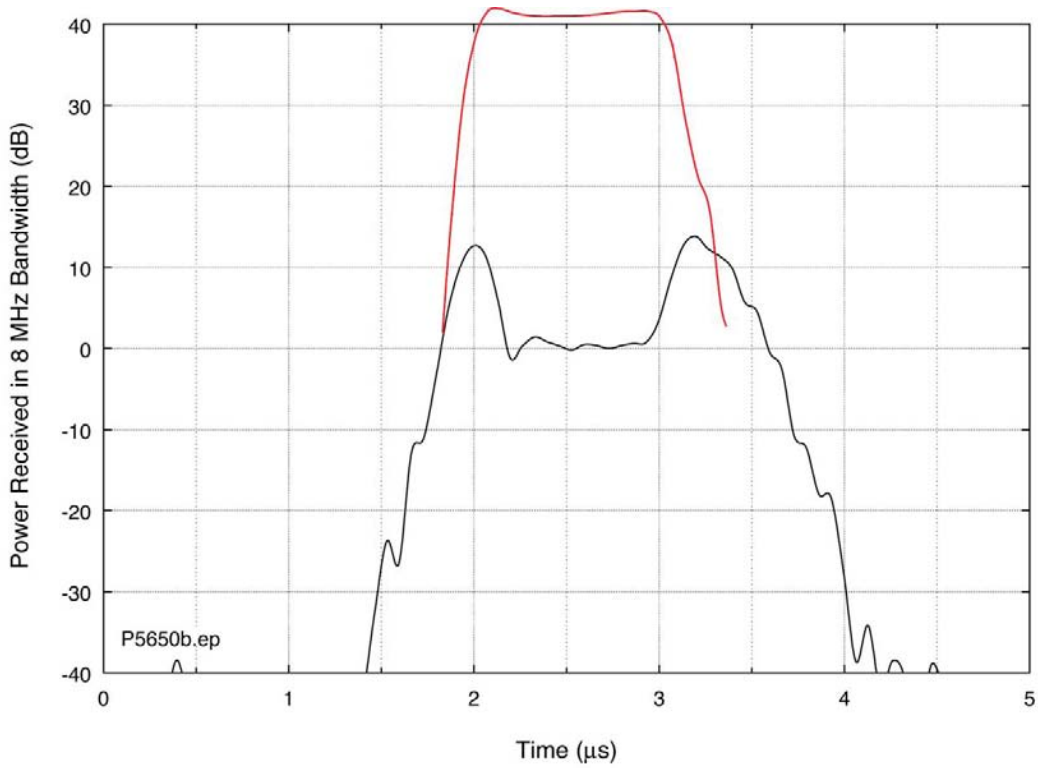


Figure 70. Pulse envelope, Point N ($\Delta f = +30$ MHz) in the TDWR Channel B spectrum.

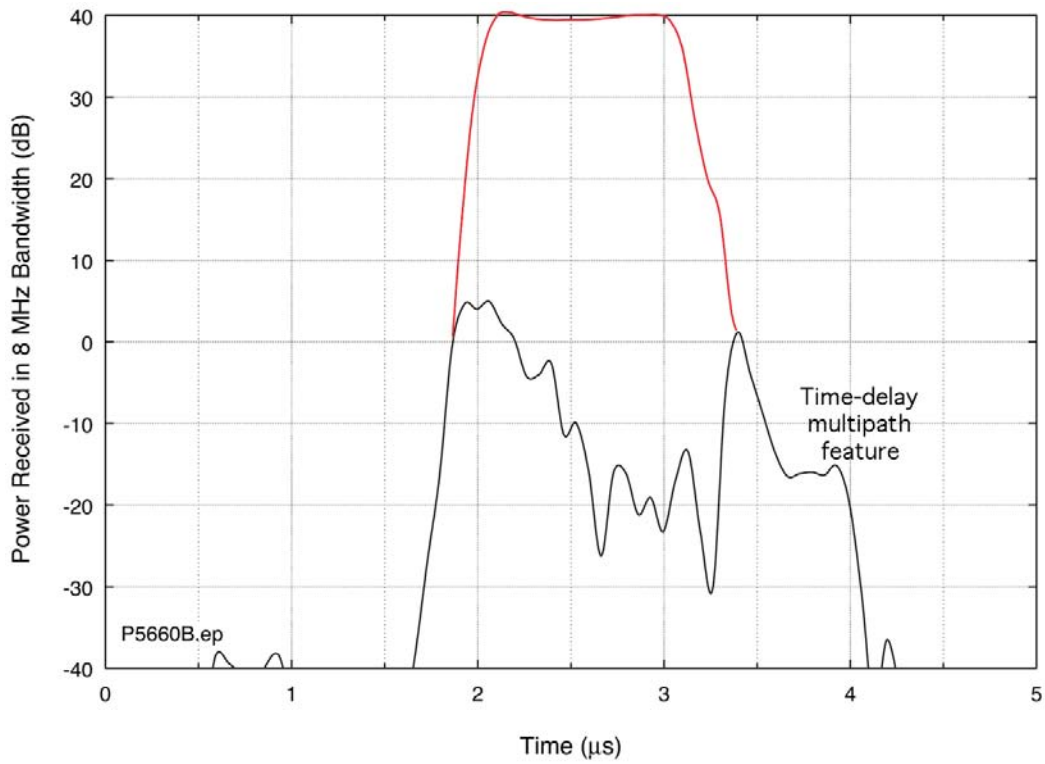


Figure 71. Pulse envelope, Point P ($\Delta f = +40$ MHz) in the TDWR Channel B spectrum.

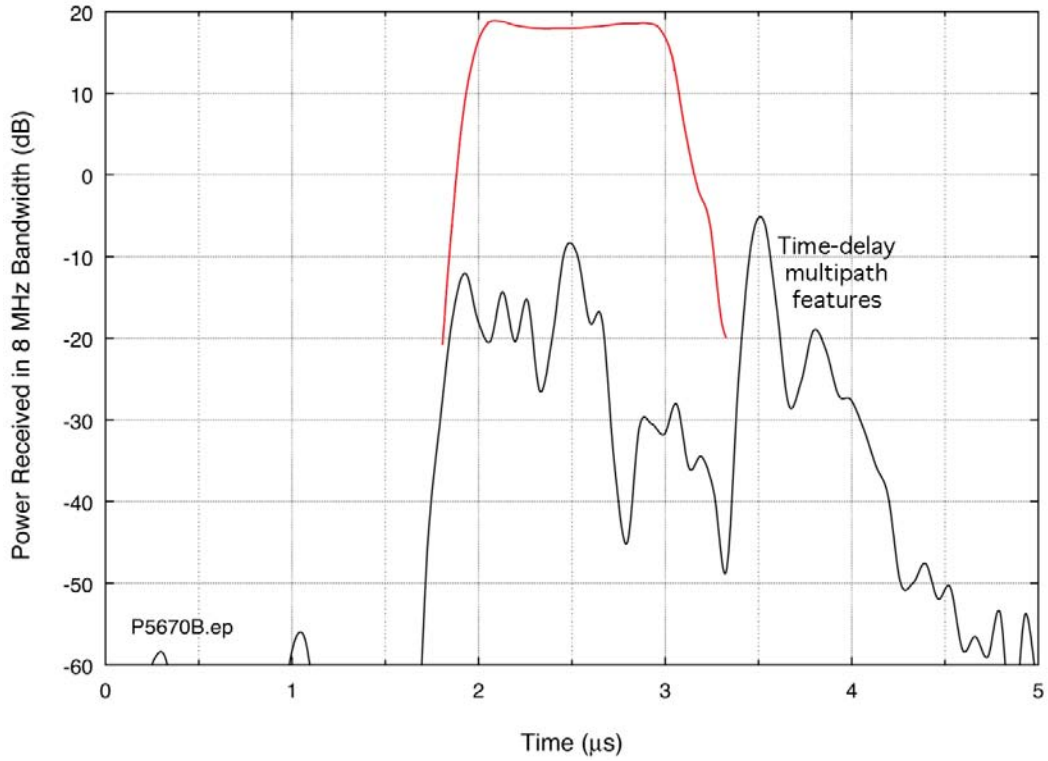


Figure 72. Pulse envelope, Point Q ($\Delta f = +50$ MHz) in the TDWR Channel B spectrum.

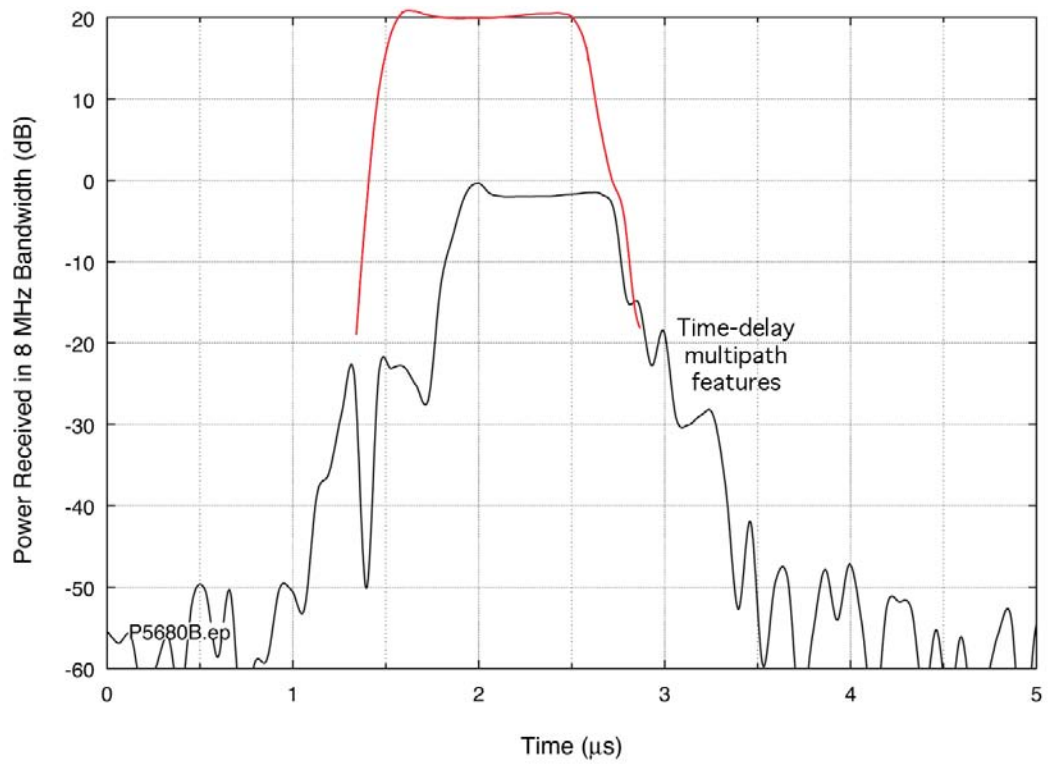


Figure 73. Pulse envelope, Point R ($\Delta f = +60$ MHz) in the TDWR Channel B spectrum.

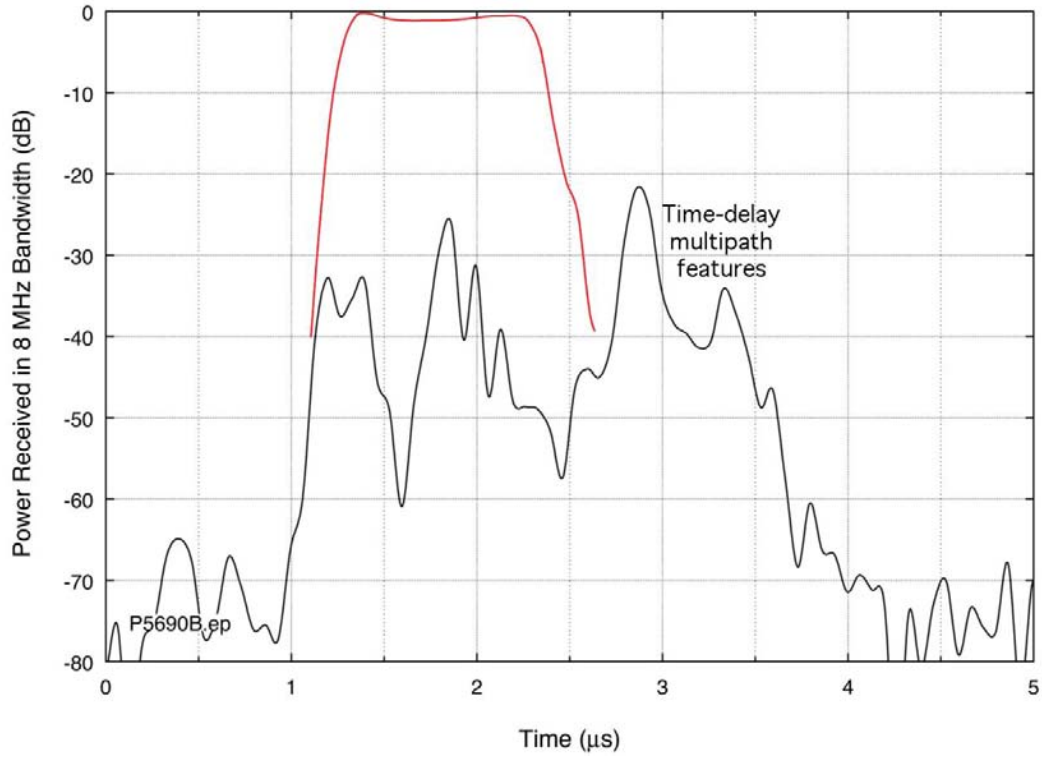


Figure 74. Pulse envelope, Point S ($\Delta f = +70$ MHz) in the TDWR Channel B spectrum.

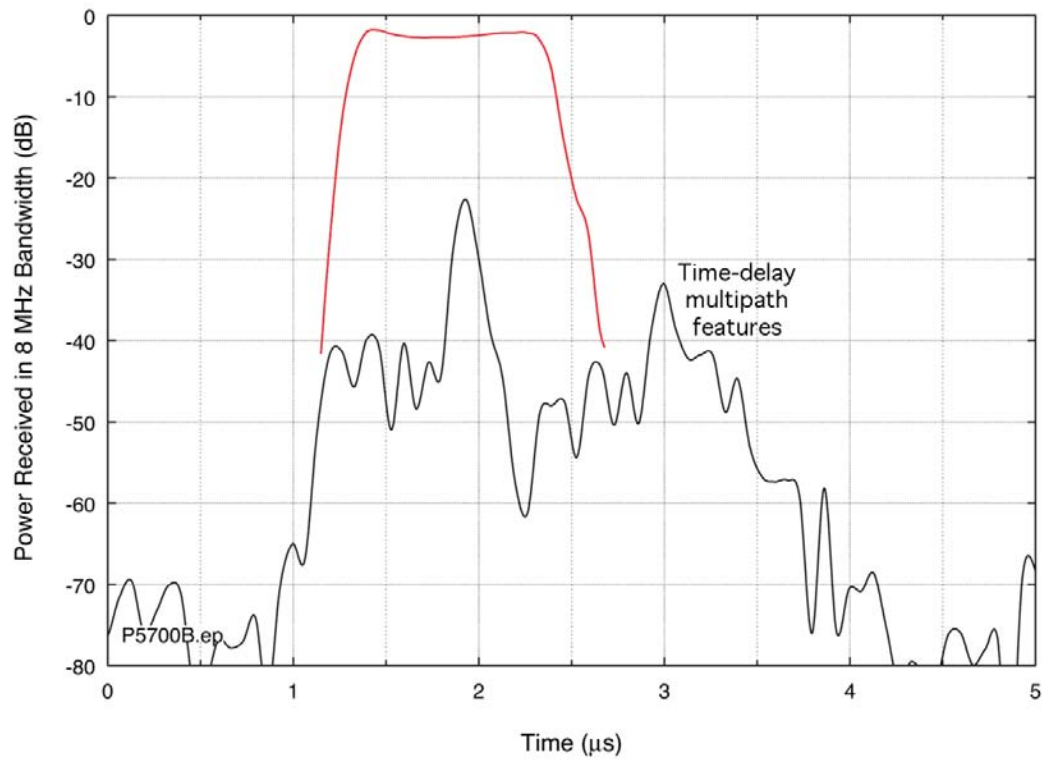


Figure 75. Pulse envelope, Point T ($\Delta f = +80$ MHz) in the TDWR Channel B spectrum.

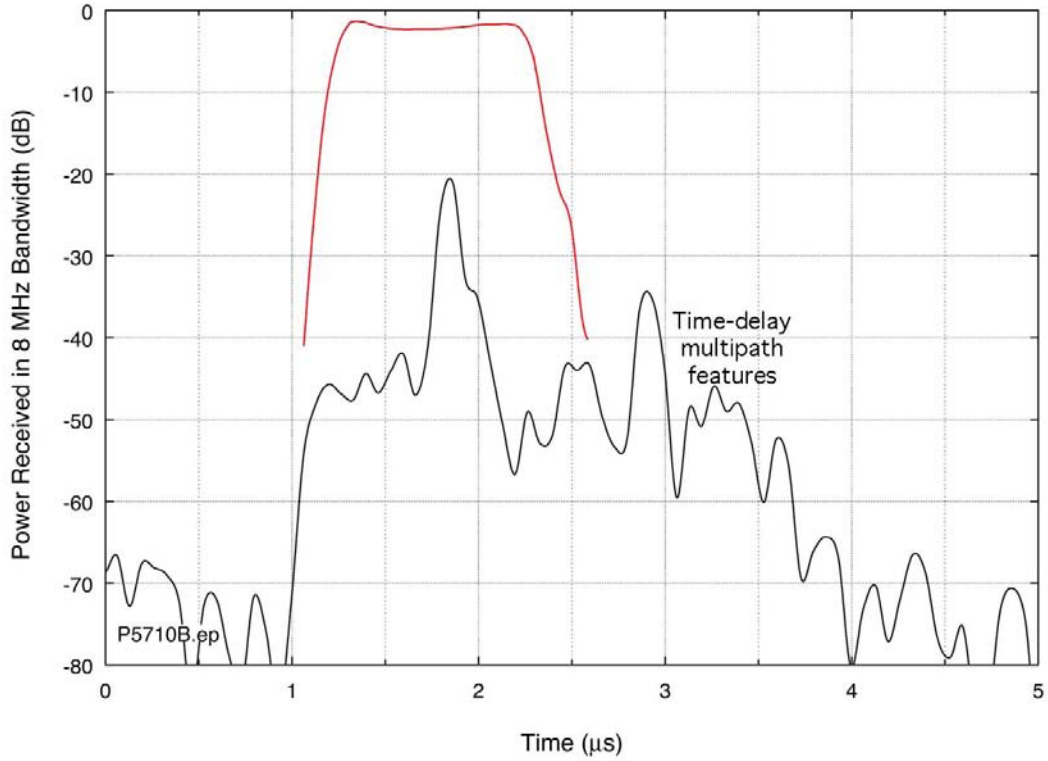


Figure 76. Pulse envelope, Point U ($\Delta f = +90$ MHz) in the TDWR Channel B spectrum.

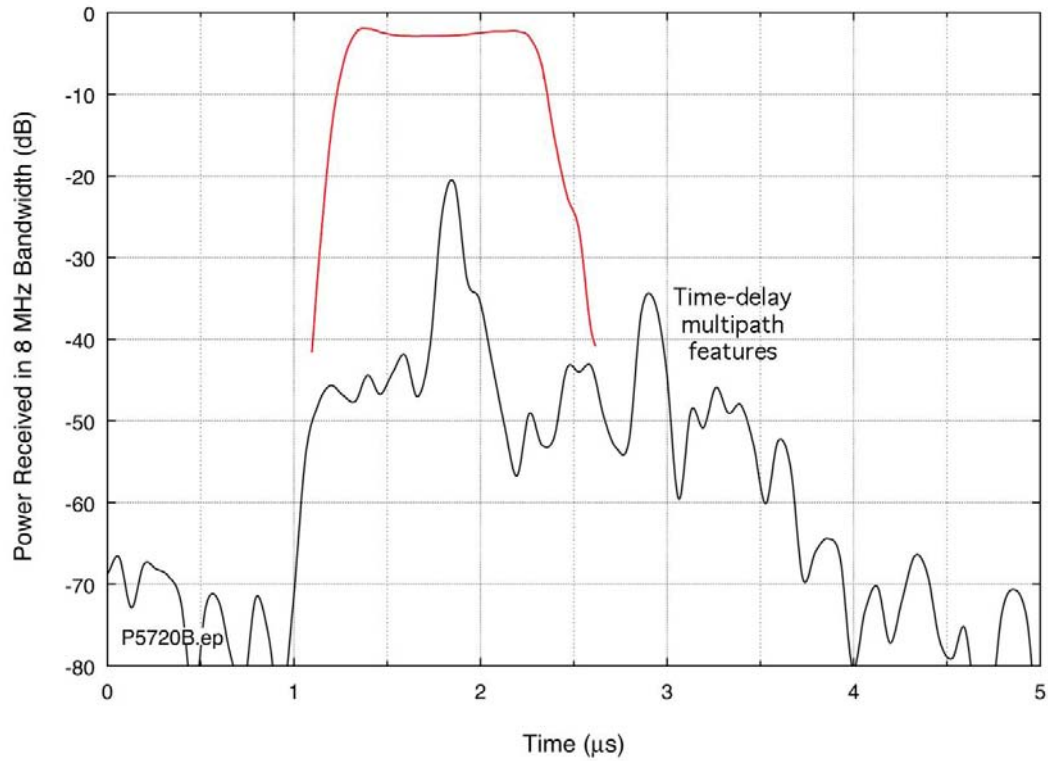


Figure 77. Pulse envelope, Point V ($\Delta f = +100$ MHz) in the TDWR Channel B spectrum.

3 OBSERVATIONS OF RABBIT EARS MORPHOLOGIES AND IMPLICATIONS FOR OFF-FUNDAMENTAL DETECTION OF PULSED SIGNALS

3.1 Observed Rabbit Ears Morphologies

Rabbit ears morphologies observed in the off-fundamental pulses measured from the WR-100 and TDWR 5 GHz weather radars include: pairs of high-amplitude rising and falling edges with lower-amplitude noise in-between (“classic rabbit ears”); single rising edges followed by lower-amplitude noise; single falling edges preceded by lower-amplitude noise; and noise-like pulses with no prominent rising or falling edges. These morphologies vary continuously across the measured emission spectra. They vary as a function of location in the spectrum and of measurement bandwidth. No method is known for predicting *a priori* the morphology that will be observed on any given frequency in any given measurement bandwidth.

3.2 Implications for Off-Fundamental Detection of Pulsed Signals

If off-fundamental detection of pulsed signals needs to be performed (as for example in dynamic frequency selection (DFS) systems), then designers of such systems should be aware of the rabbit ears phenomenon. Off-fundamental detection techniques that depend on sensing of pulse widths, for example, may not be as robust as desired if the short rabbit ears spikes (and pairs of short rabbit ears spikes) are detected in a receiver’s bandwidth instead of the expected center-frequency pulse width of the transmitter. Designers should also be aware that the observed widths of the spikes will vary as a function of their receivers’ detection bandwidths.

Conversely, if DFS or other spectrum-sharing algorithms do not depend on sensing of pulse widths, but instead rely on (for example) the PRI patterns from pulse to pulse, then the rabbit ears effect may not necessarily be a concern. This is because the rabbit ears effect only applies to *individual* pulses but does not affect the PRIs between pulses.

3.3 Multipath Effects

Although not the subject of this study, it is noted that some multipath effects are observed in some of the measured data. Multipath effects are a function of the geometries between measurement systems and DFS receivers. As with the rabbit ears effect, multipath effects would tend to complicate DFS sensing that is dependent on pulse widths but might pose little or no problem for DFS techniques that rely on PRIs.

4 PRACTICAL APPLICATION: USING THE RABBIT EARS EFFECT TO MEASURE PARAMETERS OF CHIRPED-FREQUENCY PULSES

4.1 Frequency-Modulated (Chirped) Pulses

Many radar systems use frequency-modulated (FM) pulses as a method of pulse compression. Chirping, as this technique is called, allows radar receivers to sustain a high degree of range resolution (via compression techniques in radar receivers) even though the transmitted pulse widths are lengthened to compensate for the limited peak power generated by solid-state transmitters. In modern solid-state radars it is not uncommon to encounter chirped pulse durations that are 100 μs long and chirped bandwidths that are 100 MHz wide. This is in contrast to conventional radar pulse widths that might be about 1 μs long and are not chirped.

4.2 Measurement of Chirped Pulse Parameters through Use of the Rabbit Ears Effect

Vector signal analyzers (VSAs) can be used to measure the characteristics of chirped pulses up to a point. VSAs sample at high speed (typically at about 95 megasamples (Msa, 10^6) per second) in the time domain and then perform Fourier transforms to show pulse duration and chirp bandwidth information. VSAs are powerful measurement devices but they do not necessarily have enough bandwidth to directly measure the wider chirp bandwidths of modern radars. A 95 Msa/sec VSA digitizer, for example, will only provide up to about 36 MHz of measurement bandwidth, just a fraction of the bandwidth of some types of chirped radar transmitters.

The rabbit ears effect can be used as a practical tool to measure both the duration and bandwidth of arbitrarily long-duration and wide-bandwidth chirped pulses. Furthermore, the effect can be used with both spectrum analyzers (SAs) and VSAs. The author has used this effect to measure the chirped-pulse characteristics of highly sophisticated, state-of-the-art radars in places and times where he either did not have a VSA or else the pulse characteristics exceeded even the capabilities of the best available VSAs. In the author's experience, the rabbit ears effect can be used to achieve chirped-pulse characteristics measurements with greater speed and ease than direct measurements of these characteristics. (Related information on engineering aspects of the rabbit ears effect in bandwidth-limited receivers is provided in [2].)

This measurement technique is founded on the recognition that, if the measurement system is bandwidth-limited compared to the chirp width of the pulses to be measured, then the carrier frequencies of each of the chirped pulses will spend some time *outside* the convolution bandwidth of the measurement system. Therefore chirped pulses are measured *off their fundamental frequencies* by bandwidth-limited measurement systems during part of each of their cycles, even if the measurement system is center-tuned to their center frequencies. The conclusion drawn from this observation is that *bandwidth-limited measurement of wide-bandwidth chirped pulses is equivalent to the rabbit ears measurement of non-chirped pulses*.

Imagine that a measurement system has a smaller convolution bandwidth than the bandwidth of the chirped pulses that are to be measured, and that it is center-tuned to the same frequency as the center of the intentional FM chirp range of the pulses. Then the chirped pulses' carriers begin and end on frequencies outside the measurement system bandwidth, and the pulses sweep

through the measurement system bandwidth between the two spikes. The measurement system will show a rabbit ear spike in the time domain at the beginning and ending of each pulse; the time between those rabbit ears must be the pulse duration.

As the chirp carrier tunes (frequency modulates) through the measurement system bandwidth, a bump will be formed in the time domain. This bump will be centered between the two rabbit ear spikes if the measurement is tuned to the center frequency of the chirped pulses. If the measurement system's tuned frequency is offset slightly below or above that fundamental frequency then the bump will move slightly left or right, respectively, in the time domain between the rabbit ears.

The ratio of the width of the time-domain bump to the time between the rabbit ears is equal to the ratio of the measurement bandwidth to the bandwidth of the chirped pulses. If the chirp bandwidth is B_c , the measurement bandwidth is B_{meas} , the pulse width determined from the rabbit ears spike spacing is T , and the duration of the bump between the rabbit ears is t_{delta} , then the proportionality relationship between these parameters is³:

$$\frac{B_{meas}}{B_c} = \frac{t_{delta}}{T} \quad (1a)$$

and therefore

$$B_c = B_{meas} \cdot \left(\frac{T}{t_{delta}} \right) \quad (1b)$$

4.3 Example Chirp-Parameter Measurement Using the Rabbit Ears Effect

The author has used this technique for many years in measurements of chirped pulses transmitted by operational and developmental radar systems; he has undertaken a simple demonstration of the technique for this NTIA Report. For this demonstration a vector signal generator (VSG) output is fed to an SA. The VSG is programmed to produce RF pulses at 5500 MHz that are 60 μ s long with a chirp bandwidth of 20 MHz, the chirp direction running in time from lower frequency to higher frequency. Although the 20 MHz chirp bandwidth is within the bandwidth capabilities of existing VSAs, it exceeds the maximum 8 MHz bandwidth of the SA used for this demonstration. In any event, the purpose of the exercise is simply to provide an example of this measurement technique.

The rabbit ears measurement of chirped-pulse bandwidth is performed with the SA parameters shown in Table 1. Figures 78–80 show the results from the SA display.

³ This relationship is strictly true only if the FM of the chirped pulses is linear. However, non-linear FM (NLFM) in chirped pulses of existing radars is so close to linear FM (LFM) in existing radar designs that for practical purposes the linear ratio may be used as a good approximation even for NLFM chirped pulses.

Table 1. SA settings for chirped-pulse parameter measurements.

SA Parameter	SA Parameter Setting
frequency span	zero hertz (time domain)
detection	positive peak
trace mode	clear-write
resolution (IF) bandwidth (RBW)	widest available in SA being used
video bandwidth (VBW)	at least as wide as RBW
sweep time	longer than the likely chirped-pulse duration
RF attenuation	as much as needed to prevent IF-stage overload
reference Level	highest possible with the selected RF attenuation

Figures 78 and 79 show the rabbit ears that are observed when the spectrum analyzer is tuned 10 MHz below and above the center frequency of 20 MHz chirped pulses, respectively. Each of these two figures shows classic pairs of time domain spikes that can be used to determine chirped pulse duration, T , by measuring the time interval between them. In these two figures, however, the chirp bandwidth cannot be determined because of the large amount of off-tuning of the measurement system from the center frequency of the chirp range.

Figure 80 shows the SA display when the measurement system is tuned to the center frequency of the chirp range. The data in this figure may be used to determine *both* the pulse duration, T , and the FM range of the chirped pulses, B_c . In this figure the pulse carrier successively enters the SA convolution bandwidth (its intermediate frequency (IF), or resolution bandwidth (RBW)) of 8 MHz, passes through the SA's tuned frequency (coincident with the center frequency of the chirping), and finally passes out of the SA's convolution bandwidth. The bump between the rabbit ears is actually the *convolution* of the SA RBW with the chirp-pulse carrier; the chirp-pulse carrier sweeps out the shape of the SA RBW as it passes through the tuned frequency of the SA. Thus the 3 dB bandwidth of the bump is the 3 dB bandwidth of the SA RBW.

In addition to the measurement of T from the interval between the rabbit ears, another interval, t_{delta} , is measured at the 3 dB points of the bump between the rabbit ears, as shown in Figure 80. The chirp bandwidth, B_c , is then computed by multiplying the value of the SA RBW, B_{meas} , by the pulse duration, T , and dividing by t_{delta} . These computations are shown in red in Figure 80.

In Figure 80 the convolution of the SA RBW is centered between the pulses because the SA is center-tuned to the chirped-pulse FM range. If the SA were off-tuned slightly below or above the center of the chirped-pulse FM range then the bump would be moved slightly to the left or right, respectively, but it would still be possible to measure the critically important value of t_{delta} and therefore still compute B_c . If the amount of off-tuning were to become too large, however, then the bump would be moved so far to the left or right that the result would become what is shown in Figures 78 and 79. In that case it becomes impossible to measure t_{delta} and then B_c cannot be computed. It is reiterated that this measurement technique for parameters of chirped pulses can be used with any bandwidth-limited measurement system, including both SAs and VSAs.

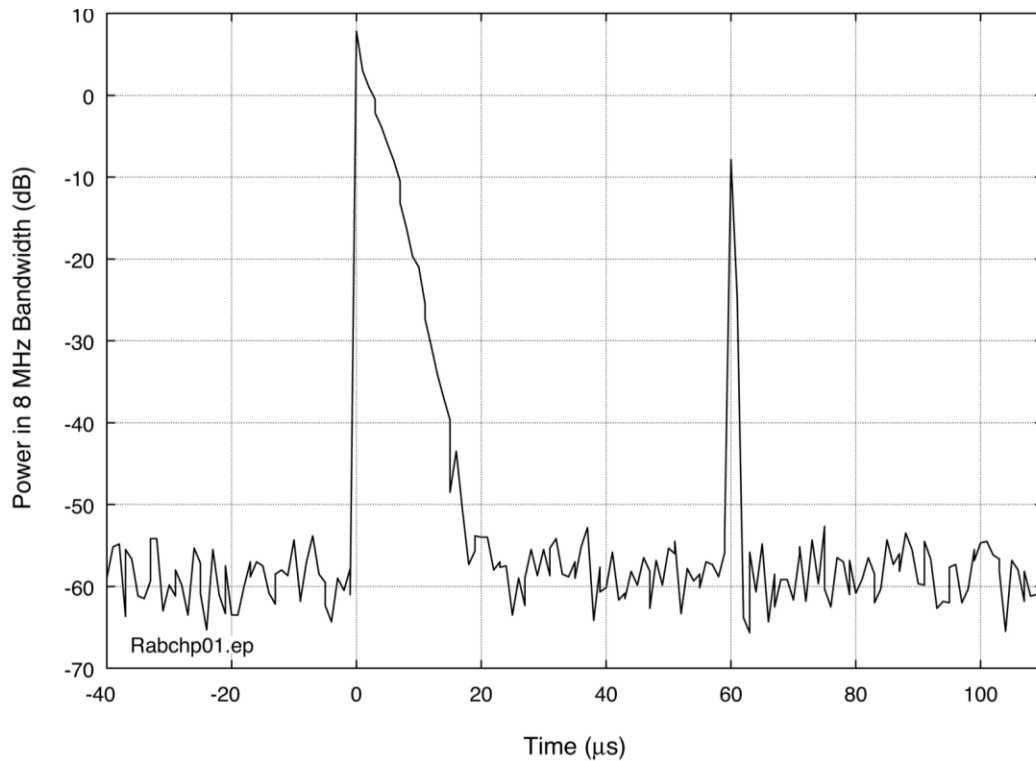


Figure 78. SA display of rabbit ears when SA tuned frequency was 10 MHz below the center of 20 MHz wide chirped-pulse carrier. SA settings were as shown in Table 1, with RBW = 8 MHz.

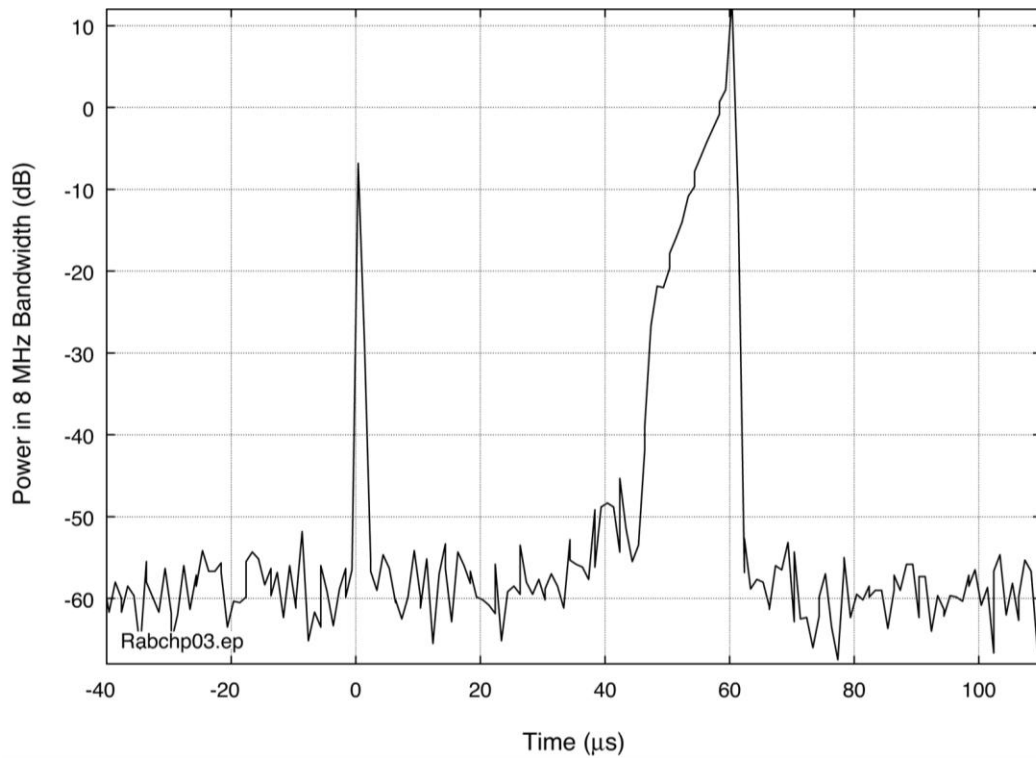


Figure 79. SA display of rabbit ears when SA tuned frequency was 10 MHz above the center of the 20 MHz wide chirped-pulse carrier. Pulse duration of 60 μs is observed between the rabbit ears in both Figures 78 and 79.

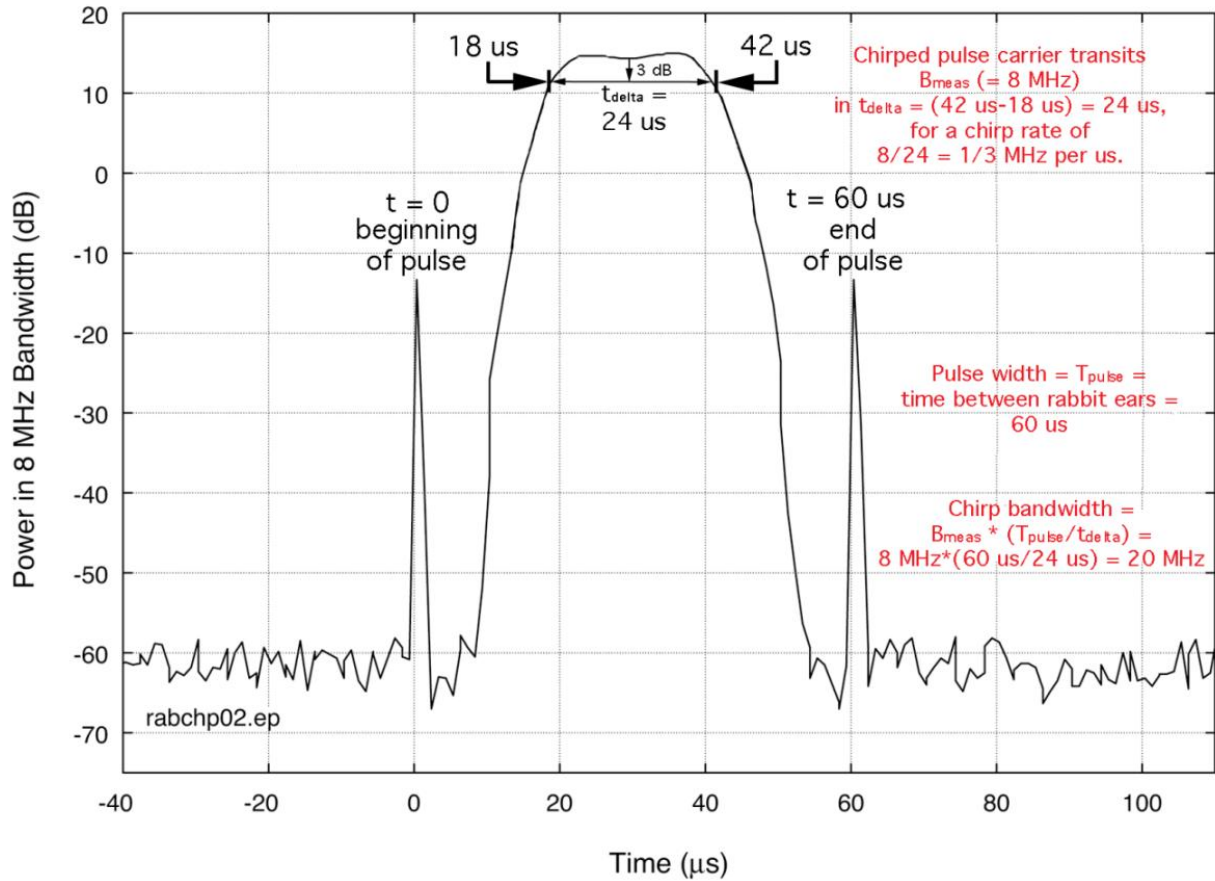


Figure 80. SA display when tuned to the center of the chirped-pulse FM range. Calculation of pulse duration and FM range is shown in notes in red.

5 SUMMARY

When RF pulse envelopes are observed away from their fundamental frequency their shapes differ from those at their fundamental frequency. Off-fundamental pulse envelopes tend to exhibit spikes at their rising and falling edges with lower-amplitude energy between the spikes, a phenomenon called the rabbit ears effect. This time-domain phenomenon results from the convolution by a bandwidth-limited measurement system or radio receiver of a limited number of off-fundamental Fourier lines in the emission spectra of pulsed signals. Examples of rabbit ears pulse envelopes have been provided in this report in a mathematical simulation and in measurements of off-fundamental pulse envelopes of two models of 5 GHz weather radars.

The morphologies of rabbit ears pulses show a wide range of variation. The shapes of rabbit ears on any given frequency and in any given receiver bandwidth are not predictable *a priori* on any available theoretical basis—they can only be observed on an *ad hoc* basis on each frequency in any particular receiver or measurement bandwidth.

The characteristics of rabbit ears would complicate DFS techniques that depend on off-frequency sensing of pulse widths or pulse shapes. Conversely, on-frequency DFS sensing would not be affected. The rabbit ears effect has no effect on transmitted PRI sequences. Therefore DFS techniques that use PRI information to avoid radar frequencies would not be impacted by this effect.

The rabbit ears phenomenon has a useful, practical application. This is the measurement of pulse durations and FM bandwidths of chirped radar pulses with measurement systems that are themselves bandwidth-limited. This is useful and important because state-of-the-art solid-state radars that transmit chirped pulses often generate chirped FM ranges that exceed the direct-measurement capabilities of even the most capable VSAs. Furthermore, the rabbit ears method of measuring chirped-pulse parameters works with any bandwidth-limited measurement system, including both SAs and VSAs.

6 ACKNOWLEDGEMENTS

Mr. Geoff Sanders of ITS is thanked for generating the mathematical creations of the rabbit ears effect in Figures 1–7 using the software product MATLAB©. Mr. John Carroll of ITS and Mr. Bob Sole of NTIA’s Office of Spectrum Measurement (OSM) were instrumental in the measurement of TDWR rabbit ears pulse envelopes. The staff of the TDWR Program Support Facility at the Federal Aviation Administration’s Mike Monroney Aeronautical Center in Oklahoma City, Oklahoma are thanked for making the TDWR available for the pulse-shape measurements. Ms. Kristen Davis of ITS is thanked for her preparation and formatting of this Technical Report.

7 REFERENCES

- [1] Sanders, F. H., R. L. Hinkle, and B. J. Ramsey, “Measurement Procedures for the Radar Spectrum Engineering Criteria (RSEC)”, NTIA Report TR-05-420, NTIA, U.S. Department of Commerce, March 2005. <http://www.its.bldrdoc.gov/publications/2450.aspx>
- [2] Sanders, F. H., and R. Sole, “Test results and simulations illustrating the effective duty cycle of frequency modulated pulsed radiolocation and EESS system waveforms in marine radionavigation receivers”, ITU-R Report M.2128, International Telecommunications Union Radiocommunication Sector (ITU-R), 2008. <http://www.itu.int/pub/R-REP-M.2128>

BIBLIOGRAPHIC DATA SHEET

1. PUBLICATION NO.	2. Government Accession No.	3. Recipient's Accession No.
4. TITLE AND SUBTITLE The Rabbit Ears Pulse-Envelope Phenomenon in Off-Fundamental Detection of Pulsed Signals		5. Publication Date July 2012
		6. Performing Organization Code NTIA/ITS.T
7. AUTHOR(S) Frank H. Sanders		9. Project/Task/Work Unit No. 6462000-200
8. PERFORMING ORGANIZATION NAME AND ADDRESS Institute for Telecommunication Sciences National Telecommunications & Information Administration U.S. Department of Commerce 325 Broadway Boulder, CO 80305		10. Contract/Grant Number.
		12. Type of Report and Period Covered
11. Sponsoring Organization Name and Address National Telecommunications & Information Administration Herbert C. Hoover Building 14 th & Constitution Ave., NW Washington, DC 20230		
14. SUPPLEMENTARY NOTES		
15. ABSTRACT (A 200-word or less factual summary of most significant information. If document includes a significant bibliography or literature survey, mention it here.) When radiofrequency pulse envelopes are observed away from their fundamental frequency their shapes differ from those at their fundamental frequency. Off-fundamental pulse envelopes tend to exhibit spikes at their rising and falling edges with lower-amplitude energy between the spikes. This phenomenon, called the rabbit ears effect, is described in this NTIA Report. Examples of rabbit ears pulse envelopes are provided in a mathematical simulation and from measurements of off-fundamental pulse envelopes of two models of 5 GHz weather radars. Morphologies of rabbit ears pulses are examined. A method is provided for using this effect to determine the durations and bandwidths of chirped pulses in bandwidth-limited measurement systems. Implications for off-fundamental detection of pulsed signals for dynamic frequency selection (DFS) algorithms are considered.		
16. Key Words (Alphabetical order, separated by semicolons) chirped pulses; dynamic frequency selection (DFS); off-fundamental signal detection; pulsed radiofrequency (RF) signals; rabbit ears; radar spectrum		
17. AVAILABILITY STATEMENT <input checked="" type="checkbox"/> UNLIMITED. <input type="checkbox"/> FOR OFFICIAL DISTRIBUTION.	18. Security Class. (This report) Unclassified	20. Number of pages 66
	19. Security Class. (This page) Unclassified	21. Price:

NTIA FORMAL PUBLICATION SERIES

NTIA MONOGRAPH (MG)

A scholarly, professionally oriented publication dealing with state-of-the-art research or an authoritative treatment of a broad area. Expected to have long-lasting value.

NTIA SPECIAL PUBLICATION (SP)

Conference proceedings, bibliographies, selected speeches, course and instructional materials, directories, and major studies mandated by Congress.

NTIA REPORT (TR)

Important contributions to existing knowledge of less breadth than a monograph, such as results of completed projects and major activities. Subsets of this series include:

NTIA RESTRICTED REPORT (RR)

Contributions that are limited in distribution because of national security classification or Departmental constraints.

NTIA CONTRACTOR REPORT (CR)

Information generated under an NTIA contract or grant, written by the contractor, and considered an important contribution to existing knowledge.

JOINT NTIA/OTHER-AGENCY REPORT (JR)

This report receives both local NTIA and other agency review. Both agencies' logos and report series numbering appear on the cover.

NTIA SOFTWARE & DATA PRODUCTS (SD)

Software such as programs, test data, and sound/video files. This series can be used to transfer technology to U.S. industry.

NTIA HANDBOOK (HB)

Information pertaining to technical procedures, reference and data guides, and formal user's manuals that are expected to be pertinent for a long time.

NTIA TECHNICAL MEMORANDUM (TM)

Technical information typically of less breadth than an NTIA Report. The series includes data, preliminary project results, and information for a specific, limited audience.

For information about NTIA publications, contact the NTIA/ITS Technical Publications Office at 325 Broadway, Boulder, CO, 80305 Tel. (303) 497-3572 or e-mail info@its.blrdoc.gov.

This report is for sale by the National Technical Information Service, 5285 Port Royal Road, Springfield, VA 22161, Tel. (800) 553-6847.